Limits of Adaptation in the Vergence System

A Dissertation

SUBMITTED TO THE FACULTY OF

UNIVERSITY OF MINNESOTA

BY

Elizabeth M. Fast

IN PARTIAL FULFILLMENT OF THE REQUIREMENTS

FOR THE DEGREE OF

DOCTOR OF PHILOSOPHY

Advisor: Stephen A. Engel, Ph.D.

May 2022

Acknowledgements

I would like to express gratitude to my advisor Dr. Stephen Engel for his valuable guidance and support through this long journey. I would also like to thank the other members of my dissertation committee, Dr. Daniel Kersten, Dr. Gordon Legge, and Dr. Linda McLoon.

I also want to express deep and sincere gratitude to Dr. Anahita Mehta; I would not have been able to do this without your constant encouragement and support. Thank you for all your invaluable insight, and honest feedback, and for always having the perfect balance of compassion and “bad cop.”

Thank you also to everyone from the Engel lab, my other UMN colleagues and friends. Special thanks go to Dr. Yihwa Baek and Dr. Jackson Graves, for walking this path with me, and for becoming lifelong friends. I’m so happy for you guys, and proud of you, and plan to do a victory vacation and visit both of you.

I would like to extend my sincere thanks to Sara. You have taught me so much. I cherish all the memories of our silly college shenanigans, and the serious talks as well. I know no matter what you will always have my back, and be my biggest cheerleader.

Thank you also to Em and Kyla. You two always inspire me to be a better version of myself. Our regular Zoom chats helped keep me sane the last few years. I'm so proud of us for the people we are growing into, and for the dreams we are all following.

I very much appreciate Sari, my # 1 walking buddy. I appreciate your insight so much, and your sense of humor can always make me feel better. I love our mutual admiration of Physical Therapists and salty foods. Thank you for always having the perfect blend of positivity and a dry sense of humor.

Ashlee, Ariana, Nat and Nelle, I am so glad you all have recently come into my life. Thank you for always being a source of validation and encouragement. Thank you for being so understanding of what it means to live the chronic illness life. Thank you for making me laugh and smile, even in the darkest situations. And thank you for always letting me know you believe in me.

And I would also like to thank all the rest of my friends, from all over the globe. From the frivolous to the sincere, thank you for all the fun and laughter, as well as the genuine support and understanding.

Profound thanks to Mom and Dad for supporting and nurturing me into the person I am today. Thank you for nurturing a spirit of curiosity in our home, and

letting me make a mess when I worked on projects. Thank you also to David and Kathleen, my first partners in crime, my dune climbing buddies, and entrepreneurial associates.

Thank you to Tilda for being the best dog, and my constant companion. Even though you take it a step too far, and bark ferociously at “attackers” with all 12 pounds of your very fluffy body, I appreciate that you always want to protect me. But even more, thank you for endless cuddles on the couch, despite your ceaseless demand for scratches.

Finally, deepest thanks to Mackenzie, for your constant support in everything, for keeping me sane, well fed, and for making sure I was sleeping. These last few years you have really stepped up to the plate and helped in more ways than ever before, and I could never fully express how much that has meant to me. Most of all, thank you for being my best friend, and always knowing how to cheer me up.

Abstract

Vergence eye movements, used to align the eyes and avoid diplopia, are controlled by several interacting components. One, the tonic component can be thought of as a “baseline” position of the eyes, and this baseline can be adapted through recent history of eye positions. We tested the limits of this adaptation, with the dual goals of measuring the maximum increase in the amount of divergence that can be obtained through adaptation and understanding what factors determine this maximum. We used a dual stereoscope/eye-tracker to measure fusional limits (maximal divergence before experiencing diplopia) and phorias (eye movements indicative of incomplete adaptation); both were also measured behaviorally. Experiments 1-3 adapted participants stepwise in 5 minute blocks of increasing vergence demand (implemented by shifting one image location toward the periphery), and found that adaptation did shift fusional limits. But ultimately adaptation failed to keep up with vergence demand, and phorias increased in size across blocks. This indicated that adaptation was becoming less efficient as vergence demand increased; however the slope of phoria reduction did not decrease with increasing vergence demand, suggesting that the rate of adaptation did not change. We hypothesized that the 5 minute blocks were simply not enough time to adapt completely, and tested this in Experiment 4 where block duration was allowed to vary. As vergence demand increased, block duration also increased, suggesting that the rate of adaptation was in fact slowing as vergence demand increased. However, even with the

variable block length, adaptation became less complete across blocks, as indicated by larger and larger phorias. Future work can determine the causes of these remaining limits on adaptation.

Table of Contents

List of Figures

Chapter 1: Introduction

What determines the range of eye movements we can make? The answer to this question has important clinical relevance. In the vergence system, which brings the eyes into alignment so that objects of interest fall on corresponding parts of the two eyes retinae, eye movements can be limited in problematic, and clinically relevant, ways. In convergence insufficiency, for example, the eyes turn inadequately inward, while in certain forms of strabismus, one eye turns inadequately outward.

This dissertation presents multiple experiments on vergence adaptation, and explores how one component of the vergence system, the tonic component, contributes to setting fusional limits, which are the largest image disparities that can be overcome by fusional eye movements to prevent diplopia. More specifically we ask whether adapting to divergent eye positions increases fusional limits in the direction of adaptation, and why vergence adaptation ultimately fails.

The goal of this chapter is to provide the background and context needed to motivate and understand those experiments. Specifically, this chapter discusses how the eyes work together in visual perception, including the topics of binocular fusion, vergence eye movements and their control, and vergence adaptation.

Vergence Eye Movements

Although we have two eyes, and therefore two retinal images, we almost always experience single vision. The process of creating one percept from two retinal images is called binocular fusion, and attaining fusion is one goal of vergence eye movements. The eyes usually align so that objects of interest fall on or near corresponding retinal locations in the two eyes. When objects do not fall on corresponding locations, retinal disparity is produced; if the disparity is large, it must be corrected by vergence in order to attain fusion and avoid diplopia.

Vergence eye movements are any disjunctive movement of the eye, defined as when the axes of the eyes move in opposing directions (Figure 1). This is in contrast with versions, or conjugate eye movements, where the eyes move in parallel (Rashbass & Westheimer, 1961). Versions are used for saccades and smooth pursuit eye movements (Gegenfurtner, 2016).

Vergence eye movements can be classified by direction of motion (e.g. Howard et al., 2000). If the eye rotates horizontally about the vertical axis, the movement is either convergence (esotropic, with the eyes moving nasally) or divergence (exotropic, with the eyes moving temporally). Convergent and divergent eye movements are used to maintain stability in fixation in the horizontal meridian. This is most clearly seen after a change in depth of fixation; if the eyes move to

an object that is closer, they will converge, and they will diverge to fixate on an object farther away. Convergent and divergent eye movement signals are also used to compensate for eso- and exophorias, underlying deviations of the eyes, noticeable when binocular viewing is prevented.

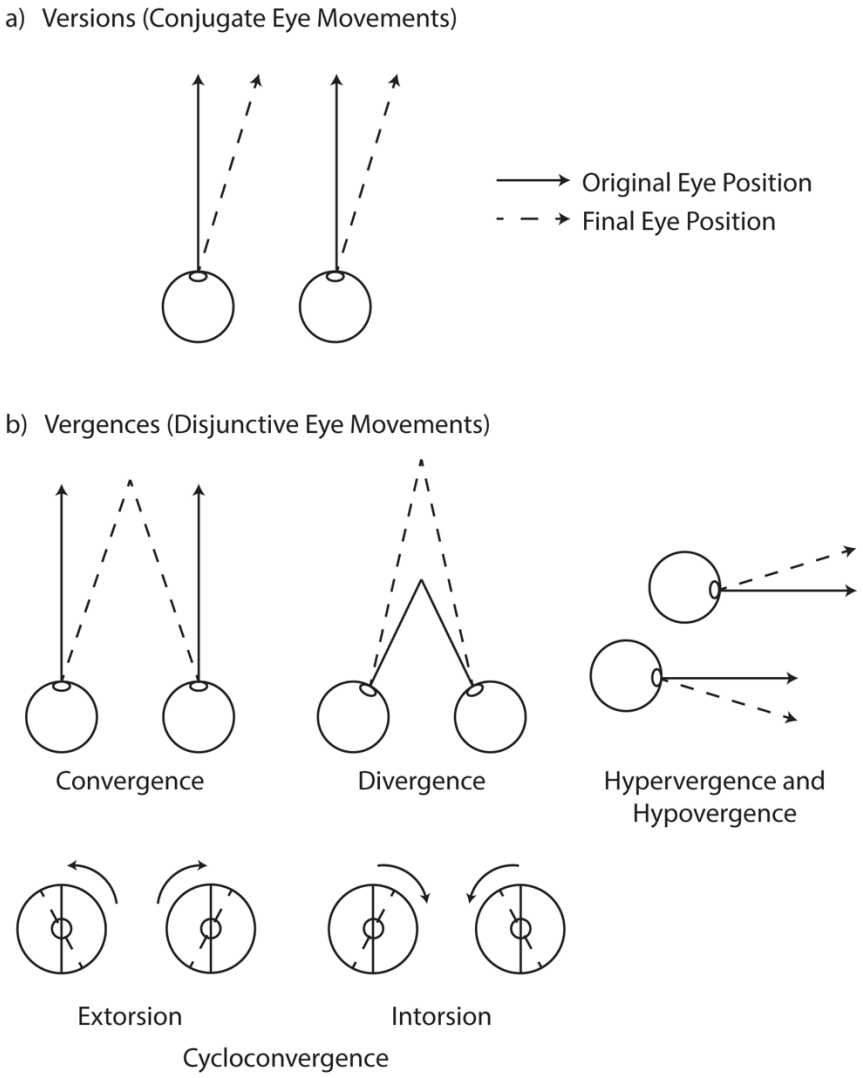

Figure 1. Types of eye movements. a) Versions, or conjugate eye movements, occur when the eyes move in the same direction. b) In vergences, the axes of the eye move in opposing directions. These movements can occur in the horizontal meridian (convergence or divergence), the vertical meridian (hypervergence or hypovergence), or rotationally about the visual axis (extorsion and intorsion).

If the eye rotates about the horizontal axis, moving vertically, the movement is either hypervergence (upward) or hypovergence (downward).

These relatively rare eye movements maintain stability of fixation in the vertical meridian (which is particularly useful when focusing on objects in the oblique gaze, Ogle & Prangen, 1953) as well as compensating for hyper- and hypo-phorias.

The last type of vergence movement is the torsional movement of the eyes. If the eye rotates about the visual axis, the movement is termed a cyclovergence (e.g. Siderov et al., 1999). All of these eye movements are performed by the extraocular muscles. A discussion of the different extraocular muscles, and their specific functions, is in Appendix A.

Retinal Disparity

Because we have two eyes laterally placed on the front of our heads, large portions of the visual field overlap. If our eyes are not pointed to the same location in space, objects will land on different portions of the retina, and this difference will, if large enough, produce double vision (diplopia). Vergence eye movements maintain alignment, and help the visual system avoid diplopia.

When an image of an object lands on different portions of the retina in the two eyes, it is called retinal disparity (Figure 2). As a person navigates the world, they must continually compensate for retinal disparities when focusing on objects of different depths. After moving their eyes to a new location, retinal disparity from a change in location and depth will initiate a vergence response to reduce the disparity and avoid diplopia.

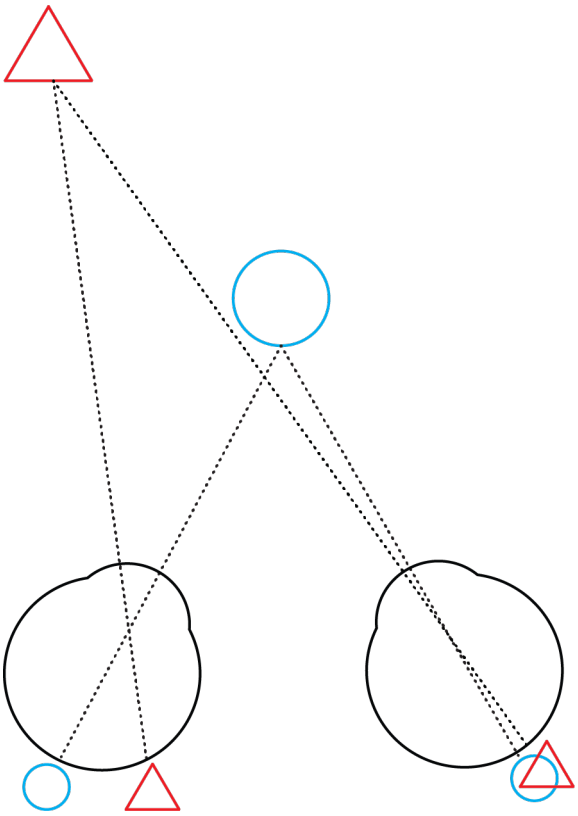

Figure 2. Retinal Disparity. Assume a person fixates on a point centrally aligned with their eyes. This fixated point will project onto the fovea. Space to the left of the object will project to the right side of the fovea, and vice versa. If the fixated object falls on the same retinal location in both eyes, the object can be fused, and the percept will be a single image, as is the case with the blue circle. If there is retinal disparity, meaning that the object does not project to the same retinal locations in both eyes, as seen with the red triangle, fusional vergences will be

employed possibly along with versions, to align the eyes so that the disparity is eliminated, if this is chosen as the new object of interest. For more reading, see Kalloniatis & Luu, 2005.

All points in space that produce no retinal disparity fall on an arc called the horopter. The horopter can be defined geometrically and empirically. The geometric horopter, also called the Vieth-Müller circle, is a line that passes through the nodal point of both eyes, and the fixation point (Howarth, 2011). Any point on the V-M circle will project to the same retinal location in both eyes, meaning that an object at any point along the circle would be seen as singular. This geometrical horopter makes several simplifying assumptions, such as assuming that the nodal point of the eye is located at the center of rotation of the eye; also, it assumes that if the two eyes were superimposed, corresponding points on the retina would be congruent (Harrold & Grove, 2015).

The horopter can also be measured empirically as the points in space that elicit singular vision (Shipley & Rawlings, 1970a,b). By this definition, the horopter increasingly deviates from the Vieth-Müller circle as eccentricity increases, resulting in a horopter which is less concave than the Vieth-Müller circle. Some studies have also found that the horopter is increasingly concave with farther fixation distances (Shipley & Rawlings, 1970b); however, this effect is eliminated if several factors are controlled; because the nodal point can shift with increasing eccentricity, it can lead to conflicting results. Hillis and Banks (2001) eliminated the effect of nodal point translation by assembling a stereoscope that would

project to the same retinal points with all fixation distances. They also controlled for vergence fixation errors, and did not present large accommodative demands. After compensating for these potential confounds, they found no evidence for an increasingly flattening horopter with decreasing viewing distance.

Not all retinal disparity will result in diplopia. Each point in the eye possesses an area or a range of points in the other eye, Panum's Fusional Area that can align with that point. It defines the tolerable amount of retinal disparity that can occur without experiencing diplopia (e.g. Mitchell, 1966, Fender & Julesz, 1967, Schor & Tyler, 1981). Panum's fusional area becomes larger moving away from the fovea, for example Mitchell (1966) found the size of Panum's Fusional Area to be 10-14 mins of arc, and Ogle (1952) found that slightly larger amounts of retinal disparity were tolerable when measuring out to 7° past the fovea.

The ability to fuse images, despite retinal disparity, is affected by factors such as size, complexity and eccentricity of the images to be fused. For example, Panum's Fusional Area can be extended by slowly increasing the retinal disparity (Fender & Julesz, 1967), as well as using a complex stimulus and a larger stimulus (Kertez, 1981), as compared to measuring fusional limits with only a fixation point. Foveal disparities are easiest to fuse, but peripheral stimuli are also able to stimulate fusional eye movements, albeit not as strongly, up to 12 degrees horizontal and 0.75 degrees vertical eccentricity (Burian, 1939); in

addition, images must be larger, if they are farther from the fovea, to stimulate fusional vergence. Interestingly, peripheral elements can induce fusional vergence even if they are too indistinct to report whether the peripheral elements are fused or not. And despite the fact that the foveal contribution is the more important cue for fusing, if peripheral elements are large enough they can also prevent or disrupt central images with no disparity (Burian, 1939).

Retinal disparity is also a cue for stereopsis, stereo depth vision. Objects that lie within the Horopter would be said to have crossed disparity, and would be seen as closer; objects that lie beyond the Horopter would be said to have uncrossed disparity and would be seen as farther (i.e. Ogle,1962). Stereoscopic depth is experienced before vision breaks into diplopia. However, interestingly, diplopic vision can still carry a stereoscopic phenomenon to it and appear to be seen in depth, up to a certain point. Ogle (1952) found that although fusion broke well below 1° of retinal disparity at all measured retinal locations, stereoscopic perception continued foveally for several more minutes of arc of retinal disparity, and at 5° past the fovea, depending on the method of measurement, stereoscopic depth perception continued when the retinal disparity was increased to the range of 1°-3°. Stereoscopic depth is supported neurally by disparity detecting neurons which have been found in V1, V2, V3 (Poggio, Gonzalez, & Krause, 1988) & MT (Maunsell & Van Essen, 1983).

One potential point of confusion could arise from the many uses of the word ‘disparity’ in this paper. Retinal disparity, as is used in Panum’s Fusional Area, is the difference between the location of an image on the two eyes’ retinas. Fixation disparity is related to how far the eyes’ directions of gaze are from fusion, with zero indicating that the eyes are fixated on the same point in the image plane, and higher numbers mean farther from fixation, as the eyes are not fixating at the same point.

In this paper, *image offset* will be used to describe the difference between two images’ locations in the virtual image plane, at the viewing distance of the images. In the current study, we increased image offset by moving the image presented to one eye outwards. This induced a retinal disparity large enough to produce diplopia, and thus caused a vergence eye movement.

We will use the term *fixation offset* to mean the difference between the pointing directions of the eyes, where zero is the initial position that produces fusion of the moving image. As image offset increases, fixation offset should as well. And if the participants perfectly track the image, and maintain fusion the entire experiment, fixation offset should be equivalent to image offset the entire experiment. Fixation offset differs from fixation disparity, where larger numbers mean the participant is not fused; in our experiments larger fixation offsets aid fusion, and for optimal fusion fixation offset and image offset are equivalent.

Appendix B discusses how these quantities and their units of measurement are calculated.

Components of Vergence Eye Movements

Mechanisms of Vergence Eye Movements

Vergence eye movements are controlled by several interacting mechanisms, or components, as identified by Maddox in 1893. Although his classifications were based on his clinical experience and not empirical observation (Morgan, 1980), his thorough description has been the basis of many following empirical studies and formal models of vergence movements.

Maddox identified four interacting mechanisms that together control vergence: the fusional, tonic, accommodative, and proximal components. The fusional component responds to retinal disparity. The tonic component is the resting muscle tonus or resting innervation that brings the axes of the eyes from the divergent anatomical position of rest to the more or less parallel physiological position of rest (Rosenfield, 1997; Schor 2011). The accommodative component is the vergence response induced by a refractive shift of the eye, when the ciliary muscles of the eye contract and change shape of the lens, due to the yoked responses of accommodation and vergence. The proximal component responds to the many non-disparity (monocular) cues that affect the perception of

nearness, for example causing the eyes to converge when an object is perceived to be near. Below, I briefly review the evidence for each of these components.

Fusional Vergence

Fusional vergence is the component that responds to, and corrects for, retinal disparity. The fusional component is activated by the detection of retinal disparity, and produces disparity reducing eye movements. It also has the ability to compensate for any over- or under-contribution of any of the other components.

Retinal disparity that drives vergence to avoid diplopia is known as the *vergence demand*. For example, if a 2 diopter (Δ) base-out prism was placed before the right eye, it would shift that eye's image laterally, producing 2Δ of disparity, and the eye would rotate inward; this means the vergence demand was 2Δ (Figure 3). The maximum vergence demand the system is able to overcome, i.e. the largest vergence movements the eyes can make, to produce fusion is known as the fusional amplitudes, or fusional limits. If a vergence demand is less than the fusional limits, the remaining fusional power is called the fusional reserves. For example, if a person with convergence limits of 25Δ is placed under a demand of 20Δ, then there is a fusional reserve of 5Δ.

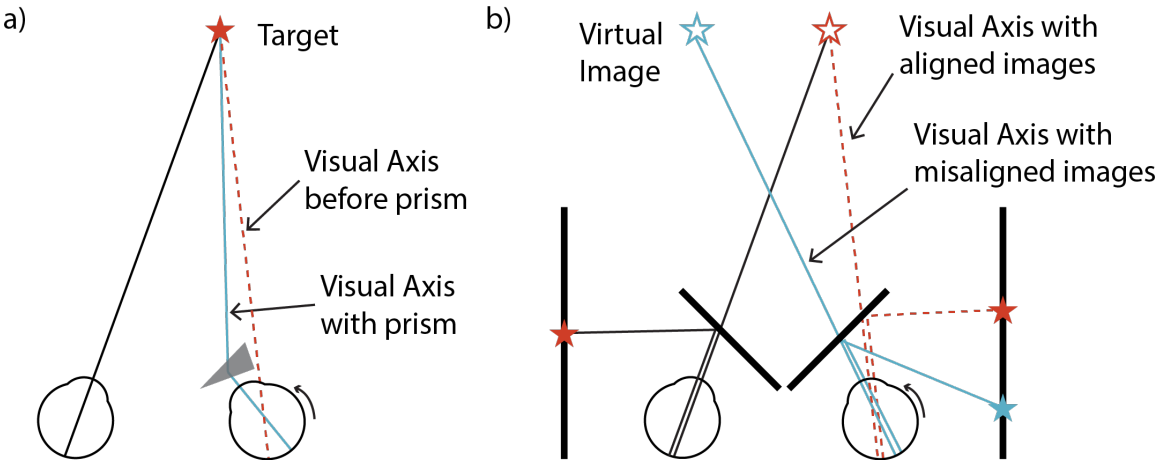

Figure 3. Vergence demand induced by a prism and a stereoscope. Vergence demand can be induced with a prism (a) or a mirror stereoscope (b). In both panels, the red dotted line shows the position of the eyes needed to fuse the images when there is no added vergence demand, and the solid blue line shows the eye position needed to fuse the images after the demand has been introduced. (Adapted from Noorden & Campos, 2002, p. 179.) Our experiments used a stereoscope as in panel b, and the distance between the red and blue virtual images is termed the image offset. More information about these quantities, and how they are calculated in Appendix B.

Fusional limits are often reported as the strength of the largest prism a person could wear while still maintaining fusion. The strength of the prism is reported in prism diopters (Δ), which is calculated as the displacement of an image in cm at a given distance, divided by that distance in meters. So if a prism displaces an image by 1 cm at a distance of 1 m, the prism has the strength of 1 Δ. And if a prism displaced an image 2 cm at the distance of 1 m, it is a 2 Δ prism. Diopters can be converted to visual angle by taking the inverse tangent of prism strength in diopters/100. The strength in diopters must divided by 100 in order to convert

the displacement to meters, because the displacement and viewing distance must be in the same unit when calculating visual angle.

Fusional limits mainly reflect fusional vergence (plus the size of Panum's fusion area in the relevant part of the visual field), and are very different for varying viewing directions and viewing distances. For example, a typical convergence limit at a distance of 6 m is 20-25Δ, whereas at a near distance of 1/3 m that limit would be 30-35Δ; the limits for divergence are much smaller- at far distance they are 5-7Δ, and 10-20Δ near (Fray, 2013).

Tonic Vergence

In the absence of innervation, the eyes would fall to a divergent anatomical position of rest (Maddox, 1893), for example under anesthesia, during deep sleep, and in death before rigor mortis sets in; this divergent position is in the range of mostly parallel to 20° divergent, depending on the individual (Rosenfield, 1997). Tonic vergence is the component that brings the eyes from the anatomical position of rest to the physiological position of rest, the position the eyes would fall to in the absence of any visual cues, which is parallel or slightly convergent, under most circumstances (Schor, 2011).

This is also known as dark vergence – the position of the eyes in a dark room without any visual cues. Dark vergence typically is measured on average, in the

range of 1 meter viewing distance, but individuals range from 40 cm to infinity (Jaschinski & Walper, 2007). And the measure is quite stable over time, over the course of hours and weeks (Fisher et al., 1988). However, if dark vergence is measured in a way that minimizes the effects of the accommodative and proximal components, then the viewing distance for dark vergence is measured closer to 3.4 meters (Rosenfield et al., 1991). And if dark vergence is measured over time, while the participant sits in a dark room for 2 hours, then the viewing distance increases from approximately 1 meter on average, out past 4 meters on average (Fisher et al., 1988).

Evidence for a tonic component, distinct from the fusional component, comes from studies that measured eye position with no external fusional cues following prolonged exposure to an artificially introduced vergence demand, for example with a prism. If the vergence demand was present for long enough the eyes will stay in position for some amount of time following the removal of the external fusion cues (e.g. disparity). This Vergence Adaptation is reviewed more thoroughly below and is interpreted as arising from ongoing activity in the tonic component.

The tonic component also can be dissociated from the fusional component by its likely source of input. The fusional component is driven by disparity and responds to changes in retinal disparity in less than 1 second (Rashbass & Westheimer,

1961). Schor (1979a) measured the decay of disparity induced vergence over 30 seconds when no fusional cues were present. The eye remained in the new position only if the vergence was induced for at least 30 seconds, well beyond the 1 second needed to correct the disparity. Therefore, unlike the fusional component, the tonic component is not directly driven by retinal disparity, as during most of the 30 seconds needed to change the resting position of the eye no disparity was present, because fusion had already corrected it.

The tonic component instead appears to be driven by the activity of the fusional component. Although there is no direct evidence for this, there is indirect evidence. For example, the tonic component is not adapted if the prism used to induce vergence has a power too great to fuse, and therefore does not induce vergence (Carter, 1965), suggesting that fusion must be present in order for the tonic component to be activated. In general, if binocular fusion is prevented, the tonic component will not adapt (Schor, 1979 b). Also, if binocular vision is prevented after adaptation, the tonic component will not decay. This has been tested out to 8 hours (Carter, 1963). Taken together, it seems that the tonic component is only altered when fusion is allowed, but does not change when fusion is prevented, suggesting that it is the activation of the fusional component that activates the tonic component. A proposed evolutionary benefit of this system is that the fusional component can reduce disparity quickly, and then the

lower energy, less effortful, and tonic component can take over, meaning less effort of the fast system is required.

Hofmann & Bielchowsky (1900) completed one of the first empirical studies on the effects of prism adaptation. They speculated that there were fast and slow components driving vergence. The fast acting mechanism would align the eyes and the slow component would maintain binocular alignment. They thought the slow component was important for comfortable binocular vision, as the fast component was very fatiguing.

Since then, many computational studies have been completed to determine the interaction of the fast fusional component, and the slow tonic component. For example, Krishnan & Stark (1977) started with an established model of conjugate (version) eye movements, and showed that two integrating elements, one with a fast time constant and one with a slow time constant, better predicted eye-tracker data of vergence eye movements, rather than a single element. Schor (1979b) used fast and slow integrators to develop a negative feedback, leaky neural integrator model, where fixation disparity is the steady state error to the system (Figure 4). The Schor model (1985) better predicts the interactions of accommodation and vergence (see below), but is most accurate only with step inputs. There is also another class of models developed by Hung and colleagues (e.g. Hung et. al., 1986), which more accurately predicts behavior to more

complex stimuli (e.g. pulse, ramp, step, step-pulse and sinusoidal), but is not as accurate at predicting the accommodative/vergence crosslinks.

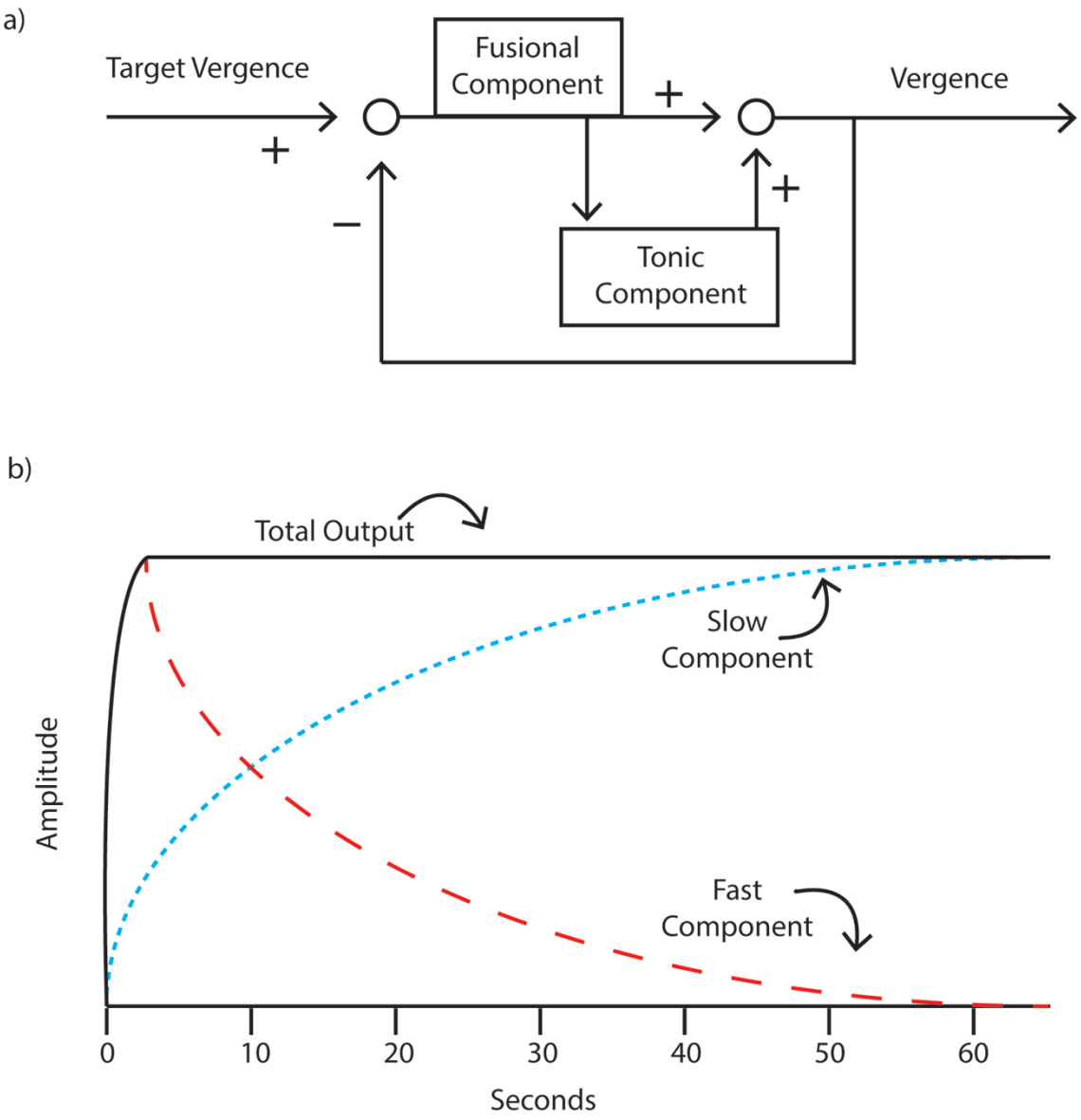

Figure 4. Schor's model of fast and slow interacting components. Fixation disparity is the steady state error to this system, which uses this negative feedback to control the fast and slow components, which are leaky neural integrators. a) A simplified graphic of Schor's model. The difference between actual vergence and target vergence (fixation disparity) is the input for the

system. The output is the sum of the fast and slow components. b) Behavior of the model, with complete adaptation, in a closed loop setting. The total output of the model is the sum of the fast and slow components. As the slow component increases its output, the fast component decreases its output.

Accommodation vergence crosslink

Accommodation occurs when the ciliary muscles of the eye contract and change the shape of the lens, thereby changing the refractive power of the eye. The stimulus for accommodation is blur on the retina (von Noorden & Campos, 2002). The range of accommodation goes from the near point of accommodation to optical infinity, the far point of accommodation, where there is effectively no accommodation (von Noorden & Campos, 2002).

Vergence and accommodation are linked, such that one will induce the other. When a change in accommodation occurs, the vergence that is induced is called accommodative vergence (e.g. Schor, 1985). Conversely, convergence accommodation is the change in accommodation that is stimulated by a change in convergence (Kersten & Legge, 1983). These effects are often quantified as the accommodative convergence/accommodation ratio (AC/A) and the convergence accommodation/convergence ratio (CA/C) (von Noorden & Campos, 2002). Measuring the AC/A ratio requires opening the convergence loop by presenting stimuli monocularly (Schor, 1985). Measuring the CA/C ratio requires opening the accommodation loop by presenting low spatial frequency images that do not stimulate accommodation, or viewing through pinhole pupils

(Schor, 1985). Drugs that reduce the accommodative response increase the AC/A ratio because there is more accommodative effort, and thus a stronger induced vergence. Miotics, which decrease pupil size, and therefore increase the depth of focus, decrease the AC/A ratio (von Noorden & Campos, 2002). Similar logic also applies to the CA/C ratio; drugs that block accommodation decrease the CA/C ratio, and drugs that enhance the accommodative response increase the CA/C ratio (Schor, 1985).

Several models of the interaction between accommodation and vergence have been proposed. For example, Maddox thought the primary interaction was accommodative convergence, driven by blur (Maddox, 1893), and Fincham and Walton proposed that the main interaction was convergence accommodation, driven by disparity (Fincham & Walton, 1957; Fincham, 1951). Others have proposed models of mutual interactions, where both blur and disparity are used for convergence accommodation and accommodative convergence. If the two models do mutually interact, AC and CA could occur in parallel, or in serial. If in parallel, the interactions could feed forward, or feedback. And if in serial, the two components could occur in either order. Schor (1985) tested all six of these models (two single interaction models and four dual interaction models) against empirical data. The model with feed forward parallel crosslinks between convergence and accommodation was found to best fit the clinical and empirical data.

Proximal Vergence

Proximal vergence is the vergence response induced from the perception of depth (nearness or farness) from various monocular depth cues. It is the least studied component, perhaps because Maddox considered it a part of the accommodative response, not a separate component (Maddox, 1893), or perhaps because unlike blur and disparity, that can be physically measured, perception of nearness is a psychological construct, making it harder to understand and model.

Proximal cues can induce accommodation (Rosenfield et al., 1990 a; Rosenfield et al., 1990 b; Rosenfield et al., 1991; North et al., 1993) and vergence (Rosenfield et al., 1991; North et al., 1993). This can be observed by measuring tonic accommodation and tonic vergence under open loop (no feedback) settings, where there are no blur or disparity cues. The change in tonic states can then be attributed to proximal cues (Rosenfield et al., 1990 a; Rosenfield et al., 1990 b; Rosenfield et al.,1991). The proximal contribution can also be demonstrated in a cue disharmony experiment where two of the three cues (blur, disparity, and perceived distance) are correct for equivalent viewing distances, but the third is artificially set to a different distance (North et al., 1993).

There is some debate on the relative contribution that proximal cues have on accommodation and vergence. They appear to have a significant contribution

(Rosenfield et al., 1990 b) from near viewing to 3m, at which point the contribution asymptotes to little or no effect (Rosenfield et al., 1991). Under the cue disharmony conditions, it seems that proximal cues are roughly equal in contribution to disparity cues, and outweigh the relative contribution of blur cues (North et al., 1993). However, when measured under closed loop settings that are most similar to natural viewing, proximal cues seem to contribute very little (Hung et al., 1996).

Vergence Adaptation

As noted above, the tonic component reflects an underlying resting position of the eyes, which is flexible and altered based on recent sensory experience, a process called vergence adaptation. Vergence adaptation can be most simply understood in the case of prism adaptation. For example, if a base-out prism is placed in front of the right eye, it will create a virtual image of the object that is leftward of the physical location of the object. If the right eye is fixated on a point that corresponded with the location of the physical object, then there will be disparity between the two eyes; the projection of the virtual image on the right eye will fall farther to the right of the retinal location of the image in the left eye, creating a vergence demand.

In order to eliminate the disparity and align the images, the right eye will rotate nasally, a disparity driven vergence movement driven by the fusional component (Figure 3a). If the prism is momentarily placed before the eye, and the eye is

covered while the other eye fixates a target, the eye will naturally resume its original position from before the prism was placed in front of the eye. This is because covering the eye removes all disparity cues for vergence, and its position is driven by the tonic component.

However, if a person views a scene through a prism for an extended period of time, their vergence system will adapt; the new position of the eye will temporarily become the ‘default’. This is apparent if the eye is again covered. If vergence adaptation has occurred while viewing through the prism, the eye will not change positions when covered.

The shift of an eye, after it has been covered, is termed *phoria* (Figure 5b). When the prism is first set in place, the phoria is equal and opposite to the strength of the prism, as the eye shifts back to its original position, driven by the tonic component (as long as the strength of the prism is not so great that it prevents fusion). Over the course of several minutes, as the tonic component adapts, the phoria slowly reduces in magnitude towards zero (Henson & North, 1980), Figure 5e.

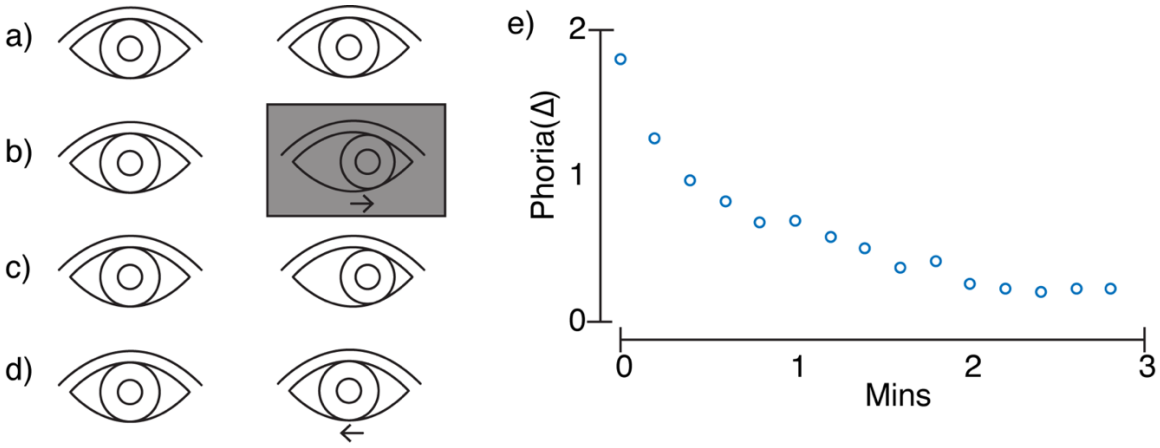

Figure 5. Typical vergence adaptation findings. a-d) Eye position during a cover-uncover test, revealing a phoria. a) With binocular fusion cues, the eyes are aligned. b) When one eye is covered, disrupting binocular vision, the eye returns to its 'baseline' position. c) At first, when the eye is uncovered, the eyes are still misaligned. d) Now that binocular vision is restored, fusional cues are used to realign the eyes. Phoria is calculated as the difference in eye position between panels a and c) Phorias decrease over time, as participants adapt to a prism-induced vergence demand. Typical vergence adaptation findings, from Henson & North, 1980. Over the course of several minutes, the size of the phoria decreases.

Vergence adaptation can also occur in normal viewing situations. For example, Owens & Wolf-Kelly (1987) found that vergence adaptation (and accommodative adaptation) occurred after participants read at a close distance. After one hour of near reading, participants had adapted to their state of convergence (and had also become temporarily more myopic). However, it is more common for vergence adaptation to be studied under conditions of artificially induced disparity. Disparity can be artificially created by the use of prisms (Figure 3a) or by a stereoscope (Figure 3b).

The classic pattern of vergence adaptation, as demonstrated with behavioral phoria measurements, was discovered by Henson and North (1980). Prior to their study, vergence adaptation was measured with fixation disparity tasks, which do not reflect the tonic component as directly (ex. Ogle & Prangen, 1953; Carter, 1965; Schor, 1979 a). Henson and North found the pattern of decreasing phoria, as described above, and demonstrated that on average, the rates of adaptation were equivalent for both directions of vertical adaptation, but that adaptation was faster and more complete for convergence as compared to divergence.

Stephens and Jones (1990), measured adaptation using phoria across increasing prism strengths, while also measuring fusional limits. They found that fusional limits and phoria increased linearly with adaptation to increasing prism strength, until the prism strength became too large. Overall, they found fusional limits of approximately 8-12Δ base-in and 25-30Δ base-out. They also calculated fusional amplitudes, the range of fusible disparities around the tonic position, by subtracting the phoria from the fusional limits. Across the image disparities at which participants adapted, fusional amplitudes remained constant, except at the extreme image disparities, suggesting that under normal viewing conditions there is a fairly constant fusional amplitude.

Vergence adaptation was also studied by Neveu et al. (2010), who examined the effect vergence adaptation had on the entire binocular system, by inducing a conflict between vergence and accommodative demands. They increased convergence with a telestereoscope (a device that changes vergence demands without changing accommodative demands), and found that vergence limits and phorias shifted towards convergence after adapting, showing that their telestereoscope did induce vergence adaptation. They adapted both eyes with more convergence (relative to the viewing distance and accommodative cues) and the divergence limits also shifted towards convergence. They also measured the effect on stereoscopic thresholds, and accommodation, both of which were affected by the adaptation, showing that the whole system is affected by a change in one binocular component.

Temporal Aspects of Vergence Adaptation

The rate of adaptation can be measured as the rate of change of phorias over the adaptation duration. An exponential function can be fit to the phoria curves, to quantify this rate (ex. Sethi & Henson, 1985; Sethi & Henson, 1984; Sethi & North, 1987). There is some evidence that adaptation might be faster with decreasing prism disparity, and larger fusional reserves (e.g. adapting to base-out prism was faster than base-in or vertical prism adaptation; Sethi & North, 1987). However, this is an area of sparse research with only one paper, using just a few participants.

The decay of adaptation is another temporal aspect of vergence adaptation, and is affected by the preceding adaptation duration. For example, after adapting for 5 seconds to 8.8 degrees adduction (base-out/convergence), the relaxation of phoria to the initial position happens over the course of 10-15 seconds (Ludvigh et al., 1964). But if the duration of adaptation is 40 seconds, then the decay of adaptation may not be complete even after 30 seconds (Schor, 1979 b).

The decay of adaptation is aided and significantly speeded by binocular vision. Ogle and Prangen (1953) found that after adapting to a total of 6Δ of prismatic deviation in the vertical Meridian in 2Δ steps for 45-115 minutes, participants experienced approximately 15 minutes of diplopia. Once participants regained the ability to fuse, adaptation decayed over the course of 12-20 minutes, as measured with a fixation disparity task. However, if binocular vision was prevented, the vergence system did not decay back to the baseline even after 2.5 hours. They also speculated that the decay they did see was due to their testing methods (which allowed for brief moments of binocular vision), and without testing the decay could have been even slower. Others have speculated that the decay of adaptation without fusion could happen over 8 hours or more (Carter, 1963).

Most studies of vergence adaptation have looked at the effects of adapting for seconds, minutes or hours. However, Sethi & Henson (1984) adapted participants to 2Δ base-out prisms, inducing convergence, for 1 to 3 days, and were occasionally tested with a further 2Δ, for a total of 4Δ. Behavioral measures were used to observe the decline of the phoria while participants adapted. For most participants, over time the rate of adapting to the further 2Δ prism increased, meaning that when they adapted, they adapted faster. With two participants, the rate of adapting to the further 2Δ increased back to the rate of adapting to the initial 2Δ. The rate of adaptation was unchanged for one participant, and for two participants the rate increased with the further 2Δ, but never increased back to the initial rate. This demonstrates that although phorias alone are often used as to determine when adaptation is complete, they may be insufficient to determine if a person is fully adapted; it may be necessary to also measure the rate of adaptation to determine when adaptation has completed.

Chapter 2

Introduction

What determines our range of possible eye movements? Here we investigate divergence in normal observers as a model system for understanding what limits the range of the vergence system. As reviewed in Chapter 1, vergence eye movements are controlled by multiple interacting components, including a fusional component that responds to retinal disparity, and a slow tonic component, which can be thought of as the baseline eye position, and responds to the activation of the fusional component (Maddox, 1893). The tonic component can be adapted. This adaptation is quantified by measuring the phoria, which is the difference in eye position between binocular viewing conditions vs. monocular viewing conditions. Monocular conditions should reflect the tonic component without the contributions of the fusional component, because there are no disparity cues.

The experiments in this chapter were designed to explore how the tonic component contributes to fusional limits (the range of image offsets that can be overcome by vergence eye movements, and fused). Many studies have demonstrated how adapting to vergence demands (retinal disparity that drives the fusional component) results in an increase in fusional limits in the direction of adaptation (e.g. Ogle & Prangen, 1953; Henson & North, 1980; Sethi & North,

1983; Sethi & Henson, 1984; Sethi & North, 1987; Stephens & Jones, 1990; Neveu et al., 2010). For example, Ogle and Prangen (1953), and Henson and North (1980) both demonstrated that adapting to increasing vergence demand can increase the range of fusional limit in the direction of adaptation, and Stephens and Jones (1990), and Neveu et al. (2010), demonstrated how the range of the fusional amplitudes (the range of achievable eye positions at a certain adaptive state) is independent of different adaptive states, suggesting there is a constant fusional amplitude around the tonic state when adapting to increasing vergence demand.

It remains unknown, however, how far this component can be adapted. This question is important because if adaptation can extend fusional limits by large amounts, then it could possibly be used to aid patients with disordered eye movements, such as convergence insufficiency or strabismus.

Furthermore, if there is a point beyond which adaptation can no longer increase fusional limits then an important unanswered issue would be its cause: It may be, for example, that adaptation ultimately stops improving fusional limits because the amount and/or rate of adaptation decreased in some way with increasing vergence demand. Suggestively, Sethi & Henson (1984) conducted a study with successively increasing vergence demand and found that the rate of adaptation following a second 2Δ step of demand was at a slower rate, at least initially.

In the present experiment, we gradually shifted the image seen by one eye, increasing demands for divergence, while giving participants time to adapt to the demands. We hypothesized that eventually, participants would nevertheless reach a fusional limit; their eyes would fail to diverge adequately, leading stereo fusion to fail and diplopia to ensue. We hypothesized that this would occur when the tonic component could no longer adapt to the increasing vergence demands.

To explore the potential reasons for this failure to adapt, we measured the rate and amplitude of adaptation, using both eye-tracking and behavioral measures of phoria and fixation offset. If either the rate or amplitude of adaptation decreased with increasing vergence demand, then there would be evidence that the ultimate fusional limits were determined by the inability of the tonic component to adapt. Understanding the interaction of the tonic component and fusional limits could aid in the development of future therapies for patients with abnormal binocular vision.

Methods

Common Methods to All Experiments

Participants

Experiments 1, 2 and 3 enrolled 8, 10, and 8 participants respectively. Some participants participated in more than one of the experiments. The University of Minnesota Institutional Review Board approved the experimental procedures.

Participants reported that they did not have a history of visual disorders, had normal or corrected to normal vision, and were screened to confirm they were not stereoblind, and were instructed that, during the experiment they may experience eye discomfort, but to stop immediately if they experienced any pain. Although most participants reported that their eyes felt “weird” during the experiment, none reported any pain, and all completed the experiment.

Equipment

Eye-position was measured using an Eyelink 1000 Eye-tracker (Ottawa, Ontario, Canada) with a sampling rate of 500 Hz. Calibration used the built in Eyelink 9-point calibration, and the cognitive pre-set thresholds to determine start and end points of saccades, and the data from those saccades were filtered out. Because we were only interested in stable eye positions, and not small eye movements, data were averaged into 1 second bins. Any session where 35% of the eyetracker data or more was missing, likely due to a poor calibration or the participant moving their head, was excluded from analyses. When possible, another session was completed to replace the excluded session.

Images were presented on a modified Wheatstone stereoscope (Figure 6), with two mirrors for viewing two identical monitors placed on the outside facing inwards. The mirrors were “cold” mirrors, invisible to the infrared eye-trackers, yet reflecting the image from the monitors for participant viewing.

To calibrate the stereoscope, the virtual image from each mirror was aligned in one plane so that the fusional, accommodative and proximal cues were all in agreement. A black point was drawn on the white wall, 75 cm from the participant's eyes. Because the cold mirrors allow as much as 5% of visible light to pass through, if the monitors are presenting a black screen, then a high contrast point on the wall behind the mirrors can be dimly seen when the room is dark. A white point was drawn at the center of each monitor, and the mirrors were rotated until the white points were superimposed on the black point; by doing this, the mirrors were adjusted as though participants were looking at a virtual point 75 cm ahead, with a vergence angle of 2.5° (assuming an inter-pupillary distance of 6.5 cm). This was done monocularly for each eye to prevent fusion from driving the points to appear improperly aligned.

During the experiment, the room was dimly lit, because if the room was fully darkened the LEDs from the eye-tracker were highly visible through the mirrors, and could have provided a potentially fusible target when no fusion cues were presented on the screen. If the room were brighter, the peripheral content beyond the mirrors might also have provided a fusional cue.

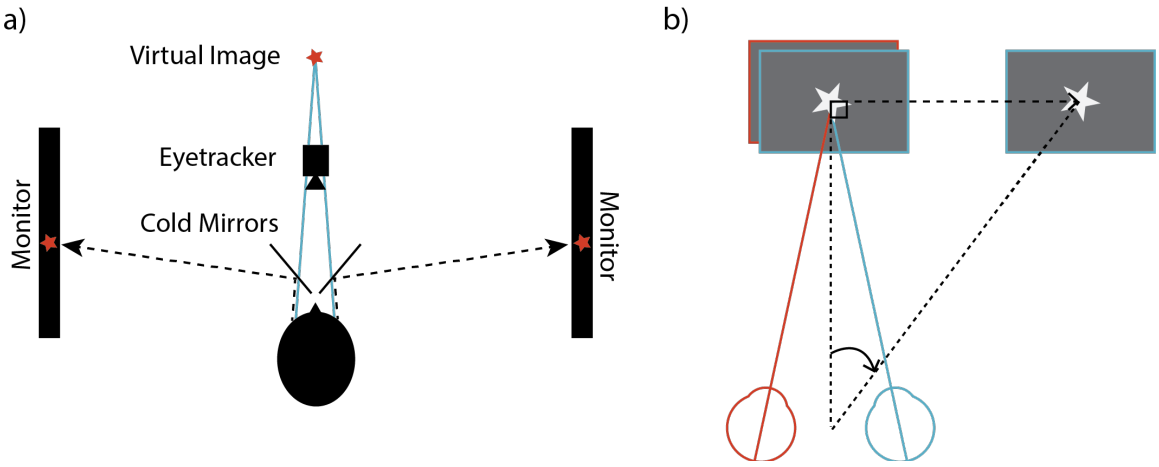

Figure 6. The experimental setup. a) A dual-monitor stereoscope, with cold mirrors allowing the infrared eye-tracker to track the eyes through the mirrors. b) *Image offset* was calculated as the angle subtended by the distance between the original image location, and the offset image location, at the viewing distance. *Fixation offset* was calculated as the angle subtended by the distance between the two eyes' fixation locations in the virtual image plane, at the viewing distance. In the case of image b, angle a is both the fixation offset and image offset. If participants were perfectly fusing the images throughout the experiment, then fixation offset would be identical to image offset. They are calculated the same way that visual angle is calculated. See Appendix B for more information on how these measurements are calculated.

The Image and Its Locations

Participants viewed a grayscale image of a complex urban scene (Figure 7), 7.3 degrees large, presented binocularly at a viewing distance of 75 cm, the distance to the virtual image. Over time, the image presented to one eye shifted outward, with different time courses in different experiments. (Figure 9). For example, in Experiment 1, an initial 4 degree shift was followed by a 5 minute period of constant image offset, followed by additional 1 degree shifts every 5 minutes. All experiments contained periods of stable image offset followed by shifts, termed "blocks", but the image offset step size of the blocks was different in different experiments.

The shifts increased the distance between the images in the virtual image plane, which we call the image offset (Figure 6). Image Offset was measured in degrees, as the angle subtended by the distance between the centers of the images, at the viewing distance. See appendix B for a more complete description of the calculations. Image offset is then the vergence demand that the system must overcome to achieve fusion.

Figure 7. The black and white urban image that was used for all the experiments.

Fixation Offset and Phoria: Eye-tracker

Fixation offset from the eye-tracker data was calculated as the distance between the two eyes' fixation locations in the virtual (fused) image plane. This was calculated as the angle subtended by the distance between left and right eye fixation locations in the virtual image plane, at the viewing distance (Figure 6b). This distance between the eyes was calculated using the x-axis position of each

eye from the eye-tracker data; the right eye distance was subtracted from the left eye distance, meaning negative numbers reflect crossed disparity. Calculating it this way also allows fixation offset measurements to be directly compared to image offset, which uses the distance between the center of the two images; that is if image offset increases, and the eye makes a vergence eye movement to maintain fusion, then fixation offset will increase by an identical amount.

Phoria, the shift in eye position when fusional cues are present vs. when they are restricted (i.e. binocular vs monocular viewing), was calculated as the fixation offset in a monocular condition, minus the fixation offset during binocular viewing (Figure 8a, e.g.). This difference reflects how far the eye drifted back towards baseline, when fusional cues were absent, a measure of the state of adaptation to the vergence demands, i.e. image offset, at that moment. The different experiments used different protocols to measure this, as noted below. For example, in Experiment 1, between image shifts, the stimulus presentation was divided up into 30 second segments, 25 seconds of which was binocular viewing, followed by 5 seconds of monocular stimulus presentation (i.e. the image was blanked out in the adapting eye).

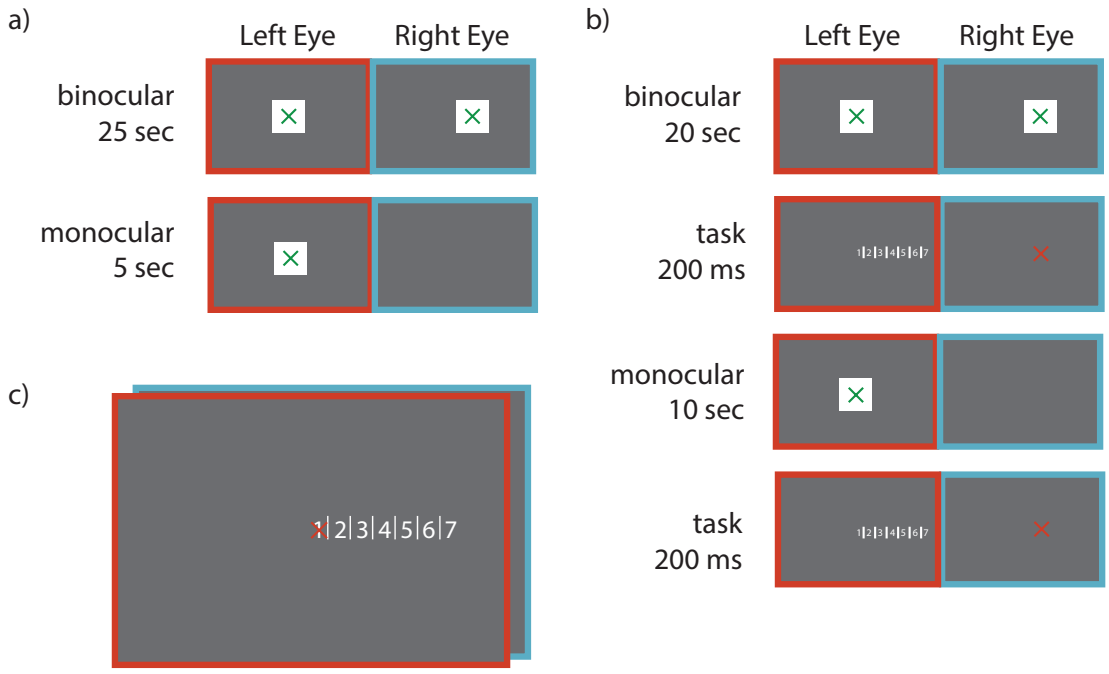

Figure 8. Phoria and fusion tasks in Experiments 1-3. a) In Experiment 1, 25 seconds of binocular image presentation alternated with 5 seconds of monocular presentation. b) Behavioral task and monocular and binocular block timings used in Experiment 2 and 3. A fixation point was presented to one eye, and a numerical spatial scale to the other. Following binocular viewing, the task yields a measure of fixation offset. Whereas, following monocular viewing, the same task provides a behavioral phoria measurement. c) The participant's percept of the task from experiments 2 and 3. The images to the two eyes have been superimposed to depict the perceived image; the red target 'X' appeared somewhere along the numbers, and participants reported that number the target appeared closest to. The number 1 and the red fixation cross are located at the center of each eye's image; if perfect fusion is maintained during the task the two will perceptually align. Note that the image is not to scale, as the numbers took up a much smaller portion of the screen, and a large portion of the screen was reported as "anywhere beyond 7." Also note that during the fixation offset version of the task in Experiment 3, the top and bottom edge of the Figure 7 image were presented in both eyes, above and below the numbers and the target, to aid in fusion.

Fixation Offset and Phoria: Behavioral Task

In Experiments 2 and 3, the eye-tracker measurements of fixation offset and phoria were corroborated with a behavioral fixation offset task (Figure 8c). The Fixation Offset task, a modified “Thorington Test”, was used as a behavioral measurement for both a fusion check, a measurement to determine if participants are fusing or not, and as a phoria measurement. During the task a ‘ruler’ with numbers 1-7 was displayed in white, spaced apart by 0.5 degrees, with vertical white lines 1 degree tall spaced evenly between the numbers. The numbers were presented on the non-adapting eye’s display with the ‘1’ located at the center of the display. This ruler remained in the same location when presented throughout the experiment.

A target, a red ‘X’ with a height of 1/6 of a degree, was presented to the adapting eye, at the center of that eye’s image given that moment’s image offset, meaning the location of the target shifted equally with the image offset. Participants reported where along the ruler they saw the target. If participants were able to keep the image fused throughout the experiment, there would be no change in the perceived location of the target along the ruler – a response of ‘1.’ Following the binocular viewing period, when participants were fusing the two images, the perceived location provided a measure of fixation offset.

Participants were instructed that they could move their gaze around the image, but not beyond the image. And tone preceded the task by one second, and participants were instructed to fixate on the fixation point when they heard the tone; this way their eyes would be appropriately positioned for the task.

Following a monocular viewing period when phoria was generated, this same task measured the size of the phoria. In more detail, if participants were rotating their eye perfectly along with the shifting image, and if their eye did not rotate back when the image was removed from one eye, then their response would be a constant '1' throughout the experiment. Normally, however, during monocular viewing, the eye rotated some amount backwards relative to its position during binocular viewing, and the response indicated how far that eye had rotated – the size of the phoria. Because of the limited retinal size of the response scale, there was a ceiling effect past 2.5 degrees in the adapting direction (i.e. beyond a response of '7'), and past 0.5 degrees in the opposite direction (i.e. less than 1).

Fusional Limits Measurement

Fusional limits, the maximum vergence demand the eyes can overcome and perceptually fuse, were measured in Experiments 1 and 3 following adaptation, which we term "divergence adapted limits" and preceding it, which we term "unadapted limits". This was done to determine the effect adaptation could have on the limits, and if limits could be increased through adaptation.

To measure the unadapted fusional limits, we used a separate procedure, in which the image was shifted smoothly outward to a maximum of 12 degrees in Experiment 1 and 15 degrees in Experiment 3. This motion triggered a divergent eye movement to keep the images aligned, up to the point of the participant's limit, at which point the eye stopped moving outwards, and began to drift back towards the original eye position. In Experiment 1, this procedure was repeated 3 times at the end of the experiment, and the maximum fixation offset of the eyes was calculated from the eye-tracker data. In Experiment 3, the task was nearly identical, except that it was calculated in a separate measurement before adaptation, and the image motion alternated between the rightward and leftward, 3 times in both directions. Altering the direction prevented adaptation buildup. The maximum fixation offset was used as the limit.

Divergence adapted fusional limits were calculated in Experiments 1-3 as the maximum fixation offset achieved during the main experimental procedure, also calculated from the eye-tracker data.

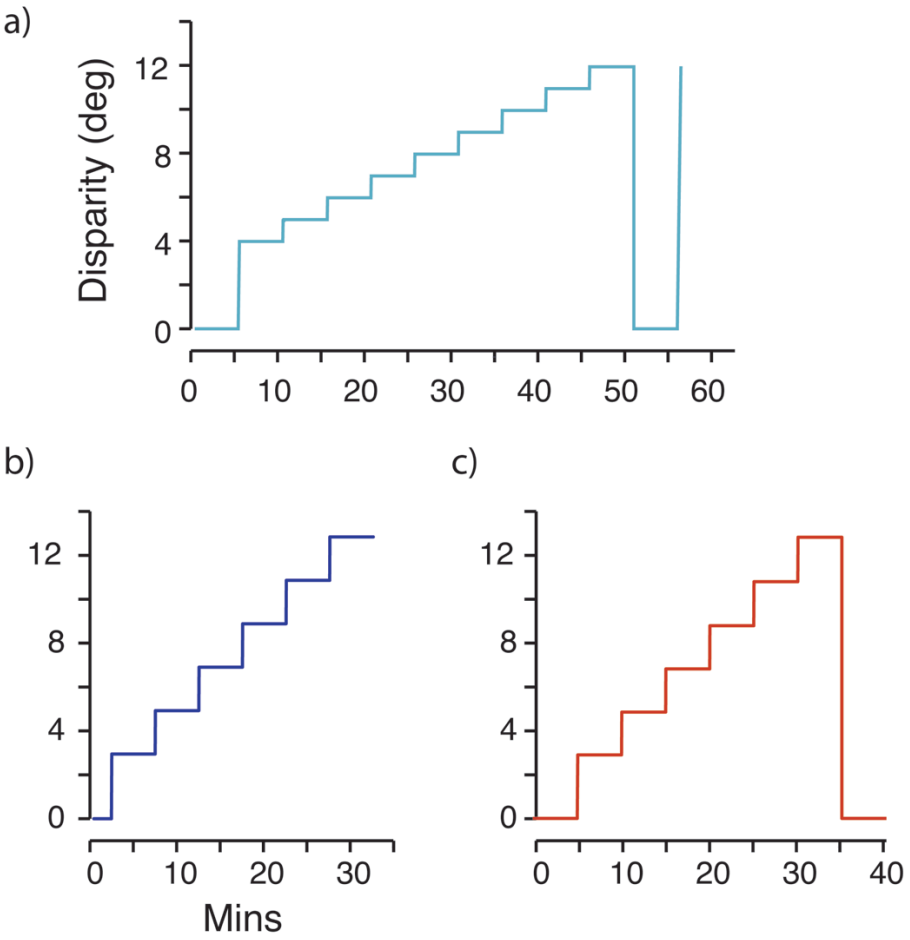

Figure 9. The image offset time-courses of the three experiments. Experiment 1 (a) started with a 5-minute baseline offset image presentation, and ended with another 5-minute baseline block followed by the unadapted fusional limit measurement. An initial 4 degree shift in image offset was followed by 1 degree steps every 5 min. Experiment 2 (b) included a 2-minute baseline at the beginning. An initial 3 degree step was followed by 2 degree steps. Experiment 3 (c) included a 5-minute baseline at the beginning and the end, and the unadapted fusional limit measurement in a separate earlier measurement.

Methods Specific to Experiment 1

Participants initially viewed the image for 5 minutes, starting at "zero image offset" where the image offset was consistent with the virtual viewing distance (Figure 9a). The image in the adapting eye then moved towards the visual periphery at a rate of 0.5 degrees/second to 4 degrees, where it remained for 5

minutes (to allow time for adaptation). At the end of 5 minutes, the image moved a further 1 degree, at the same speed, at which time it paused again for 5 minutes.

The 1 degree shifts every 5 minutes repeated until participants were unable to fuse the image for more than 75% of a 5 minute block, or to a maximum of 12 degrees. However, blocks were excluded from further analyses if it could be determined from the eye-tracker results that participants were not fused during the block. This avoided a confound of incomplete fusion; the divergence adapted fusional limit was taken as the maximum fixation offset of this last fused block in this and all experiments.

After the last 5 minute block with an image shift, the image returned to zero offset for 5 minutes to ‘readapt’ participants to zero offset, or alternatively to ‘deadapt’ from the divergence eye position. Next, to measure the unadapted fusional limit, the image moved at the same rate of 0.5 degrees/second without pause, out to 12 degrees of offset, and the maximum fixation offset before diplopia, measured using the eye-tracker data, was taken as the unadapted fusional limit (Figure 9a).

Critically, to measure the time course of adaptation throughout both phases of the experiment, the stimulus presentation during a block was divided up into 30 second segments, 25 seconds of which was binocular viewing, followed by 5

seconds of monocular stimulus presentation (i.e. the image was blanked out in the adapting eye, while staying constant in the other eye). The monocular presentation allowed measurement of phoria, the change in position of the adapted eye when binocular cues were absent (Figure 8a).

Experiment 2

Experiment 2 was a modified version of Experiment 1, with changes intended to allow us to better measure the time course of adaptation. To this end, the binocular presentation duration was decreased to 20 seconds, and the monocular periods was increased to 10 seconds (Figure 8b). In addition, in order to aid in phoria measurements, larger step sizes were used with the hope of generating larger and more detectable eye movements.

We also added the perceptual “ruler” measure of relative eye position to calculate fixation offset and phoria behaviorally (described in Common Methods, Figure 8 b-c). The 5 participants of Experiment 2a viewed a temporally moving image that caused one eye to diverge, while the 5 participants in experiment 2b viewed a nasally moving image, which induced convergence.

In Experiment 2, participants viewed “zero offset” for 2 minutes, before the image moved at a rate of 1 degree/second to 3 degrees, where the image remained for 5 minutes (Figure 9b). At that time the image moved another 2 degrees and paused for 5 minutes again. This repeated until participants did not fuse the

image for more than the last 2.5 minutes of a block, as determined by the behavioral fixation offset task (described above), at which point the experiment ended.

One participant was not included in the analyses for experiment 2.b because their behavioral data showed they never consistently achieved fusion in the experiment. They met the relatively lax “fusion threshold” to continue out to the last possible block, but analysis showed that their responses were inconsistent. It could be that they were simply poor at the task, but because it is also possible they had very unstable fusion throughout, they were excluded.

Experiment 3

A third experiment was completed with minor methodological modifications from Experiment 2: a) a “fusion lock” was added to the behavioral task during fixation offset measurements (the top and bottom 1/6 of the image, which was 1.2 degrees tall, remained on screen in both eyes, flanking the task) which provided fusion cues to assure that this was a true fixation offset task, and b) black poster board was placed around the monitors, with mismatching corrugated edges surrounding the screen in order to further prevent peripheral cues from affecting fusion during phoria measurements. Of the 8 enrolled participants, 6 completed the full experiment due to participant attrition.

Participants completed two identical sessions. First unadapted fusional limits were measured. Participants viewed 5 minutes of zero image offset, and then the image moved out in 0.5 degree jumps, every half second, to 15 degrees image offset. This was measured three times with the image shift in each eye, for a total of six measurements, alternating between left and right eyes to prevent adaptation buildup. Participants pressed a button to indicate that their fusion broke.

Participants next completed the main adaptation phase, which also began with 5 minutes of zero offset. Next, the image moved in 0.5 degree jumps every 0.5 seconds, out to 3 degrees of offset. The image remained in this location for 5 minutes, before moving at the same rate out a further 2 degrees, and pausing again for 5 minutes. This continued until participants could not fuse the image for more than the last 2 minutes of a block, as measured by a fixation offset task. At this point the image went back to zero offset again for 5 minutes (Figure 9c).

Results

Experiment 1

Results from Experiment 1 provided evidence that adaptation can increase fusional limits, up to a limit. The phoria data, however, were too noisy to determine much about the time course of the adaptation, or how thoroughly participants were able to adapt.

As expected, fixation offset tracked image offset throughout the experiment (Figure 10), meaning that participants made vergence eye movements following the moving image to maintain fusion. However, participants eventually lost fusion and experienced diplopia, following a range of 3-9 blocks (6-12 degrees), for an average of ~6 blocks (9 degrees).

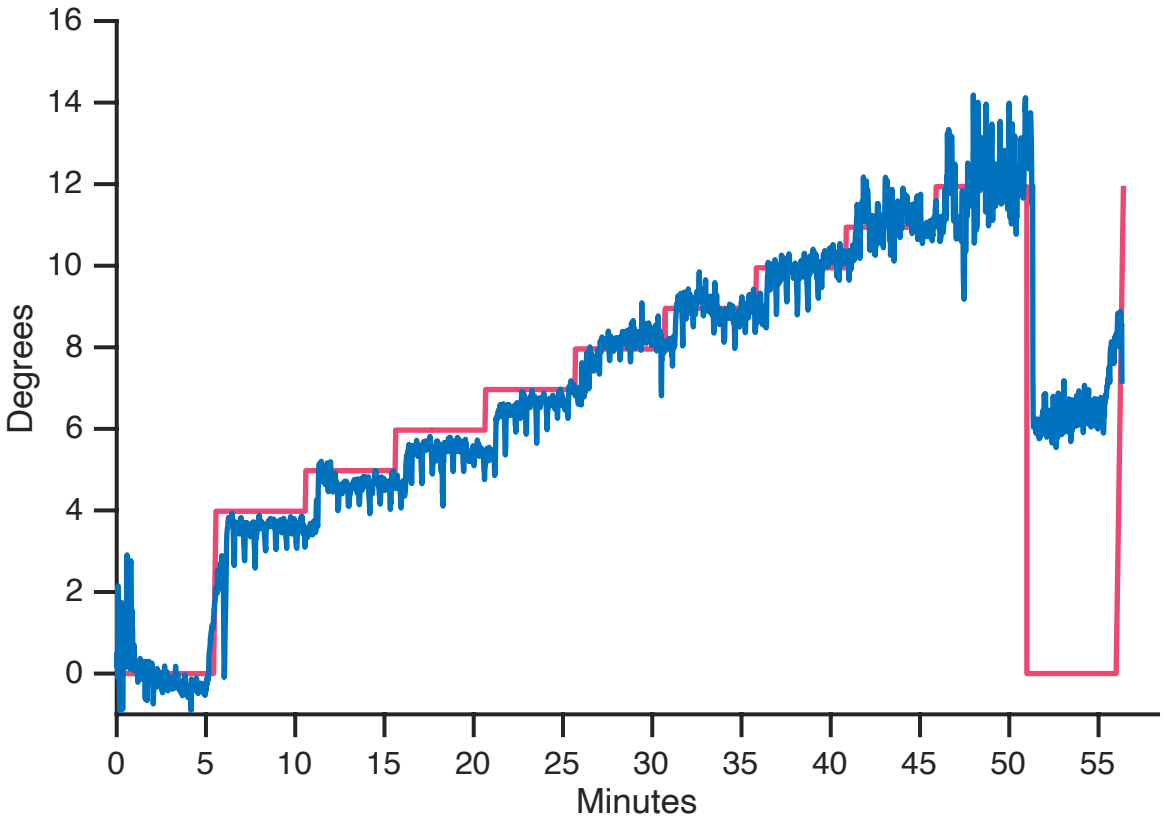

Figure 10. Experiment 1 grand average eye-tracker results. Average fixation offset across participants (blue), along with image offset (red). The small downward spikes are phorias that occurred during monocular image presentation. Fixation offset tracks image offset until the deadaptation block at the end of the experiment, where participants were not able to achieve the original fixation offset, because they had adapted to increasing image offset. The rapid increase in image offset at the end of the experiment was intended to measure “unadapted” fusional limits.

In Figure 10, the red curve plots image offset, and the blue curve plots fixation offset averaged across participants. If a participant was not fused, the block was not included in the average, or the further analysis. Because participants lost fusion at different image offset levels, in this and similar plots, different numbers of participants were averaged for different blocks. All participants are included in the baseline, as well as the first 3 blocks, and the last block. In the last block, image offset returned to zero, and the average fixation offset reflects the fact that participants had been adapted to the high image offset, so they were not able to fully fuse zero offset at that point. You can also see in this figure, as well as others throughout the paper, that the fixation offset is sometimes shifted or misaligned from the phoria offset; this is either related to the calibration of the eyetracker, or the calibration of the stereoscope, and was relatively consistent throughout an individual session.

Fusional Limits

The last increase seen in the fixation offset is the unadapted fusional limit measurement at the very end of the experiment. Because the 5-minute deadaptation time did not fully deadapt participants, the “unadapted” fusional limit measurement at the end of the experiment most likely reflects some remaining degree of divergence adaptation. Nevertheless unadapted fusional limits were calculated as the maximum fixation offset during this measurement. This was the

maximum distance between the eye's fixation locations, in the virtual plane of the image, calculated in degrees, and was 7.09 degrees.

Divergence adapted fusional limits were measured as the maximum fixation offset during the last fused block, calculated in the same manner, and was 8.88 degrees. Divergence adapted fusional limits were on average 1.79 degrees greater than unadapted limits, and this difference was highly significant in a one-way t-test against zero (S.E. = 0.40, $p < 0.005$). Figure 11 shows a comparison between the two fusional limits.

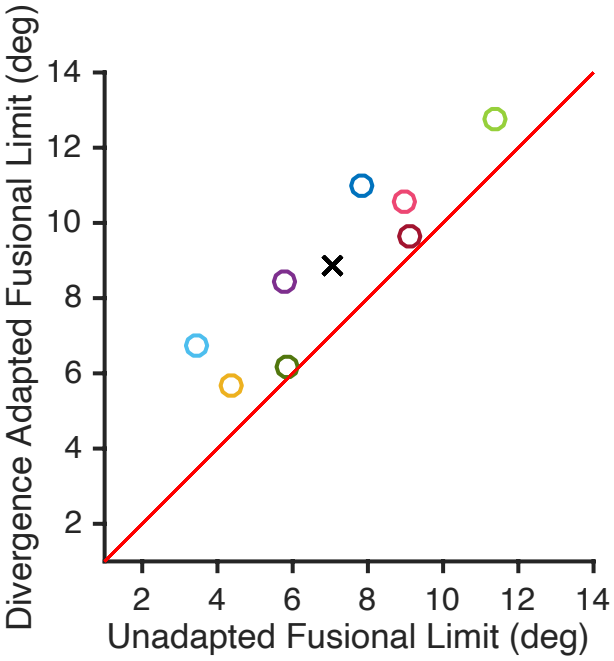

Figure 11. Experiment 1 fusional limits measurements. Each circle represents one participant, and the "x" is the participant average. The red line is unity, and represents no change in fusional limits with adaptation.

Phorias and the Time Course of Adaptation

In Figure 10, phorias are visible as the downward spikes in the blue plot towards zero, and show how far back the adapting eye drifted when its image was removed. However, these spikes only weakly show the typical pattern of decrease over time, indicative of adaptation, and were not large in absolute terms.

Phorias were quantified as the difference of the mean distance between the eye's fixations in degrees, from the last 5 seconds of monocular measurement, and the mean distance between the eye's fixations in degrees, from the preceding 10 seconds of binocular measurement. Figure 12 shows the average of each participant's phorias from the first block they completed (in blue) and the phorias from their last fused block (in red). The general downward trend is indicative of vergence adaptation- phorias decrease over time, indicating that the tonic vergence component is adapting to the current eye position (e.g. Henson and North, 1980). The decrease was smaller and noisier, however, than seen in previous work.

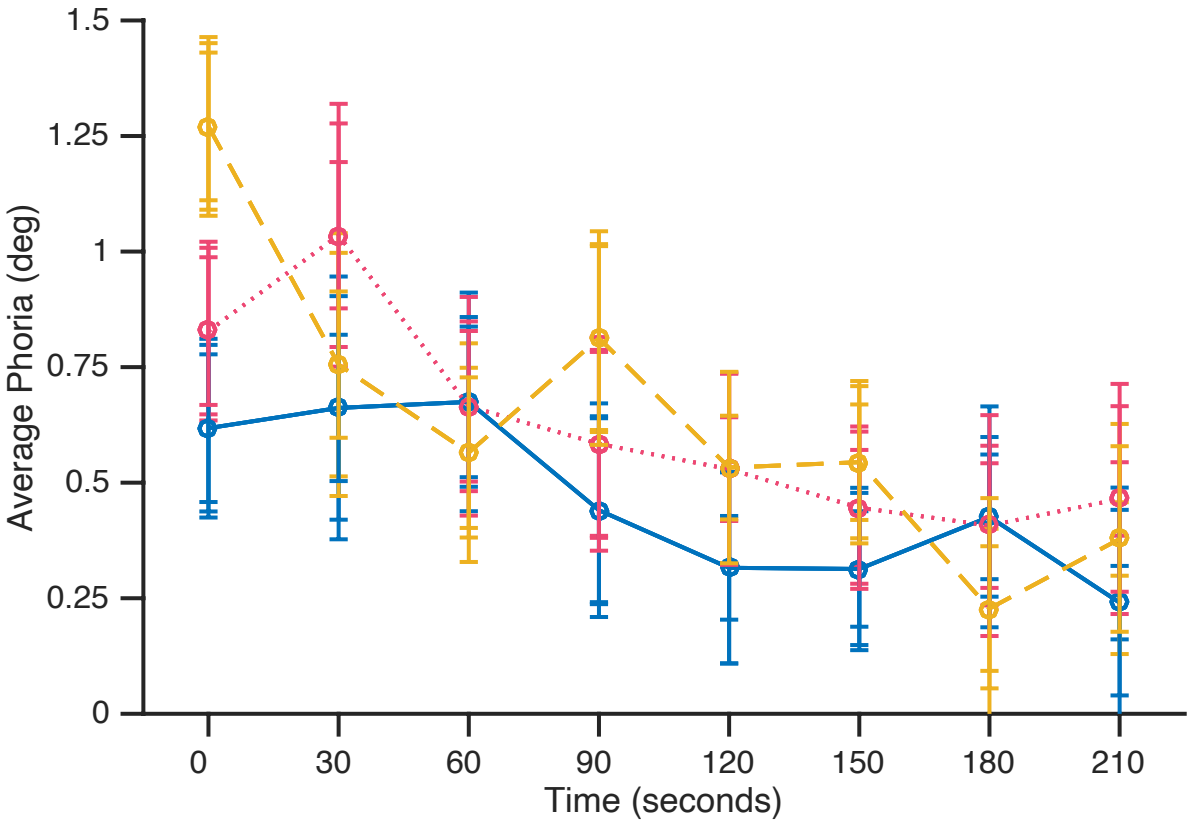

Figure 12. Experiment 1 phoria time course from first and last blocks. Phorias from the first block (blue, solid) averaged across participants versus the last block (red, dotted), as well as the second to last block (yellow, dashed) averaged across participants. Error bars are SEM.

We were particularly interested in whether adaptation decreased over successive blocks throughout the experiment, as we hypothesized lack of adaptation could be the cause of divergence limits. Because participants completed different numbers of blocks, with one participant only completing 2 blocks, analyses were done comparing the state of adaptation from the first and last blocks completed.

We first computed the mean phoria for these blocks by averaging all the phorias within each block. Phorias in the last blocks appeared to be larger than in the first

blocks, suggesting adaptation was more “complete” or “successful” earlier in the experiment. However, this difference was not statistically significant ($p > 0.05$), Figure 13 top.

The first phoria from the first block was also compared with the first phoria of the last block, to determine whether phorias started the block higher in later blocks, as compared to earlier blocks. The difference between the two blocks was also not significant ($p > 0.05$).

Finally, to compare rates of adaptation across blocks, a line of best fit was calculated for the phorias in the first and last blocks, and the slopes of those lines were compared. A smaller slope would mean that adaptation was slower. In Figure 13, bottom, the slope of the phoria change in the first block is plotted against the slope of the phoria change in the last block. Again, there was no difference between these two blocks ($p > 0.05$). Thus, we found no evidence for decreases in adaptation as participants approached their divergence limit.

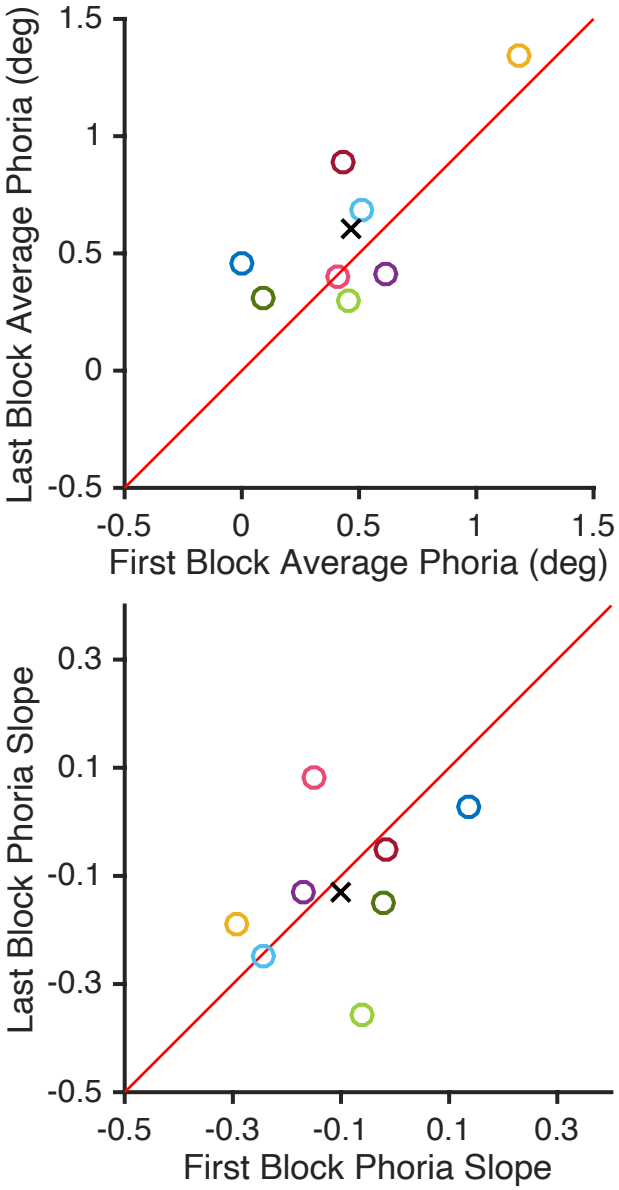

Figure 13. Experiment 1 average phoria and phoria slopes. The top graph shows each participant's average phoria from their first block versus their last block in degrees. The bottom graph shows the slope of a linear fit to the phorias from a participant's first block versus last block in degrees/minute. The red line is unity, and participant colors are corresponding between graphs.

Experiment 1 Discussion

Adapting to divergent eye positions shifted fusional limits in the same direction, allowing participants to diverge by a greater amount than without adaptation (by an average of 1.79 degrees). We found this result despite the fact that the "unadapted" limits were measured at the end of the experiment, when participants likely still were divergence adapted to a degree, meaning the difference could be larger in actuality.

Importantly, participants were unable to adapt without limit to the increasing image offsets. Most experienced diplopia before the end of the hour-long experiment, after an average of 30 minutes, comprised of 6 blocks. To explore the reason for this failure to adapt, we examined the time courses of adaptation in successive blocks. However, our measure of adaptation, plotting phoria amplitude vs time within a block, showed weaker decreases over time than the classic Henson and North (1980) phoria curves. We speculated that this pattern arose because we had a 25 second binocular duration, and only a 5 second monocular duration. If adaptation was mainly complete by the end of the first 25 second period in a block, then we would expect only to see a small phoria that did not change during the rest of the 5 minute block. Also, our image offset step sizes were not as large as those used by Henson and North, allowing the visual system to adapt more completely in that initial 25 second period.

Experiment 2a Results

Experiment 2 introduced changes to our phoria measurement procedure (longer monocular and shorter binocular periods), and the larger step sizes; these alterations were effective. The phorias were more visibly evident in the eye-tracker fixation offset time course, and clearly decreased during each block, giving a better view of the adaptation process (Figure 14 blue curve; the pattern of downward spikes of decreasing size within blocks). We also included an additional measurement of fixation offset and phorias in this experiment, using the behavioral task (Figure 14, green and purple symbols). The behavioral phorias also clearly decreased during a block, indicative of adaptation. Overall, phorias were larger in the last block as compared with the first block. This suggests adaptation became less complete as the experiment progressed. However slopes of phoria change, which measure the speed of adaptation, within a block did not vary from the first to last blocks.

As in Experiment 1, most participants eventually lost fusion and experienced diplopia, after completing differing numbers of blocks (2-4, 5-9 degrees). To try to account for this failure to adapt, we again examined the first and last blocks, to see if adaptation differed at the near and far ends of the participants' fusional limits. Unlike Experiment 1, behavioral results were used to determine the last fused block. Because sometimes the last block jumped past the participant's

limits, only the blocks where the participants started fused were used for analyses.

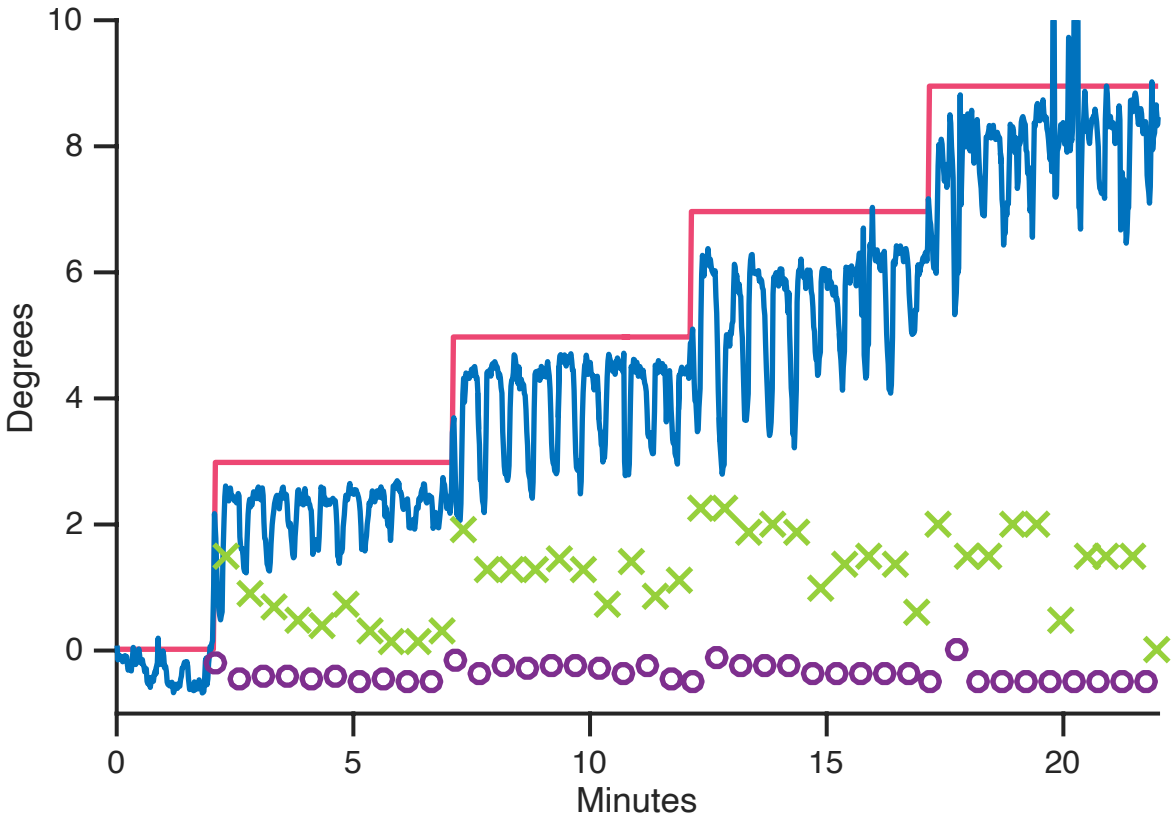

Figure 14. Grand average for Experiment 2a. Participant average fixation offset computed from eye-tracker data (blue) and image offset (red). The experiment started with 2 minutes of zero image offset, then increased by 3 degrees, and then by steps of 2 degrees, each for 5 mins. Results from the behavioral fixation offset task are plotted as the purple circles, and the behavioral phoria task results are plotted as the green "X's."

Eye-tracker Measures of Phoria and Adaptation

Figure 15 plots the average phoria measurements over time within a block. Their steady decrease during the block is the signature of vergence adaptation, and was stronger in this experiment than in Experiment 1.

Phorias tended to be larger in the last block as compared to the first block, indicating that adaptation became less complete as the experiment progressed. This was quantified using the average phoria measurements during the first and last blocks. Across all time points, phorias from the first block were 0.62 degrees, and 1.74 degrees in the last block, with a statistically significant difference of 1.12 degrees (S.E. = 0.31, p = 0.02; Figure 16, top).

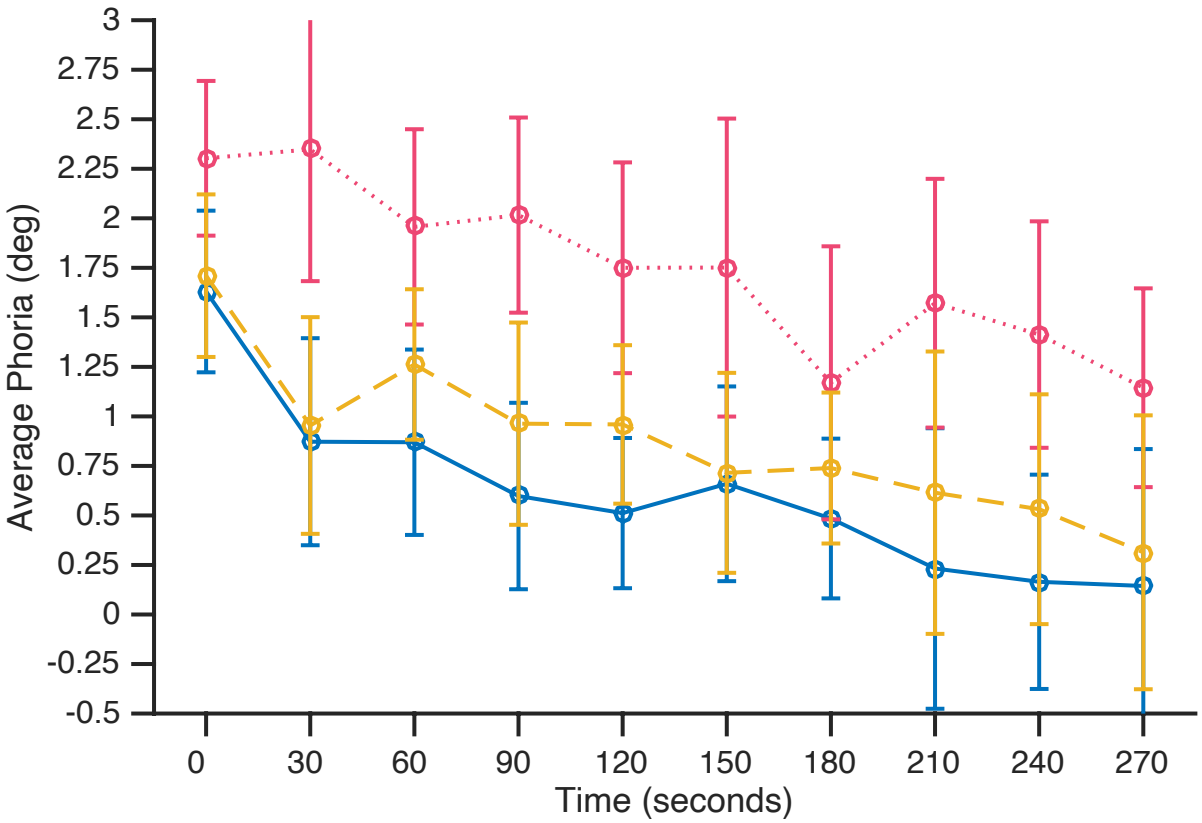

Figure 15. Grand average of phorias from first and last blocks from experiment 2a. Participants' first block (blue, solid) and last block (red, dotted) as well as the second to last block (yellow, dashed) show adaptation, as indicated by decreasing phoria over time.

We also examined the first phoria from the first block as compared to the last block, to see whether phorias were starting larger in the later blocks (Figure 15). The average first phoria from the first block was 1.63 degrees, and the average first phoria from the last block was 2.30 degrees, and the difference of 0.67 degrees was significant, when compared against zero in a one-way t-test (S.E. = 0.25, $p = 0.05$).

Finally, the slope of the line of best fit of the average phoria time course for each participant was computed, as a measure of adaptation during the block. This slope did not differ reliably between the first and last blocks ($p > .05$; Figure 16, bottom).

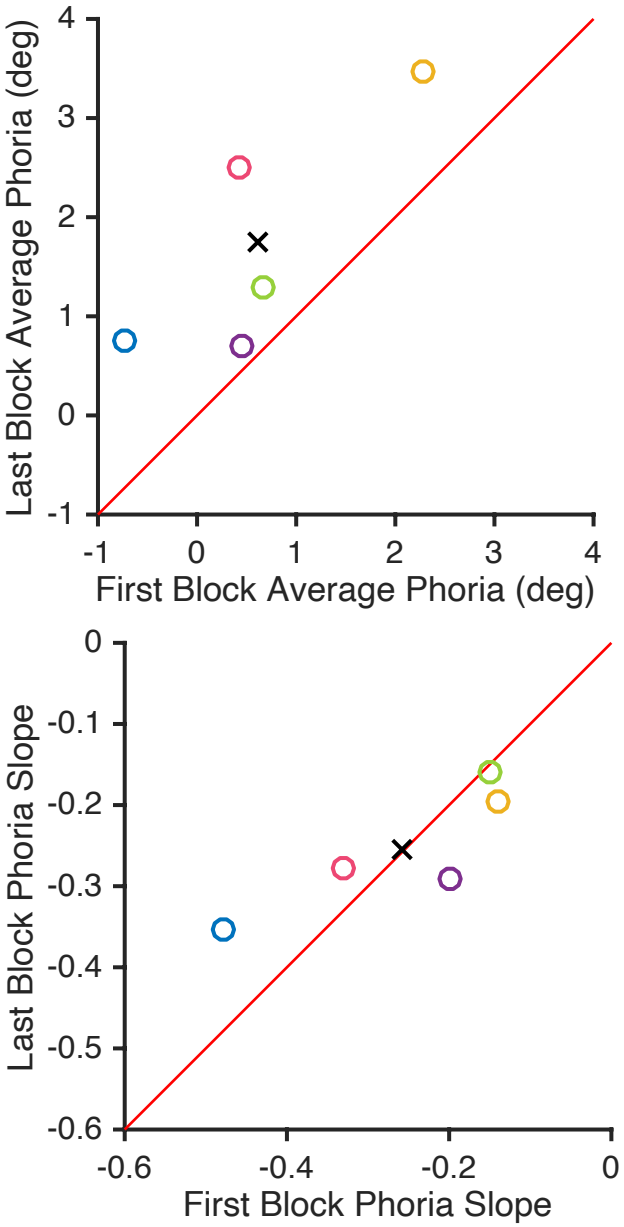

Figure 16. Average phoria and slope of phoria from eye-tracker data in Experiment 2a. Average phorias from the first block versus last block (top) and slope of phorias from first block versus last block (bottom). Each color is one participant, and the colors correspond between plots. The red line is unity.

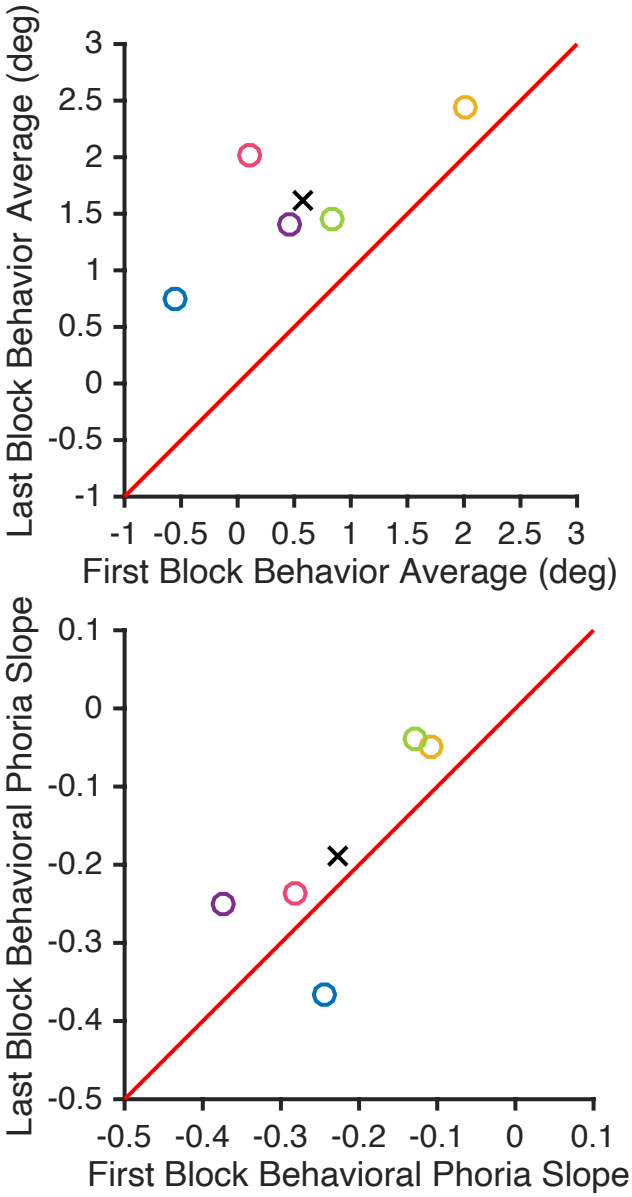

Figure 17. Behavioral phoria results for Experiment 2a. The top panel shows the behavioral average phoria size, for the first vs. last blocks, where each point is one participant, and the red line is unity. The bottom compares the slope of the phorias from the first and last blocks, and each point is one participant with colors corresponding to the figure on the top, and the red line is unity.

Behavioral Measures of Phoria and Adaptation

Phorias were also measured behaviorally, and the average behavioral phoria for each participant's first block was compared with their last block, as well as the

slope of the behavioral phorias from the first and last blocks. Results were consistent with the eye-tracker data. The cross-participant average phoria from the first block of each session was 0.56 degrees, and the averaged last block phoria was 1.61 degrees. The difference between these was 1.05 degrees, and was significantly greater than zero (S.E. = 0.26, $p = 0.016$; Figure 17). The average slope of the behavioral phoria in the first block was -0.23 degrees/minute, and the average slope of the last block was -0.19 degrees/minute. The difference was not significant ($p > 0.5$; Figure 17).

Experiment 2b Results

Experiment 2b was identical to Experiment 2a, except that the adapting eye's image was shifted nasally, causing convergence, while in all other experiments the image was shifted temporally driving divergence. Convergence limits are higher than divergence; one participant maintained fusion for 4 blocks (9 degrees), two for 5 blocks (11 degrees), one for 6 blocks (13 degrees) and one for 7 blocks (15 degrees, the maximum available on our display).

The participant who achieved 7 blocks (15 degrees) was excluded from analyses because although they were able to proceed out to the 7th block with the relatively lax threshold of 75% responses below 2 degrees of fixation offset, their behavioral data showed inconsistent fixation offset throughout the experiment. Also, several participant's last block pushed them past their fusional limits, as

detected through their responses and eye-tracker data. Those blocks were not used, and their last fused block was used for analyses.

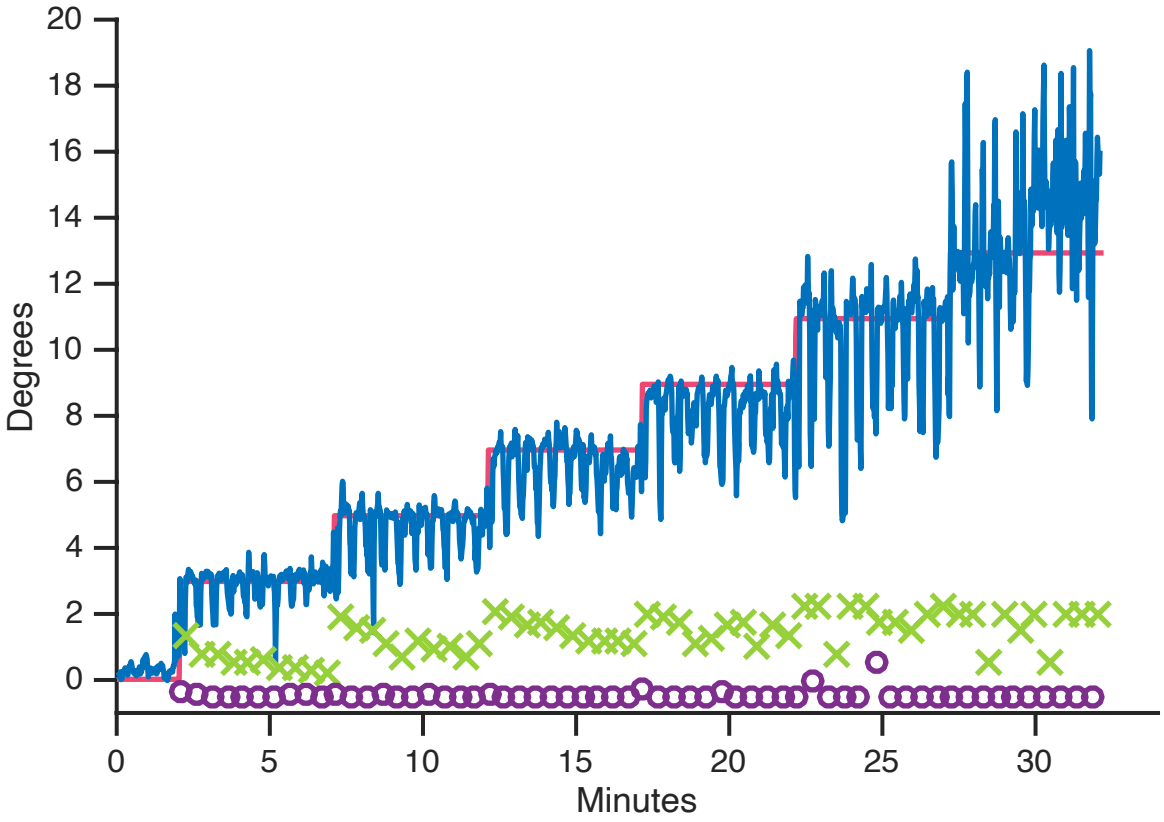

Figure 18. Grand Average for Experiment 2b. Participant average eye-tracker data (blue) and image offset (red). The experiment started with 2 mins of zero image offset, then increased by 3 degrees, and then by steps of 2 degrees, each for 5 mins. Fixation offset task is plotted as the purple circles, and phoria task is plotted as the green "X's."

Phorias, as measured by eye-tracking, were large and clearly visible in this experiment (Figure 18); phorias overall decreased within a given block, and phorias tended to be larger in the later block as compared to the first (Figure 19). When looking at the phorias averaged within the blocks, the average phoria from the first block was 0.8 degrees and the mean of the last block was 2.4 degrees.

The difference of 1.6 degrees (Figure 20) was not significant, however ($p > 0.5$). The slope of a line of best fit to the first block phorias was -0.33 degrees/minute, and the slope of the last block was -0.03 degrees/minute, but this trend was also not significant ($p > 0.5$; Figure 20). We also compared the first phoria from the first block, and the first phoria from the last block, to determine if phorias were starting larger at later blocks, but the difference was not significant ($p > 0.05$).

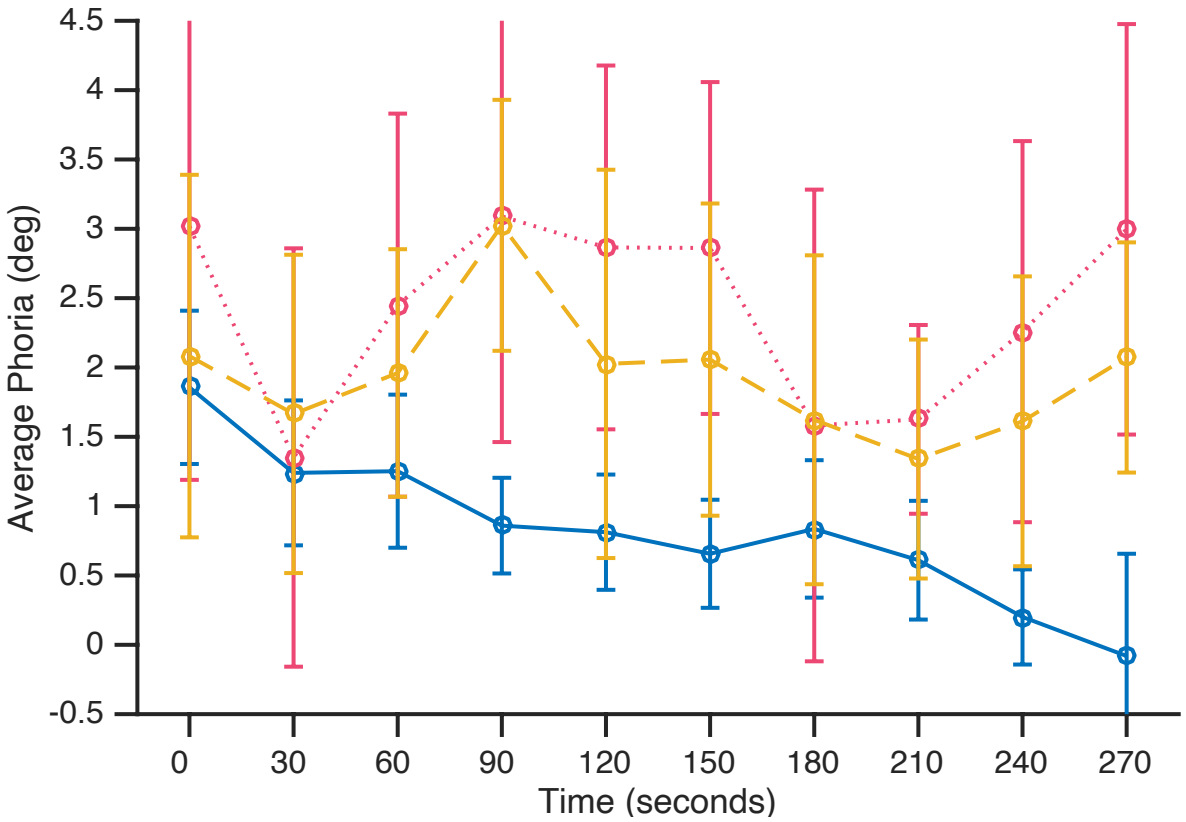

Figure 19. Grand average of phorias from first and last blocks for experiment 2b. Grand average first block time course (blue, solid) and grand average last block time course (red, dotted), as well as the second to last block (yellow, dashed).

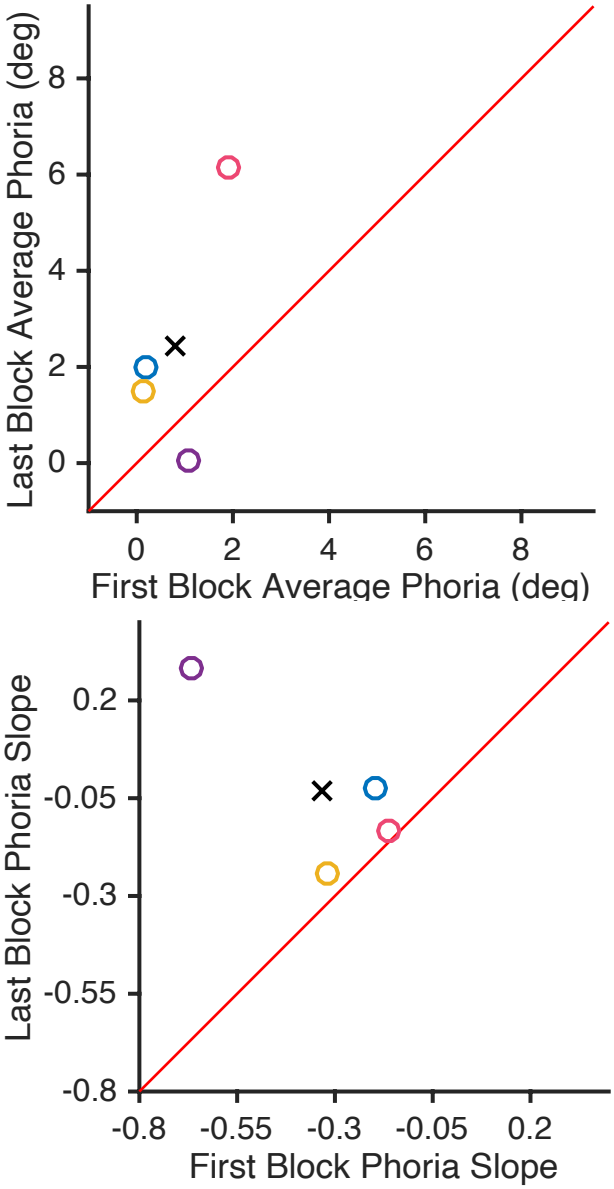

Figure 20. Results of phoria analysis from experiment 2b. Participant average phoria response from the first versus last fused blocks (top) and slope of the line of best fit of phoria responses from first versus last blocks (bottom). Each point is one participant, and the red line is unity.

Behavioral phoria responses were also analyzed to compare the average phoria value, as well as the average slopes from the first and last blocks. Consistent with other experiments, the average phoria was larger in the last block as

compared with the first block, 0.59 degrees versus 1.67 (Figure 21, top). But the difference of 1.08 was not significant ($p > 0.5$). Phoria slopes were also more negative in the first block than in the last, though this trend was also not significant ($p > 0.5$, Figure 21, bottom).

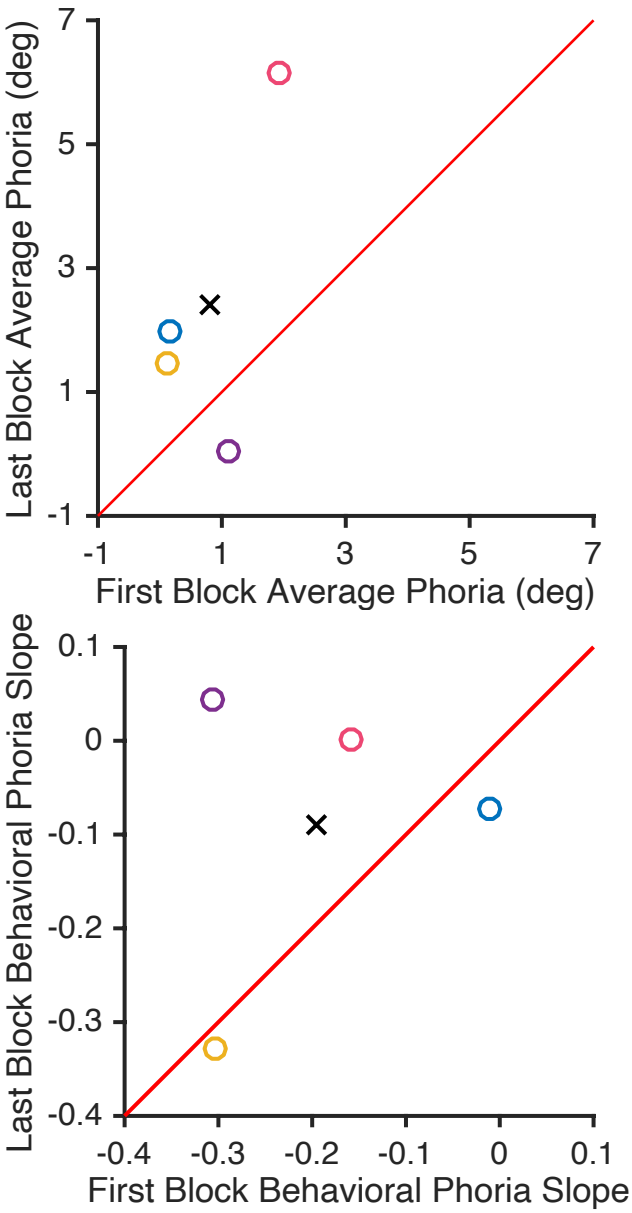

Figure 21. Behavioral phoria results for experiment 2b. The top panel shows the behavioral phoria average in degrees, for the first vs. last blocks, where each

point is one participant, and the red line is unity. The bottom panel compares the slope of the phorias from the first and last blocks, and each circle is one participant with colors corresponding to the figure on the top, and the red line is unity.

Experiment 2 Discussion

By changing the timing parameters so participants spent relatively more time with monocular stimulation, phorias were more visible in the eye-tracker time courses. They showed the expected decrease during a block, indicative of adaptation. It appears that phorias increased in later blocks, but the small number of participants prevented this from reaching significance in Experiment 2b. If true, this pattern would suggest that adaptation was less complete in later blocks. The rate of adaptation did not reliably differ across blocks in either Experiment 2a or Experiment 2b, however.

As expected, participants fused larger image offsets when converging compared to diverging. And finally, the behavioral measures we created to measure fixation offset and phoria worked well, showing the same patterns as the eye-tracker data.

Experiment 3 Results

Procedures in Experiment 3 were similar to Experiment 2a, with a few minor modifications; non-corresponding corrugated edges were placed on the perimeter of the monitors, to prevent them from aiding fusion. Also, the top and

bottom of the image remained surrounding the task during the fusion check, to help fusion.

Fusion again reached a limit, and participants experienced diplopia at the largest image offsets; participants were able to maintain fusion for an average of 3.37 blocks (7.74 degrees). One participant only maintained fusion for 2 blocks (5 degrees), one participant maintained fusion for 5 blocks (11 degrees), and the other 6 participants maintained fusion for 3 or 4 blocks (7 or 9 degrees). Some participants were only able to partially maintain fusion in their final block, as was evident from the behavioral fixation offset task; because a lack of fusion can affect the rate of adaptation (Sethi & North, 1984), these blocks, were not included in analysis.

Phorias were again highly visible in the eye-tracker traces, as downward “spikes” (Figure 22). The phorias showed a visible trend to decrease over time within a block, indicative of adaptation. Figure 22 also shows the behavioral phoria task (green), as well as the fixation offset task (purple). The fixation offset task shows that many participants, on the first response in a block, had not completely fused the new image offset, but by the next response, had achieved fusion. As can be seen in the phoria responses, phorias were larger at the beginning of a block, and were overall larger as blocks progressed (note that fewer participants data

are included in the later blocks of Figure 22 which explains why the last block of the eye-tracker data is so noisy, and extends beyond the image).

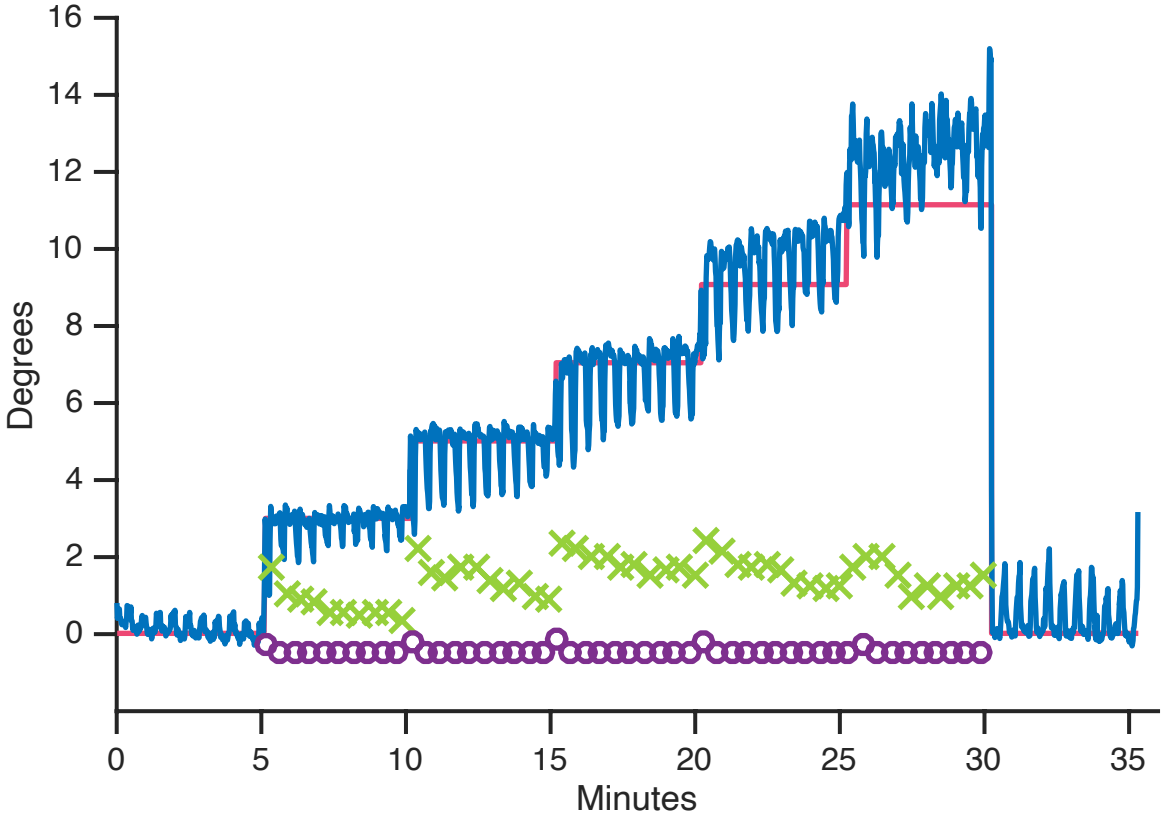

Figure 22. Grand Average of eye-tracker data for Experiment 3. Fixation offset (blue line) is plotted against image offset (red line). Purple circles are behavioral fixation offset responses, and green 'X's are phoria responses.

Fusional Limits

Unadapted- and divergence-adapted fusional limits were compared to see if adaptation changed the limits (Figure 23). Fusional limits in the unadapted condition were calculated as the maximum of the fixation offset during the unadapted fusional limits measurement, which was done 3 times prior to the main procedure. There was no trend across the three measurements, showing

testing was brief enough to not allow adaptive build-up. Averaged across participants, the unadapted fusional limit was 5.38 degrees. In the divergence adapted condition, fusional limits were calculated as the maximum fixation offset from the last fused block, which averaged across participants was 7.76 degrees. Average fusional limits increased by 2.38 degrees after divergence adaptation, and that difference was significant when tested against zero in a one-way t-test (S.E. = 0.88, $p < 0.05$).

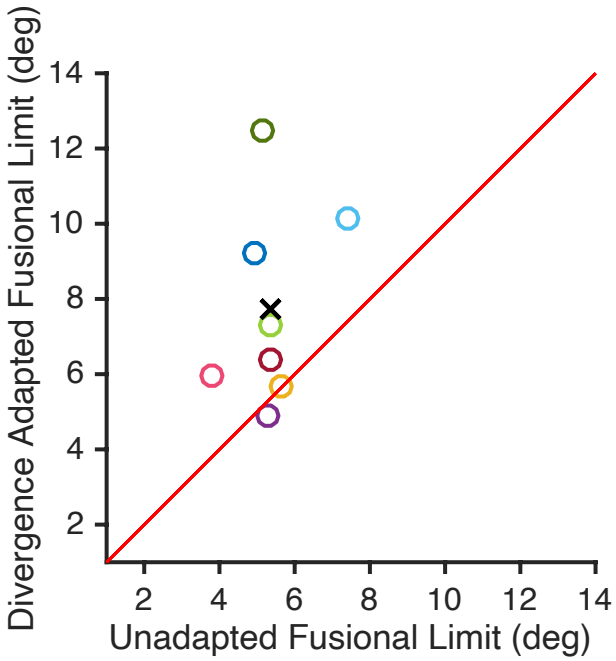

Figure 23. Unadapted vs. divergence adapted limits for Experiment 3. Unadapted limits (degrees) along the x-axis are plotted against divergence adapted limits (degrees) on the y-axis. Each circle is one participant, the red line is unity, and the black "X" is the participant average.

Eye-tracker Results: Phorias and Adaptation

Average phorias from the eye-tracker data are plotted over time within a block in Figure 24. The curves decrease, providing evidence of adaptation. Average phorias from the first block are plotted against average phorias from the last block in Figure 25, top. Phorias were smaller on average in the first block as compared to the last block, 0.56 degrees versus 1.93 degrees. The difference of 1.37 degrees was statistically significant in a one way t-test against zero (S.E. = 0.17, $p < 0.001$). The slope of the line of best fit to the phorias of the first block was -0.2 degrees/minute and last block was -0.3 degrees/minute, which did not differ significantly ($p > 0.05$; Figure 25, bottom).

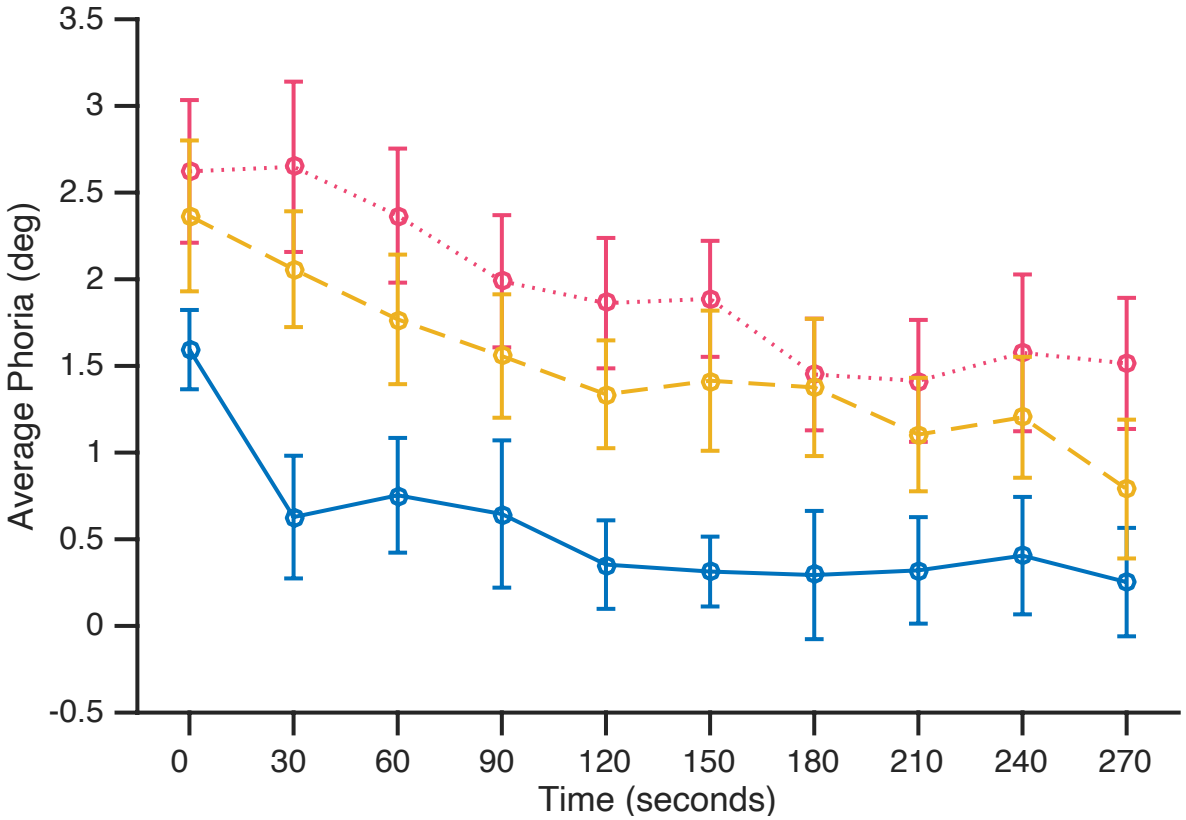

Figure 24. Grand averages of phorias computed from eye-tracker data Experiment 3. Phorias from the first blocks, averaged across participants (blue, solid), and last blocks (red, dotted), as well as the second to last (yellow, dashed) averaged across participants, plotted against time.

To test whether phorias were starting larger in later blocks, we also compared the first phoria from the first block with the first phoria from the last block. The first phoria from the first block was 1.59 degrees on average, and the first phoria from the last block was 2.62 degrees on average. This difference of 1.03 degrees was compared against zero in a one-way t-test, and was found to be significant (S.E. = 0.26, p = 0.005).

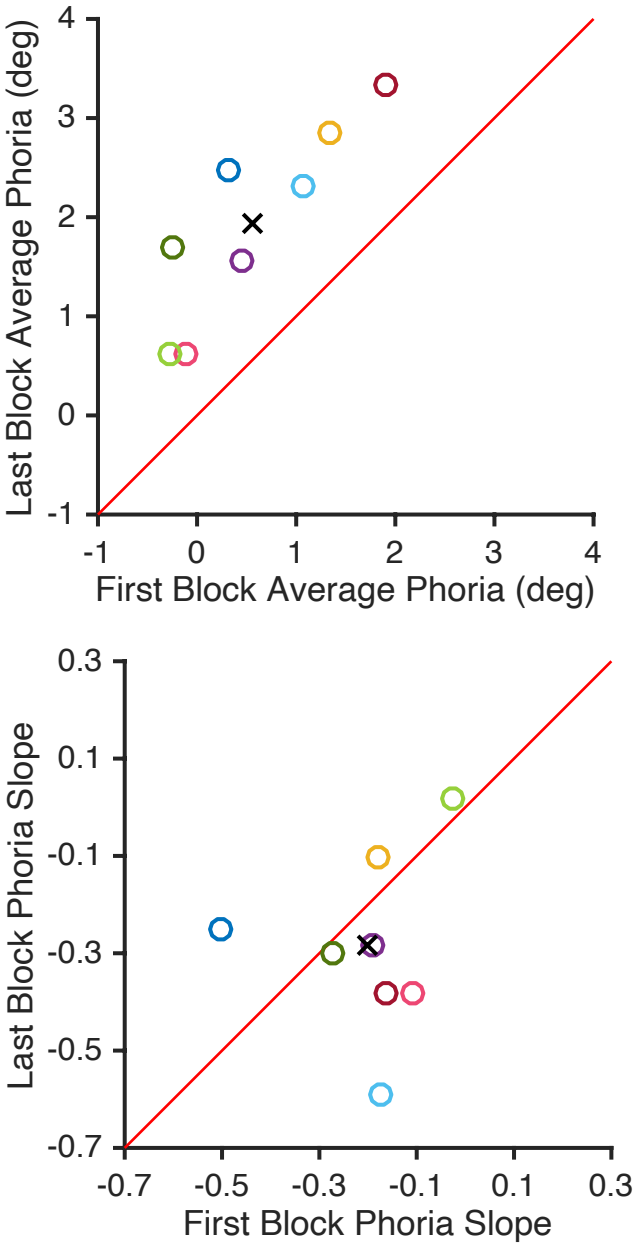

Figure 25. Eye-tracker phoria results for Experiment 3. The top panel shows the average phoria from the first block against the average phoria from the last block. The bottom panel shows the slope of the phorias from the first block against the slope of the phorias from the last block. The red lines are unity, each circle is one participant, and the colors correspond between plots, and the black 'X' is the participant average.

Behavioral Data

The phorias measured by behavior showed a similar pattern to those measured with the eye-tracker (Figure 26). The average phoria from the first block was 0.77 degrees and the average phoria from the last block was 1.80 degrees, and there was a significant difference of 1.03 degrees compared against zero in a one way t-test, (S.E = 0.16, $p = 0.001$). The average slope of the phorias from the first block was -0.22 degrees/minute and the average slope of the phorias from the last block was -0.20 degrees/minute, and the difference of 0.02 degrees/minute did not differ from zero in a one-way t-test against zero ($p > 0.05$).

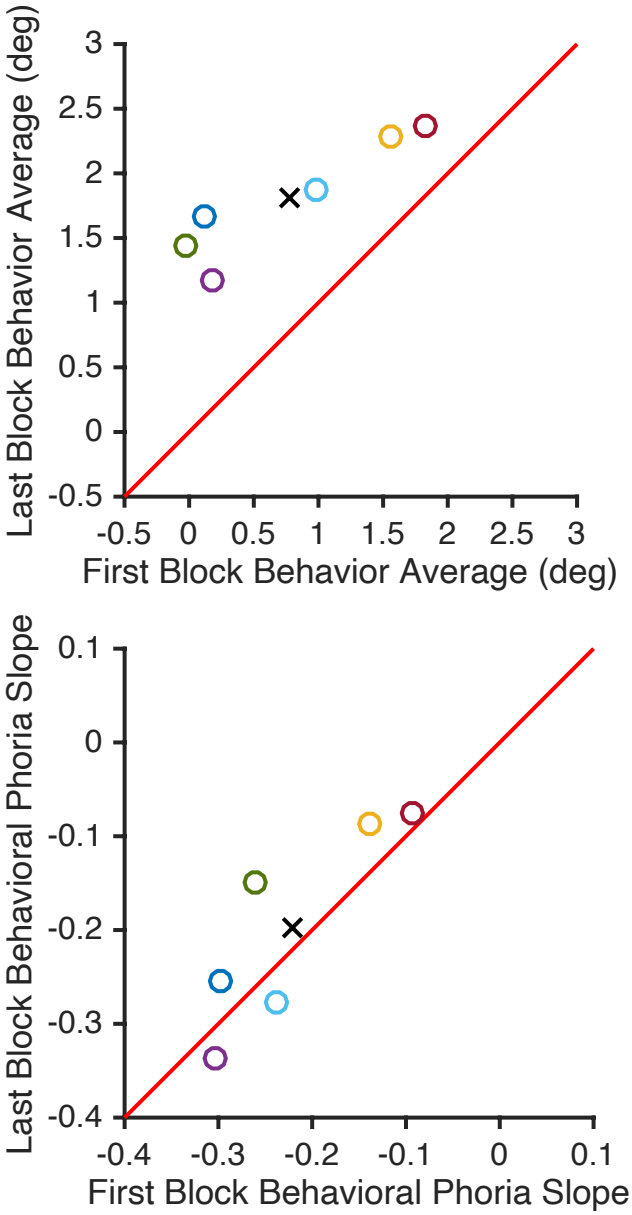

Figure 26. Behavioral phoria data from Experiment 3. Six participants completed the behavioral task. In the top panel, the first block average phoria is plotted against the last block average. On the bottom, the slope of the phorias during the first block versus the slope of the phorias during the last block. Each circle is one participant, the colors correspond between plots, the black "X" is the participant average, and the red line is unity.

Experiment 3 Discussion

The results of Experiment 3 confirm that adaptation can increase the range of achievable eye positions: Fusional limits increased by an average of 2.38 degrees, after adapting to gradually increasing divergence demand over 40 minutes. However, there were clear limits to the amount by which adaptation could increase fusion. There was additionally evidence that adaptation was not as complete in later blocks, as phorias were larger in the last block as compared with the first block. These trends were seen in both the eye-tracker and the behavioral data. Phorias were on average 1.37 degrees larger in the last block, as measured by the eyetracker, and 1.03 degrees when measured with the behavioral phoria task. And as seen in Experiments 1-2, the rate of adaptation did not seem to change between the first and last blocks – instead, the phorias were larger throughout the later block.

Interim General Discussion: Experiments 1-3

Can adapting to divergent eye positions lead to larger fusional limits? We tested this by comparing the maximal achievable eye divergence in an “unadapted” condition, where image offset increased continuously over a few minutes, to a “divergence adapted” condition, where image offset increased gradually over dozens of minutes with 5 minute constant intervals to allow adaptation. As predicted, the divergence adapted condition led to an increase in fusional limits. Eye divergence was greater in the divergence adapted condition by 1.79 degrees on average in Experiment 1, and 2.38 degrees on average in Experiment 3.

A handful of past reports are consistent with our results (e.g. Ogle & Prangen, 1953; Henson & North, 1980; Sethi & North, 1983; Sethi & Henson, 1984; Sethi & North, 1987; Stephens & Jones, 1990; Neveu et al., 2010). The increase in fusional limits through adaptation has been demonstrated by adapting participants with step-wise increase in fusional demands (Ogle & Prangen, 1953; Sethi & Henson, 1984; Sethi & North, 1987; Stephens & Jones, 1990), with the use of prisms to create an image offset (e.g. Ogle & Prangen , 1953; Henson & North, 1980; Sethi & North, 1983; Sethi & Henson, 1984; Sethi & North, 1987) as well as a telestereoscope (Neveu et al., 2010), and a dual monitor setup such as our own (Stephens & Jones, 1990). Adaptation has been measured as the time-course of phoria change over time (Henson & North, 1980; Sethi & North, 1983; Sethi & Henson, 1984; Sethi & North, 1987) as well as simply measuring how much fusional limits changed after adaptation (Stephens & Jones, 1990; Neveu et al., 2010).

Our study uniquely allowed us to examine whether adaptation itself is limited, and if so, why. We combined many of the advantages of the previous studies, specifically to measure adaptation step-wise to increasing fusional demand, and to measure the change in fusional limits, as well as the time course, by using both eye-tracker and behavioral measures. This allowed us to examine how the time course of adaptation changed with increasing fusional demand.

We also demonstrated that this form of adaptation occurs very quickly; when given 25 seconds of binocular vision relative to 5 seconds of monocular vision, adaptation occurred so rapidly that the time course of phoria reduction was harder to measure. The timing we used in Experiments 2 and 3, 20 seconds of binocular vision and 10 seconds of monocular vision, slowed adaptation down enough to more clearly measure its time course. The many studies done by Henson and North (e.g. Henson & North, 1980; Sethi & North, 1983; Sethi & Henson, 1984; Sethi & North, 1987) take this approach further and use 15 seconds for both monocular and binocular, to achieve even smoother curves.

Another advantage of our study was eliminating the blocks where participants were not fused. Sethi and Henson (1984), and Sethi and North (1987) looked at the rate of adaptation to further, and larger fusional limits, respectively. They found that the rate of adaptation to subsequent and larger vergence demands was slower than initial and smaller vergence demands. However, in some cases they used prism strengths that were beyond the fusional limits of participants, resulting in conditions where participants were not fused or were “partially” fused. As fusion is the driving force of adapting the tonic component to the current eye positions, it is unsurprising they found less and slower adaptation. They also used only 2-4 participants in each experiment, which also makes it difficult to draw conclusions.

Instead, we did not analyze the blocks where participants were diplopic, and compared the rate and amplitude of adaptation of the last fused block to the first block. Unlike Sethi and Henson (1984) and Sethi and North (1987), we found no change in the rate of adaptation. This may mean that their findings were simply the result of slower adaptation to unfused blocks, but it is also possible that our measurements were noisier than theirs and so unable to detect any changes in slope.

So, why does adaptation ultimately fail, and why can't participants achieve divergence eye positions to points on the screen easily achieved with version eye movements? One possibility is that adaptation slows down in later blocks: If this were the case, then phorias would decrease at a slower rate in later blocks than in earlier blocks. Our results did not support this hypothesis. Adaptation curves had the same slopes in both earlier and later blocks.

However, we did find an increase in average phorias across blocks in Experiment 2a and Experiment 3. The most likely explanation of this pattern is that participants were not "fully" adapted to the image offset before we shifted the image again. The larger phorias later in the experiment may be evidence of this less or not complete adaptation in the preceding block, resulting in a larger initial phoria at the start of the later block. This 'debt' of adaptation likely accumulated

over the experiment and eventually produced the failure of fusion. Together these results suggest that the reason people cannot normally diverge their eyes farther than some limit is that they perhaps have not had time to adapt to large divergences, resulting in an inadequate drive in the tonic component to reach the large divergences.

Alternatively, there could be some other limit on the tonic component; one possibility is that this partly arose because the accommodative and proximal cues were not entirely eliminated in our setup, and the conflicting cues could limit adaptation, as Neveu et al. (2010) speculated. Because the room was not entirely dark, it could be that the accommodative and proximal cues were activating and restricting/limiting how far the fusional limits could be pushed. Or perhaps there is simply a “hard” limit past which adaptation cannot shift tonic eye position.

If the first alternative were true, then slowing down adaptation further should result in more adaptation. That is, *if given more time, would participants have adapted more, and been able to fuse even larger image offsets?* The answer to this question is important for translational research (i.e. strabismus or convergence insufficiency treatment), as well as for applications such as building binocular viewing devices in virtual or altered reality. We addressed this question in our next experiment.

Chapter 3

Single vision is, for most people, a highly reliable feature of our binocular vision, most often noticed when it fails. How does this complex system work so reliably? What allows our eyes to meet the demands of so many viewing conditions?

As reviewed in Chapter 1, different viewing conditions produce different amounts of retinal disparity across the two eyes. This disparity, and other cues, drive the vergence system, which moves the eyes to lessen disparity, and place corresponding parts of the images in the two eyes on or close to corresponding locations in the two retinae. If those cues, known as vergence demands, are maintained for minutes to hours, the system adapts (e.g., Henson & North, 1980, Sethi & Henson, 1984, Stephens & Jones, 1990, Neveu et al., 2010), most likely to relieve the effort needed to sustain those eye positions. And as shown in Chapter 2, from that adapted point, the eyes are able to achieve a further position not previously attainable before adaptation.

As reviewed in previous chapters, adaptation can be measured through phoria, the distance an eye moves when fusional cues are blocked, representing the tonic position of the eye. For example, in the experiments in Chapter 2, and this chapter, we shifted the image seen by one eye outward on the screen, and that shift produced an outward movement of the eye. When the image was removed from one eye, the eye shifted back towards its “baseline position” set by the tonic

component. However, as the block continued, the eye shifted less when the image was removed. The progressive reduction of phorias was evidence of adaptation.

Our experiments in Chapter 2, however, suggested that as fusional demands are increased, eventually adaptation of the vergence system fails to keep up. What produces these limits on adaptation? Adaptation was less complete during later blocks, as average phorias were larger than in earlier blocks. But phorias at the beginning of later blocks were larger than at the beginning of earlier blocks as well. This pattern suggests that adaptation in later blocks was incomplete in some way. One reason could be that participants did not have enough time, in the 5 minute blocks, to adapt fully, and by the later blocks were less fully adapted to the step in fusional demand than in earlier blocks. We hypothesized that if participants were given more time, they would be able to more fully adapt and so achieve greater fusional limits.

In Experiment 4 we again gradually increased image offset, while again giving participants time to adapt, and measuring their adaptation via phorias. However, we allowed block duration to vary, and did not move on to the next block until participants had reached a specified high level of adaptation. We hypothesized that this procedure would allow participants to adapt more completely. If so, then this experiment should also help answer the question of how far adaptation can

push fusional limits. This in turn could be important when constructing therapy and treatment plans for people who have a disease of eye alignment.

The procedure should also give information on whether adaptation is slowed down farther from fusional limits. Adaptation may be faster or more effective when fusional demands are low, and slower when closer to fusional limits: If this is the case then in our new procedure block duration should increase for later blocks.

To achieve the largest limits possible, we also tailored step sizes of image offset shifts for each participant. This is unlike past studies which shifted images using prisms with fixed step sizes, which may put participants in different states – at a given step some participants may be nearing the edge of their limits, others may be past their limits unable to fuse, and others may still be well within their limits. By using a stereoscope, we could shift the virtual images apart with an arbitrary step size. This allowed us to scale step sizes relative to the individual limits of the participant (measured in an unadapted pre-test), to attempt to produce the largest possible increases in fusional limits.

Experiment 4

Methods

Participants

Eight participants, with normal or corrected to normal vision, and no history of eye disease or disorder, participated in the experiment. Experimental procedures were approved by the University of Minnesota Institutional Review Board. Participants were tested to confirm they were not stereoblind. Participants were told they may experience eye discomfort during the experiment, but to stop immediately if they felt any pain. Most participants reported eye discomfort, and a feeling of “wrongness”, but no participants experienced pain and all participants completed the experiment.

Equipment

The dual eye-tracking and stereoscope setup from Chapter 2 was used, with the same calibration procedures for calibrating the eye-tracker and the stereoscope.

Fusional Limits Measurement

Unlike Experiments 1 and 3, where divergence adapted fusional limits were not measured the same way that unadapted limits were, we measured the two using identical methods in the current experiment. Fusional limit measurements, for the unadapted limits, were measured the same as they were in Experiment 3, with alternating sweeps of image offset for the left and right eyes, three times in each direction. This same process was repeated to measure the divergence adapted

limits at the end of the experiment. In earlier experiments, we took the maximum fixation offset (as defined in Appendix B) that was achieved during the adaptation phase of the experiment as the divergence adapted limit. However, this likely underestimated the limit, as some participants could still fuse the images during their last block, and so could have had higher limits. In addition, measuring the unadapted and divergence adapted limits in the same way provides better experimental control.

Fixation Offset and Phoria

Fixation offsets and phorias were calculated the same way as Chapter 2, with both eye-tracking and behavioral measurements. The behavioral task used all the same parameters and procedures as Experiment 3.

Procedure

On the first day's session, after calibrating both the eye-tracker and the stereoscope, participants' unadapted fusional limits were measured, and they practiced a demo version of the fixation offset task until they were accurate to within +/- 1 degree. Fusion was ensured in the demo version, and the eyes were physically aligned. The 'ruler' (as described in Chapter 2) was presented to one eye, and the 'x' presented to the other was presented at a known, random position to the other eye, corresponding to a point along the 'ruler'. Thus we could compare the known placement of the 'x' with participants' responses to ensure they were performing the task adequately.

During the second and third day participants completed identical sessions whose data were averaged to increase the reliability of results; all sessions were 24 hours apart. The sessions again began by calibrating the eye-tracker and the stereoscope, and unadapted fusional limits were measured. The block step size for the main experiment was calculated as one third of the average of the three unadapted fusional measurements of the right eye, rounded down to the nearest 0.5°, with a minimum of 1 degree.

The main experiment began with a 5-minute baseline for the eyes to adjust to the setup at “zero” offset. The image then moved in steps of 0.5 degrees every 0.5 seconds out to the first block step size calculated as previously mentioned (as in Chapter 2, the distance moved is called the image offset). The image stayed at that offset until three consecutive behavioral phoria responses (see below for timing and frequency of phoria measurements) were at or below the “zero” response, meaning that the eye had achieved a stable and complete fusion. At that point the next block began and the image moved out another step, of the same size, and stayed there until there were three more consecutive responses at or below “zero” phoria. If, however, a participant became “stuck” at the response point one step above zero (which would be a fixation offset of 0.5-1 degrees), and their responses were at or below this level for 20 consecutive responses, which took 10 minutes, they also progressed to the next block.

This block progression continued for a total of 40 minutes, or until diplopia was experienced, at which point the divergence adapted fusional limits were measured again in the same way as they were at the beginning of the session. Then the image was placed back at “zero” offset for participants to adapt back to “real world” fusional demands before the experiment was over, for their comfort.

Two participants had one of the two adaptation sessions excluded because 35% or more of the eye-tracker data failed to record, likely because the image of the pupil was lost due to a poor calibration, so only one session was used in analysis. The other 6 participants had enough eye-tracker data to use both of their sessions.

Throughout the experiment, image presentation alternated between 20 seconds of binocular image presentation, and 10 seconds of monocular presentation, as in Experiments 2 and 3. After the 20 seconds binocular presentation, participants completed one trial of the behavioral fixation offset task (Figure 8 c) used as a measure of fusion; the top and bottom edges of the image remained on the screen, surrounding the task, as a fusion lock. During the monocular image presentation, a green ‘X’ was presented to the one eye while the other eye’s screen was blank, removing fusional cues to the two eyes; after 10 seconds they completed another trial of the behavioral fixation offset task, this time used as a phoria measurement. This task was the same as Experiments 2 and 3.

Results

On average, the experiment lasted 4.75 blocks with a range of 3-6 blocks. This number does not include any blocks that began less than 30 seconds from the end of the main part of the experiment, which were too short to include in the analyses. The “last block” used in the analyses below was always the last completed block, as we were interested in block duration, and did not want to look at the blocks where the experiment cut off in the middle of a block; the maximum completed number of blocks was 5. All participants maintained fusion until the end of the experiment and did not experience diplopia.

Figure 27 plots eye-tracking and behavioral data from the first and last 60 seconds of each block, averaged across participants. Unlike previous versions of this experiment, the block duration varied across participants and blocks, making data averaging difficult. By selecting only the beginnings and endings of each block, we could still average across sessions and participant.

Phorias are visible in both eye-tracker and behavioral data plotted in Figure 27. The eye-tracker phorias are visible as the downward spikes, when the binocular cues were removed and the eye shifted back towards baseline. As in previous experiments, phorias decayed over time, demonstrating adaptation; phorias from the first 60 seconds of a block (dark blue) were larger than the phorias of the last

60 seconds (light blue), which are almost invisible in the eye-tracker traces. Phorias in the behavioral data (green) were also larger in the first 60 seconds versus the last 60 seconds of a block. In both types of data, phorias appeared larger at the start of later blocks than at the start of the first one.

Eye-tracker data from the end of the experiment was quite noisy. Figure 27 is only a visualization of our overall results, and does not correspond to our formal analyses reported below, because participants completed different amounts of blocks: only the first 4 blocks are plotted, as the 5^{th} block was only completed by two participants, and thus the grand average was very noisy. In our later analyses, each participants' first and last blocks are compared to each other, removing any confound of number of blocks completed.

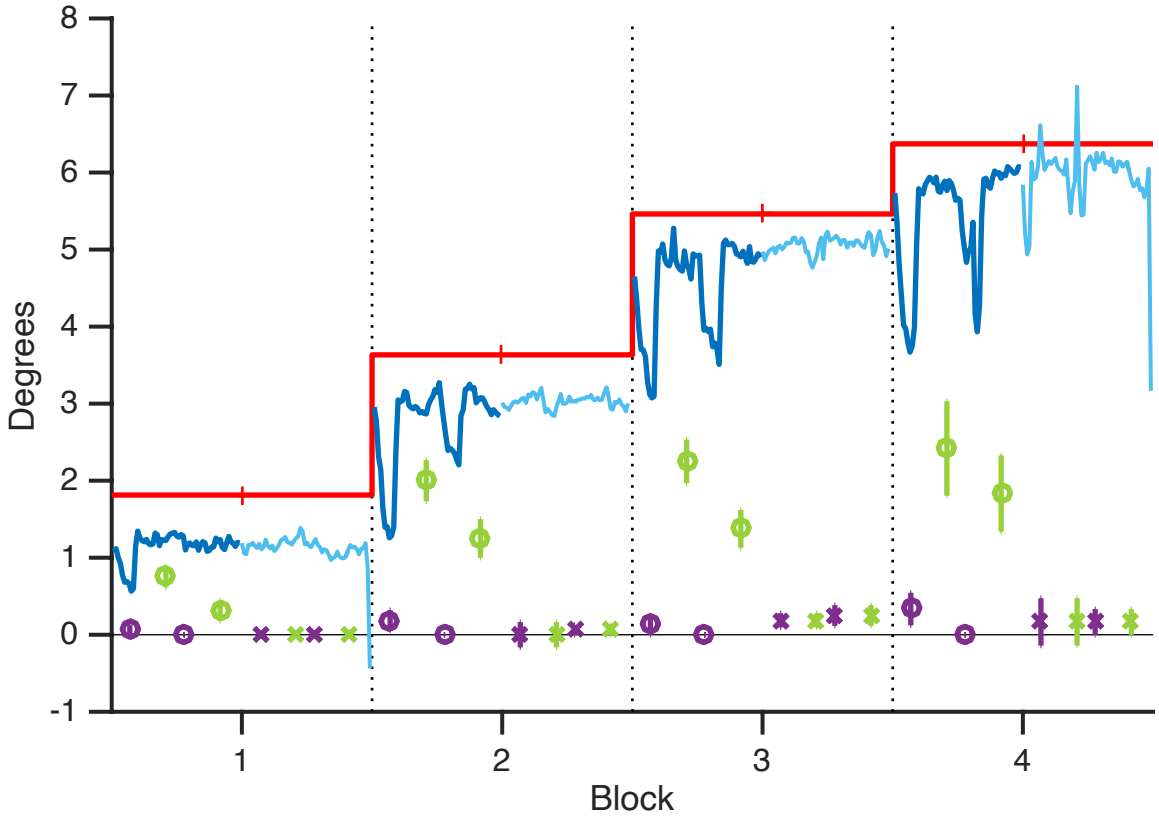

Figure 27. Grand average of eye-tracker and behavioral data in Experiment 4. The first and last 60 seconds of each block were averaged across participants. The dark blue line is the first 60 seconds of eye-tracker data for each block, the light blue is the last 60 seconds. The purple points are the fusion check responses, and the green points are the phoria task responses. Responses for both tasks from the first 60 seconds are plotted as a circle and responses from the last 60 seconds are plotted as an "x". The first 4 blocks are plotted, as only 2 participants completed 5 blocks. Image offset varied between participant and session, meaning the red line is the average image offset, averaged across session and participant; the vertical tick mark indicates the divide between the first and last 60 seconds. Error bars are SEM.

Fusional limits, and step sizes

Unadapted fusional limits were calculated by taking the maximum eye

displacement from each of the three measurements in one direction (left or right),

and averaging these maxima together. Limits ranged from 1.5°-7.4°, with a mean of 5.5° for the right eye, and 2.1°-6.39°, with a mean of 5.2° for the left eye.

Step sizes were calculated from these initial pre-adaptation limits, as one third the limit, rounded to the nearest half degree. Because small steps make observing phorias difficult (since the eye does not have much distance to shift back), the minimum step size was set to 1°, which was approximately 2/3 the limit measured for one of the participants. Across participants, step sizes ranged from 1°-2.5°, with a mean of 1.8°.

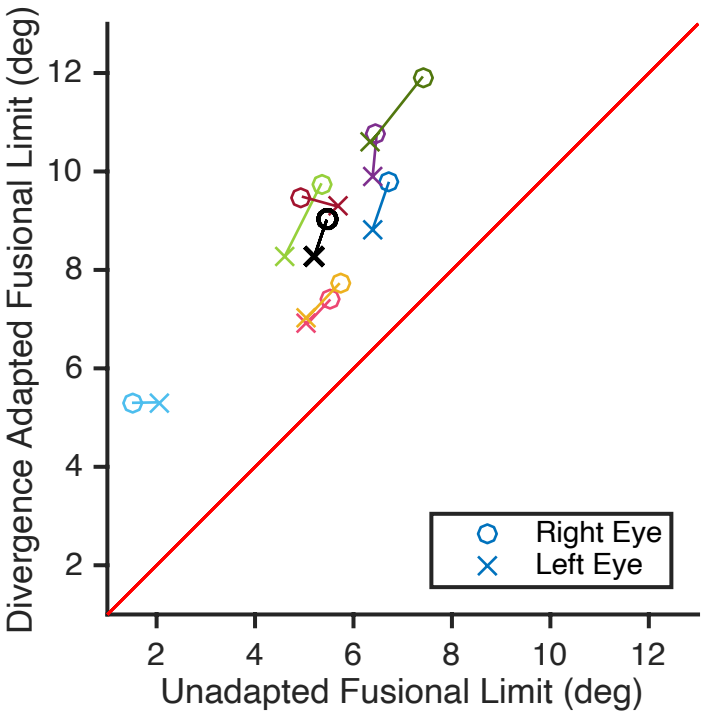

Figure 28. Fusional limits of left and right eyes Experiment 4. Before adaptation (unadapted fusional limits) and after adaptation (divergence adapted fusional limits), for both the left eye ('X') and the right eye ('O'). The black markers are the participant average. Each color is a different participant.

Fusional limits were measured for both the left and right eyes' divergence limits, before (unadapted fusional limits) and after adaptation (divergence adapted fusional limits). Unlike the previous experiments where the divergence adapted fusional limits were calculated as the maximum fixation offset from the last fused block, we measured the limits using the exact same procedures as the unadapted fusional limits measurement, immediately at the end of the adaptation phase.

The right eye, whose image was shifted, had an average unadapted fusional limit of 5.46 degrees pre adaptation and a divergence adapted fusional limit of 9.02 degrees post adaptation (Figure 28). The left eye, which remained stationary during the adaptation procedure, had a pre adaptation limit of 5.20 degrees, and post adaptation limit of 8.26 degrees. The right eye limit was significantly larger post adaptation by 3.56 degrees, (S.E. = 0.39, p <.0001), and the left eye limit increased significantly by 3.06 degrees (S.E. = 0.03, p <.0001). The change in limit was also significantly greater for the right eye than the left eye, with a mean difference of 0.50 degrees (S.E. = 0.12, p <.005).

Block Durations

If adaptation rate did not change as divergence adapted fusional limits were approached, then each block should be the same in duration as the one preceding it, reaching a similar state of adaptation in a similar amount of time to

trigger the next block, throughout the experiment. However, we found that block duration increased nearly monotonically for all participants during the course of the experiment, as image offset increased. Figure 29 shows this trend.

Block duration in the first block was 2 minutes on average, and increased to 11.6 minutes on average in block 3 (Figure 29). Recall that participants proceeded to the next block if their phoria response reduced to 0 for three consecutive responses (1.5 minutes), or 1 degree or less for 20 consecutive responses (10 min), and block durations likely would have increased much more if we had not allowed the latter. Also the mean block duration plotted in Figure 29 averages participants that completed varying numbers of blocks, making it appear to asymptote when for almost all participants it increased monotonically. For statistical analyses, we compared blocks and trends across blocks computed within each participant.

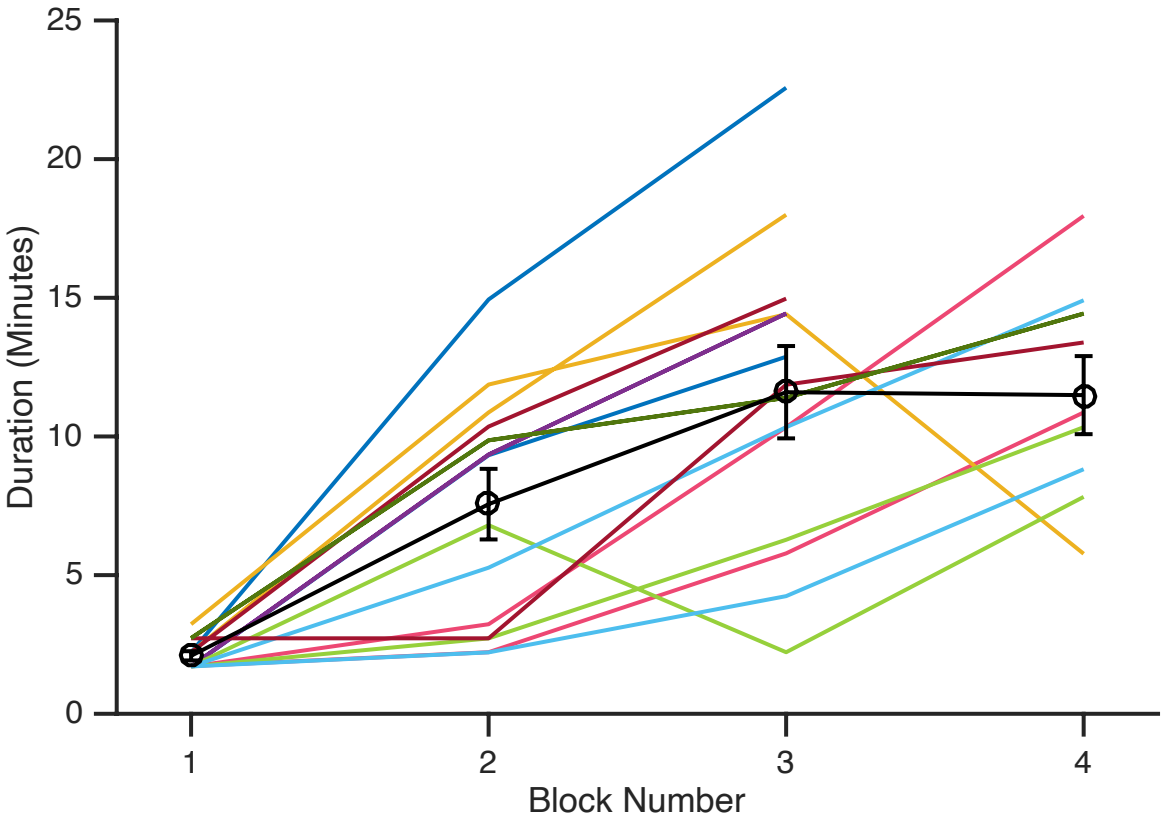

Figure 29. Block duration as a function of block number in Experiment 4. Each color represents a different participant, and most participants had valid data for two sessions. The first 4 blocks are plotted, as only 2 participants completed a 5th block. The black points are the grand average of all sessions and participants, and error bars are SEM.

Block duration increased reliably across block, as determined by the slope of the line of best fit to the block durations. Figure 30 shows the block durations for each participant (averaged across session for the participants with valid data for 2 sessions), as well as the line of best fit for each participant, which are all positive in slope. The average slope was 4.01 minutes/block, which was significantly greater than zero (SE = 0.77, p = .001).

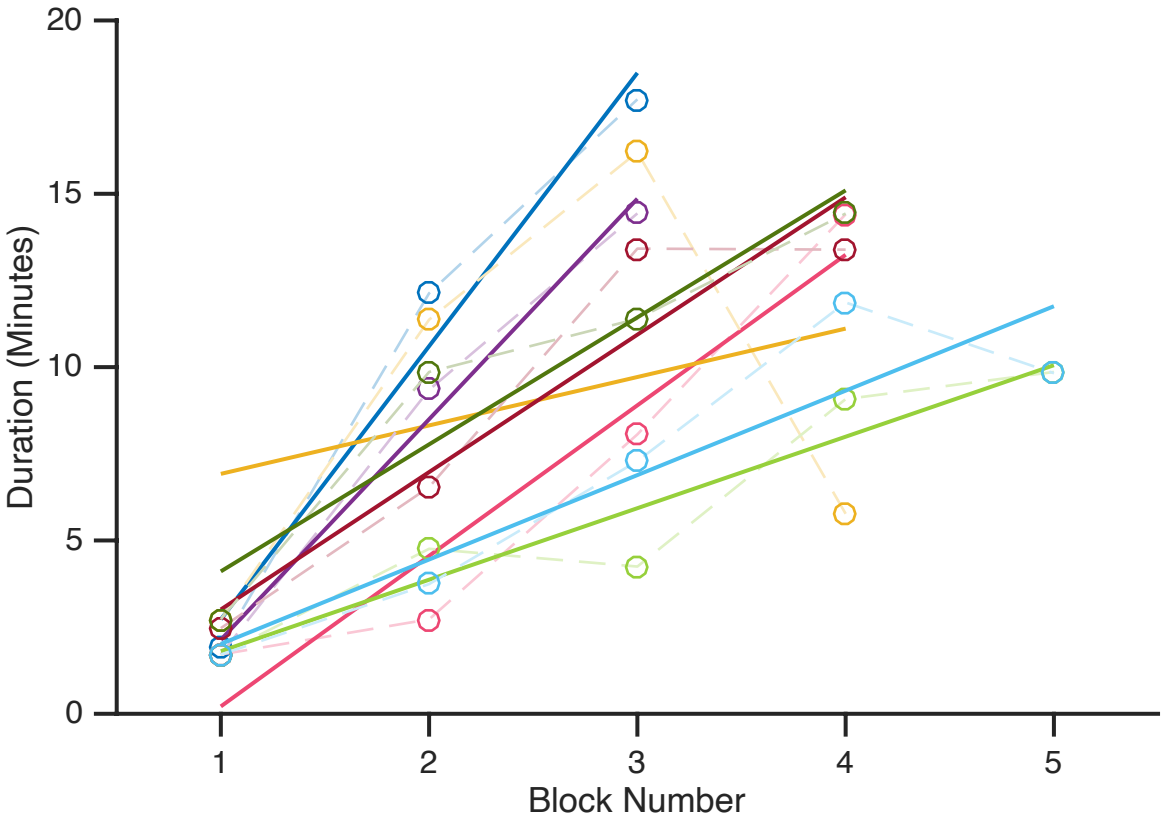

Figure 30. Average duration across blocks and lines of best fit, for Experiment 4. Block duration, averaged across sessions is plotted in the lighter dotted line, with the line of best fit for each participant plotted on top as the bolder line, in the corresponding color.

Consistent with this analysis, the blocks from the last half of the experiment were reliably longer than the blocks from the first half. Figure 31 compares the average duration of the blocks in the first half of the experiment to the average duration of blocks in the second half. First versus second half was determined individually for each participant, and if a participant completed an odd number of block, the middle block was analyzed as part of the second half. The red line is unity, and all the points fall above that line, showing that the average block duration was higher in the second half. The average last half block was 11.6 minutes, and the

first half block was 3.7 minutes, with a difference of 7.9 minutes which was significant when compared against zero in a one-way t-test (SE = 1.06, $p < 0.001$)

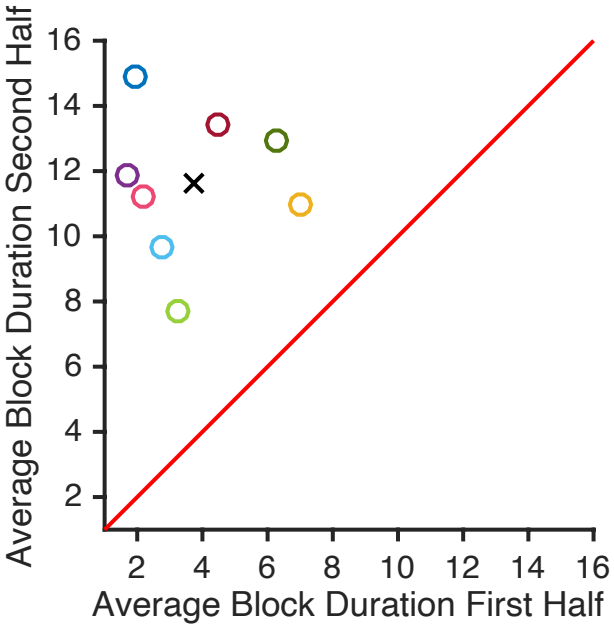

Figure 31. Average block duration of the first versus second half of Experiment 4. Block duration was averaged across the first half and compared to the average block duration of the second half. Each circle is one participant, the colors correspond across the plots, the black "X" is the participant average, and the red line is unity.

Behavioral and Eye-tracker Phorias

Phorias were calculated the same way as in Chapter 2. Figure 32 shows the individual participant average of phorias computed from the eye-tracker data during their first and last blocks, as well as the grand average of phorias during the first and last blocks. Because block lengths differed across participants, the grand average at later time points is not an average of all participants. But all

participants completed at least 4 phorias in their first and last blocks, so comparisons of the first 4 phorias are most telling. All curves show decreasing trends, indicative of adaptation.

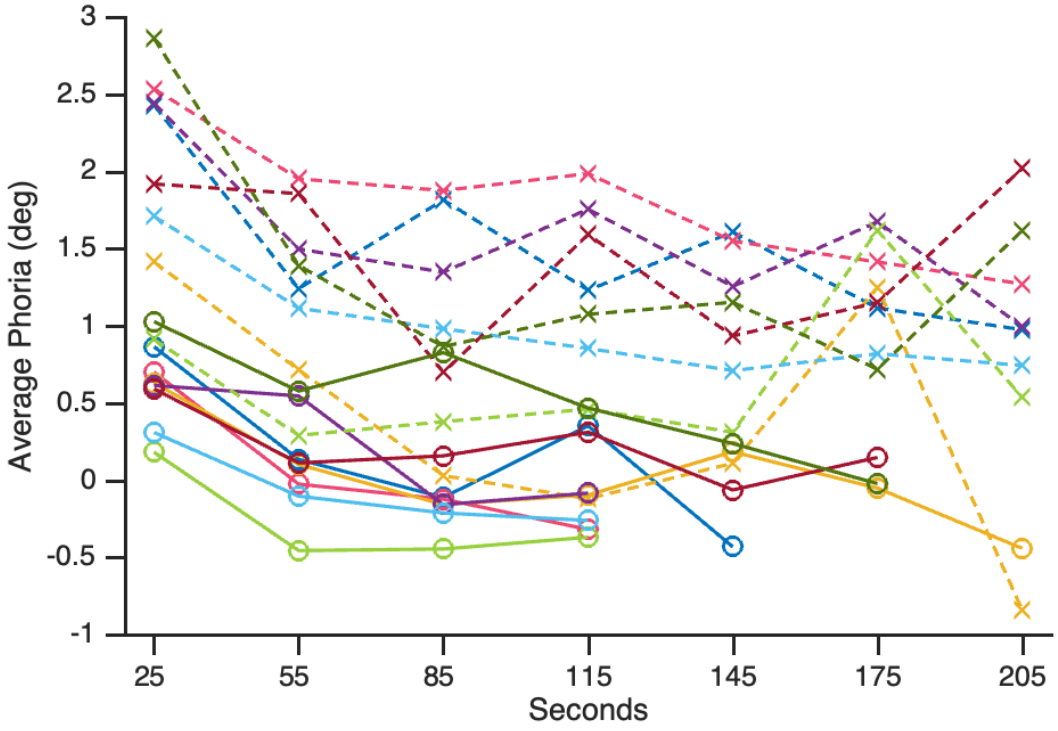
Average Phoria (deg)
3
2.5
2
1.5
1
0.5
0
-0.5
-1
25
55
85
115
145
175
205
Seconds

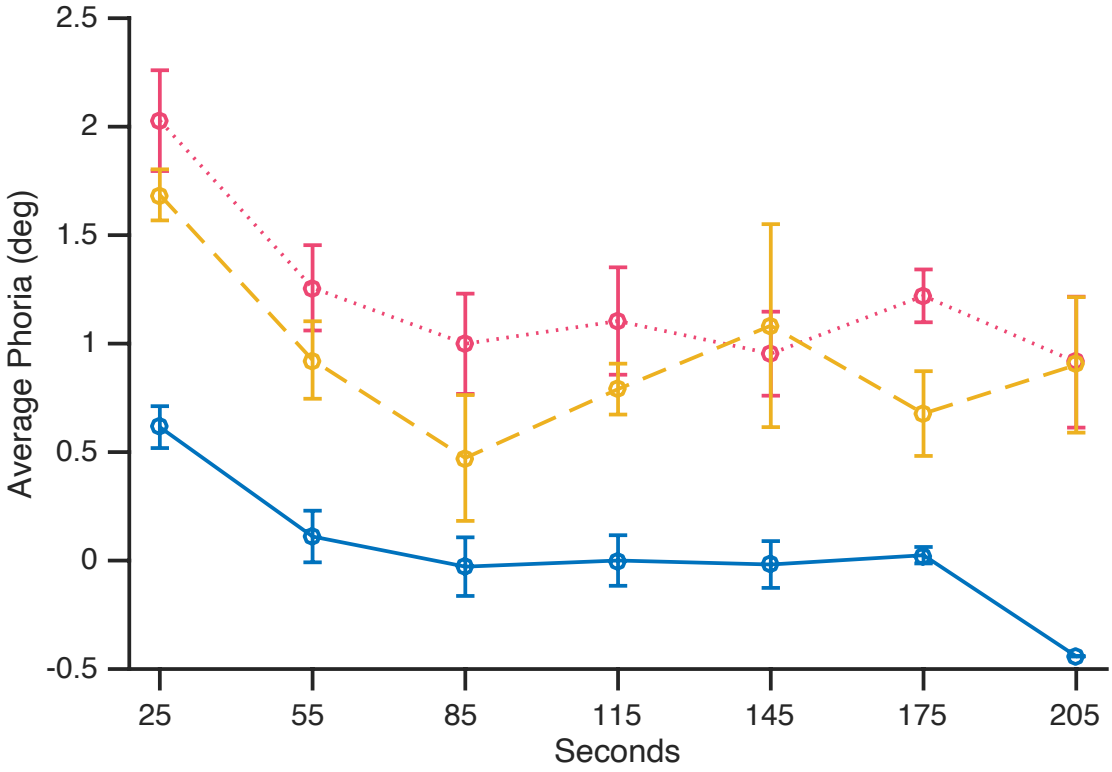
Average Phoria (deg)
2.5
2
1.5
1
0.5
0
-0.5
25
55
85
115
145
175
205
Seconds

Figure 32. Eye-tracker phorias from first and last blocks, and grand average of Experiment 4. The upper panel shows each participant's average phoria from the first block (solid line) and last block (dashed line); each color represents a different participant. The lower panel is the grand average of all participants for the first block (blue, solid line) and the last block (red, dotted line) as well as the second to last block (yellow, dashed line); error bars are SEM.

Phorias were larger in later blocks. In Figure 33, top, the average phorias from the first and last blocks of each participant's data are plotted against each other. All participants had larger phorias in the last block (an average of 0.97 degrees) as compared to the first block (0.17 degrees). The difference of 0.80 degrees was significant when compared against zero in a one way t-test (S.E = 0.06, $p < 0.001$). The first phoria in the first block was also larger than the first phoria in the last block, 0.6 degrees on average versus 2.0 degrees on average, and the difference of 1.4 degrees was significant when tested against zero in a one-way t-test (S.E. 0.16, $p < 0.001$).

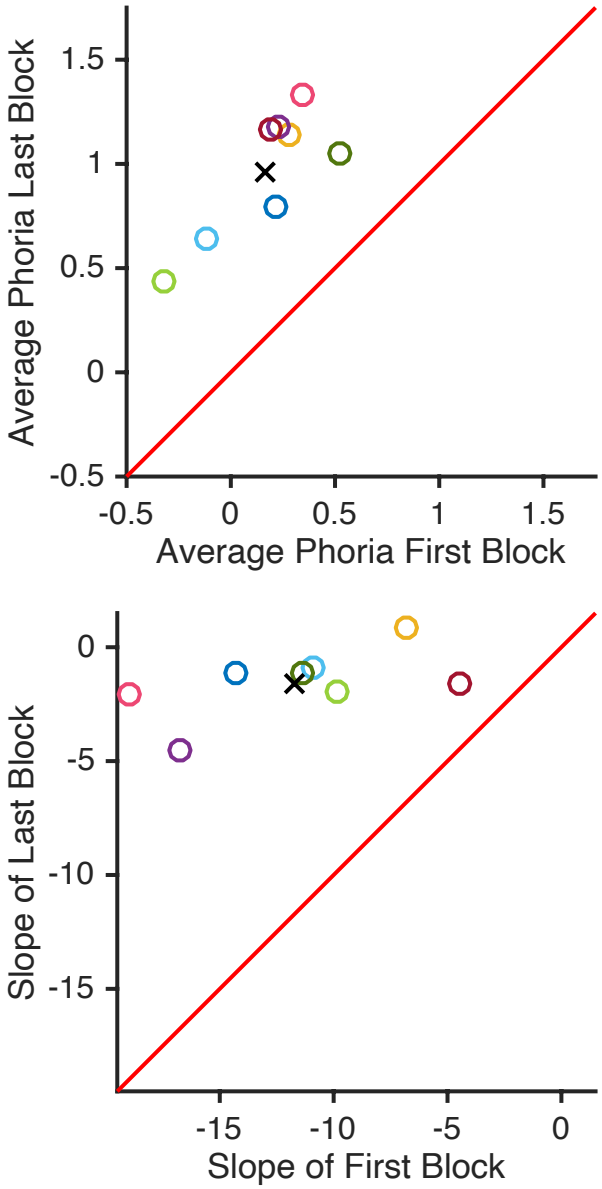

Figure 33. Phoria analyses, as measured with the eye-tracker, for Experiment 4. In the top panel, average phorias are plotted for the first versus last block. In the bottom panel, the slope of the first block phorias versus the slope of the last block phorias are plotted. Each circle is one participant, the colors correspond across the plots, the black "X" is the participant average, and the red line is unity.

The rate of adaptation within a block was faster in the first block than the last. To estimate rate, the slope of the phorias from each block was calculated as the line

of best fit to the phorias from that entire block (Figure 33, bottom). For participants who had two sessions of valid data, fits were computed for each, and slopes from the two sessions were averaged together. The average slope of the first block was -11.6 degrees/minute and the average slope of the last block was -1.5 degrees/minute. The difference of slope of -10.1 degrees/minute was significant when compared against zero in a one-way t-test (S.E. = 1.5, $p < 0.001$).

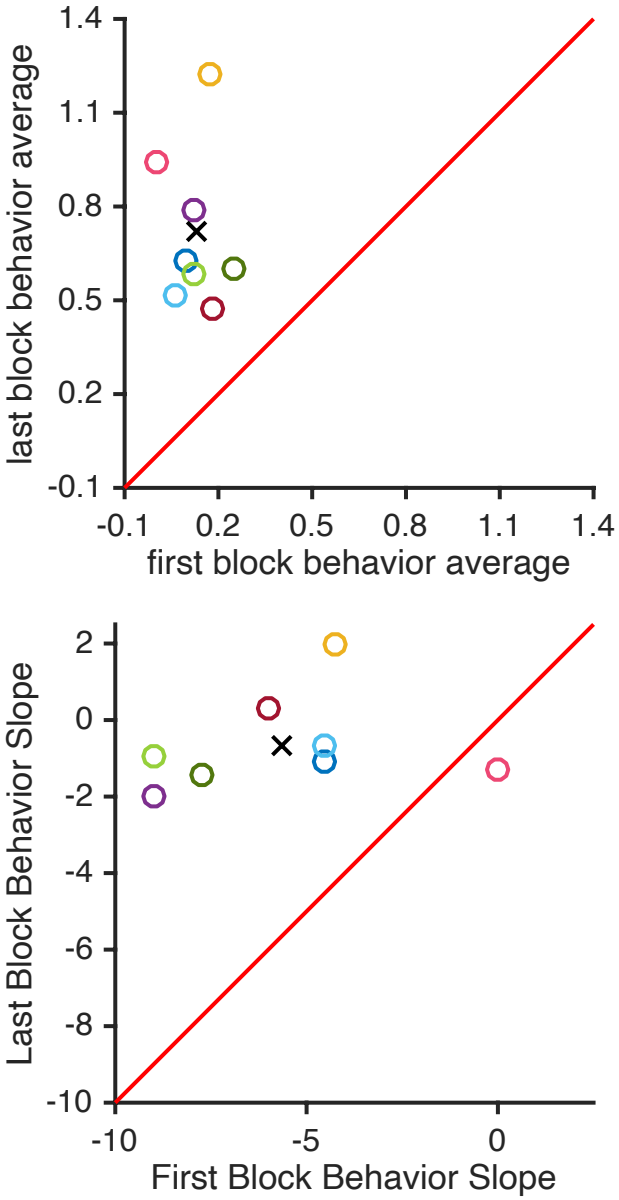

Figure 34. Behavioral phoria measurements in Experiment 4. On the top panel are the average behavioral phorias from the first block, plotted against average phorias from the last block, for each participant. The bottom panel shows the slope of the line of best fit to phorias within each block; slopes from the first block are plotted against slopes from the last block. Each circle is one participant, the colors correspond across the plots, the black "X" is the participant average, and the red line is unity.

Phorias in the experiment were measured behaviorally as well, and showed the same patterns as the eye-tracker data. As can be seen in Figure 34, top, participants' mean phoria responses from the last block were larger than for the first. The first block mean phoria was 0.13 degrees and last block was 0.72 degrees, a difference of 0.59 degrees, which was significant when compared against zero in a one-way t-test (SE = 0.10, p = 0.0005).

The rate of adaptation, as measured by the slope of behavioral phorias within a block, was also larger in the first block compared to the last block. For each participant, the slopes of the lines of best fit of the responses from the first and last blocks are plotted against each other in Figure 34, bottom. The average slope from the first block was -5.6 degrees/minute for the first block, and -0.6 degrees/minute for the last block. The difference in slope of 5.0 degrees/minute was significant when compared against zero in a one-way t-test (SE = 1.05, p = 0.002).

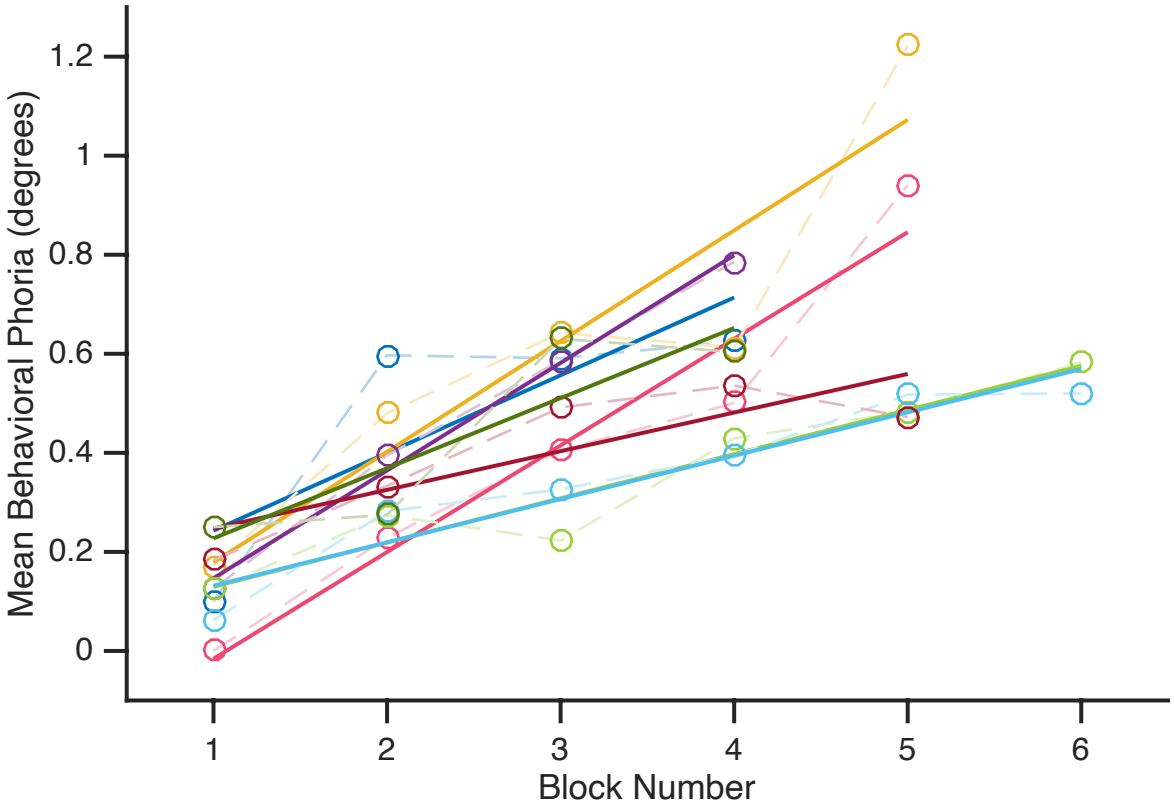

Figure 35. Average phoria across blocks, and the line of best fit, for each participant, for Experiment 4. Each color is a different participant. Each point is the mean phoria for that block, for that participant, and are connected by the dotted line. The heavy line is the line of best fit to those points, for that participant.

Average behavioral phorias increased steadily across all blocks, as can be seen in Figure 35. The mean phoria, determined by the behavioral response, for each block was plotted for each participant, and the line of best fit was plotted to those points (Figure 35). The mean phoria are generally increasing, and so the slopes of the lines of best fit were all positive, with a mean slope of 0.15 degrees/block. A one sample t-test of those slopes against zero found that difference to be significant (SE = 0.02, $p < 0.001$).

Discussion

By allowing block duration to vary as a function of the state of adaptation, we were able to test whether time was a limiting factor in our previous adaptation studies, and if having more time to adapt would result in more adaptation. Indeed, we found participants needed additional time to fully adapt in successive blocks. The increase in block duration implies that participants adapted faster in earlier blocks than they did in later blocks (see additional discussion of rate of adaptation below).

The varying block length in Experiment 4 likely allowed greater amounts of total adaptation across the experiment, which in turn increased fusional limits to a greater extent: The increase in vergence limits for this study was larger than was seen in Chapter 2. In Experiment 1, limits increased by 1.79 degrees, and in Experiment 3 limits increased by 2.38 degrees. In the current study we found limits increased by 3.56 degrees for the right eye and 3.06 for the left eye. The limits from the current experiment right eye were reliably larger than the limit increase from Experiment 1 (S.E. = 0.60, $p < 0.05$), but the trend was not significant for the comparison between Experiment 4 and Experiment 3 ($p > 0.05$).

The larger change in limits may also have been aided by customizing step size set for each individual participant. Historically prisms have been used to study

vergence adaptation. But using a stereoscope with virtually induced vergence demands allowed us to present step sizes optimized for each participant. In previous studies, the larger step sizes may have jumped past participant limits to the point where they were no longer able to adapt, and by using smaller limits were able to adapt for longer, and thus reach farther limits.

It is also likely that we measured the changes in limits more accurately, by measuring the post-adaptation limit in precisely the same way as it was measured pre-adaptation, by asking participants to track a continuous shift over the whole range of fusible image offsets. In previous experiments we simply took the maximum fusion response during the last adaptation block as the post-adaptation limit.

Most importantly, the procedures used in this experiment almost certainly could have produced even greater increases in fusional limits. Participants broke fusion in only a few sessions- every other session ended when the pre-set time limit for the adaptation procedure was reached (40 minutes). Extending the session length beyond this point would enable greater adaptation and so greater increases in fusional limits.

Rate and completeness of adaptation

Even with customized step-size and variable block duration, phorias overall grew larger in later blocks. This is likely due to two factors. First, phorias started higher at the beginning of later blocks, even though we allowed block duration to vary to allow for complete adaptation before proceeding to the next block. This increase in initial phoria size may be in part because we allowed participants to proceed to the next block if they had been at 1 degree of phoria or less for 10 mins, but were not fully able to adapt (to 0 degrees of phoria). These blocks predominately occurred later in the experiment.

Second, larger phorias in later blocks were also due to changes in adaptation. Unlike in previous experiments (Chapter 2), in Experiment 4 we found highly reliable changes in slope of phorias within a block, with decreases in phorias arising more slowly in later blocks, for both the behavior and eye-tracking data. Sethi & North (1984) and Sethi & Henson (1987) found a change in slope between first fusional demands and additional fusional demands, but the authors admit it was likely because participants were not fused at larger prism strengths. We eliminated any blocks from analysis where participants were not fused, and still found a change in slope.

Why did we detect changes in the slope of phorias in Experiment 4, but not in Experiments 1-3? This difference is likely due to the longer and variable block

lengths in Experiment 4. Examining Figure 32 shows relatively parallel adaptation curves for the first and last blocks over the first 3.5 minutes of adaptation. However, this led to complete adaptation (phorias of 0) in early blocks, while later blocks extended many more minutes, and in some cases phorias never reached 0. Thus, the slope at the beginning of the block was relatively constant across the experiment, but was greatly reduced at the end of later blocks.

Changes in adaptation

Why were block durations longer, phorias larger, and changes in phoria more gradual, during later blocks? Our data collectively suggest that larger phorias at later blocks were the result of decreased ability of the visual system to adapt.

One cause of reduced adaptation might be that the *rate* of adaptation slowed as conditions move further and further from natural viewing conditions. This could explain why phorias grew across blocks – if adaptation slowed down, even our modified procedures might have allowed unadapted vergence demand to 'build up' across blocks. In this case even longer block durations might have allowed more complete adaptation, and kept phorias more constant across blocks.

It is also possible, however, that the maximum *amplitude* of adaptation obtainable in response to a fixed increase in vergence demand decreased over time. Perhaps, for example, even given unlimited duration, adaptation could only

reduce phorias by 50% at extreme eye positions. In this case, extending durations further would not reduce the build-up of phoria across blocks.

Changes in the rate and amplitude of adaptation with vergence demand will eventually produce a “soft limit” on what can be adapted, where the system approaches an asymptote in the amplitude of adaptation gradually. This contrasts with a “hard limit” where an asymptote is reached abruptly – past a certain amount of vergence demand adaptation cannot take place. This distinction is discussed more in Chapter 4.

Transfer of adaptation across eyes

One other thing to note is that we shifted the image in only one eye towards divergence in this experiment, the right eye. Unsurprisingly, the divergence limits for the right eye increased. However, the left eye, which critically was stationary throughout the adaptation procedure, also increased its divergence limits. As far as we know this transfer of adaptation across eye has not been reported before. It suggests that the neural circuitry of vergence adaptation is happening in a central region, that controls both eyes, rather than more peripherally where representations are for individual muscles.

The limits did shift more in the right, adapting eye, than they did with the left, stationary eye. However, because we shifted the image only in that eye, this

difference could be due to an unknown difference in the right and left eye equipment, design or procedure, rather than a true difference between adapted and unadapted eyes. Future work will need to counterbalance these factors; e.g. by also adapting the left eye and measuring transfer to the right.

Other Considerations

One possibly limiting factor that we were not able to control was the accommodative cues that in natural viewing would change along with vergence changes. Vergence and accommodative cues are cross-linked, where the activation of one will activate the other (e.g. Kersten & Legge, 1983; Schor, 1985; Jiang, 1995). The mismatch between the two cues could certainly be a limiting factor in the amount of adaptation we were able to obtain.

Chapter 4. General Discussion.

General Results

We have replicated the finding that vergence adaptation can shift fusional limits (e.g. Ogle & Prangen, 1953; Henson & North, 1980; Sethi & North, 1983; Sethi & Henson, 1984; Sethi & North, 1987; Stephens & Jones, 1990; Neveu et al., 2010). By diverging one eye, we have repeatedly demonstrated that fusional limits shifted towards divergence. Fusional limits shifted towards divergence by 1.79 degrees, 2.38 degrees, and 3.56 degrees in Experiments 1, 3 and 4, respectively.

We further believe that we are the first to demonstrate that adapting one eye (the eye that shifted outward) induces a comparable but smaller shift to the other eye (which remained stationary throughout the adaptation phase). In Experiment 4, the right eye was the eye that shifted outward, and fusional limits with such a shift increased by 3.56 degrees. However, limits measured by shifting the left eye, which remained stationary during adaptation, also increased by 3.06 degrees. This would suggest that most of adaptation occurred centrally.

And indeed, Willoughby et al. (2012) used insulin-like growth factor-1 (IGF-1) on the medial rectus muscles of infant monkeys, which resulted in changes in those muscles, but also resulted in similar changes in the unaffected lateral rectus muscles. This was thought to be the result of adaptation, from proposed internuclear neurons signaling between neurons from the oculomotor nucleus, which innervates the medial rectus muscles, and neurons from the abducens nucleus, which innervate the lateral rectus muscles. Similar results were seen with adult monkeys (Christiansen et al., 2010) as well as similar changes in the superior and inferior rectus muscles, after a surgical intervention with adult rabbits (Christiansen & McLoon, 2006). These proposed internuclear neurons could explain how adaptation of the moving eye could have been signaled to the stationary eye, in our experiment.

We were also interested in whether fusional limits can be shifted to any degree through adaptation, which had not been measured in previous work. By shifting in steps, we were able to increase fusional limits in the direction of adaptation. But effects of adaptation were still limited – given 5 minutes to adapt to each step, participants in Experiments 1 and 3 eventually lost the ability to fuse the two images.

What is limiting adaptation from achieving even larger increases of fusional limits? Before adaptation, the eyes can view all points on the display, and even beyond. So the limit is not any structural limit of where each eye can point, but rather it is based on how far apart the two eyes can be diverged, as driven in part by the adaptable tonic component.

Experiments 1-3 were designed to test whether the rate of adaptation slowed across blocks, leading to the failure to adapt and eventual diplopia. However, we found no difference in the slopes of the phoria decreases between the first and last blocks of adaptation. Nevertheless, phorias of the last block started larger, and remained larger, than in the first block. This suggested that the 5 minute blocks were not long enough for adaptation to complete, so participants began later blocks with a “debt” from the previously incomplete adaptation which built up, causing subsequent blocks to start at even less complete adaptation.

To allow more complete adaptation and prevent build-up of such an adaptation deficit, in Experiment 4 we allowed block duration to vary, giving participants more time to adapt as required. This procedure did allow participants to reach greater divergence than in Experiments 1-3, supporting the idea that block-length was limiting adaptation in those experiments.

Strikingly, in Experiment 4, the block duration required to reach relatively complete adaptation increased throughout the experiment, from a mean duration of 3.7 minutes in the experiment's first half to a duration of 11.6 minutes in its second half. These results suggest that adaptation does in fact slow down as divergence demands increase. The average amount of phoria measured in later blocks was also greater than that measured in earlier blocks, and the slope of changes in phoria across blocks was greater in earlier blocks than in later ones, further supporting the notion of slowing adaptation.

Methodological Findings

The studies reported here demonstrate the benefits of using a dual stereoscope/eye-tracking setup. First, it allowed us to measure phorias over time, and that time course can signify the rate of adaptation. Second, it allowed us to measure eye-tracker and behavioral data concurrently, with each data type providing independent validation of the other.

We also showed that, in order to measure the time course of adaptation, a ratio of 25 seconds of binocular data to 5 seconds of monocular data was insufficient. When we changed the timing to 20 seconds of binocular data and 10 seconds of monocular data, we were much more able to measure clear phorias in the data.

How far could fusional limits be increased?

Almost all participants in Experiment 4 still fused the images presented during their last block of the 40 minute procedure; they only broke fusion in the fusional limits measurement at the end of the adaptation phase. However, it is highly likely that the slowing of adaptation, and resulting trend for increasing block length, would have continued if we had extended the experiment. This pattern places a limit on the maximum increase in divergence that could be obtained through our procedure, as eventually the required block length would become prohibitively long.

Experiment 4, then, supports the notion of a “soft limit” on adaptation, which arises from a decrease in efficiency as vergence demands increase. This is as opposed to a “hard limit” that would occur if there was one maximally divergent position the eyes could take. These two limits are not mutually exclusive, and so we cannot rule out the presence of a hard limit.

It nevertheless may be of interest to adapt participants for significantly longer periods of time, and see if they are able to adapt more. The methods used in Experiment 4 could be done at longer durations by employing the use of virtual reality goggles, or prism glasses, so the participant could be adapting for many hours while moving about their day. The longer amount of time would allow for blocks to be much longer. This would help determine the largest possible amplitudes of adaptation practically obtainable despite the soft, and possibly hard limits. This magnitude could in turn influence the development of therapies that use adaptation to treat disorders of the fusional systems.

Other Outstanding Questions

By documenting limits on vergence adaptation, and suggesting slowing of adaptation as a cause of this limit, our work lays the foundation for answering many additional questions beyond the main open question mentioned above (How far could fusional limits be increased?) What follows is a partial list of other questions that could be answered by building upon our initial studies. Because they are so numerous, these questions are presented relatively briefly and informally.

1. Would better measures of adaptation allowed fusional limits to be increased further? Sethi and Henson (1987) and Sethi and North (1984) also found a decreased rate of adaptation to larger and subsequent vergence demands. Although their results may be due to participants unable to fuse the larger vergence demands, in discussing their results

they raise a good point. They speculate that phoria alone may be insufficient to determine whether adaptation is “complete,” as day(s) of adaptation at the lower vergence demand caused the rate of adaptation to a higher demand to increase, for some participants. They suggest that phorias returning to zero should not be used as a determination that adaptation is complete, but rather that adaptation may only be complete when the rate that participants adapt to subsequent demands decreases to the rate of an earlier block. Using this measure of completeness may better allow very long-term paradigms to produce the largest possible amounts of adaptation.

2. Could changes in accommodation allow greater vergence adaptation? It is possible that the mismatch in accommodative and vergence cues was hindering the maximum adaptation we were able to attain. Perhaps, for example, the accommodative crosslink limited the amount of adaptation, because of the growing incongruences between the fusional and accommodative cues. This suggests that if we had included a matched accommodation change along with the fusional cues, participants may have been able to adapt further.
3. Is the partial transfer of adaptation across eyes a genuine effect? In Experiment 4, we found that the amount of adaptation that transferred was less for the stationary eye than it was for the moving eye. This finding is important because it implies that vergence adaptation can be broken into

two components with some (that transferred eyes) arising at a central location, and some (that was eye specific) arising at a different, likely more peripheral site. However, as all participants' right eye was the moving eye, and their left eye was the stationary eye, there is still the question of whether this was an artifact of our setup, or some other potential confound. Counterbalancing the image shift across eyes would determine if our finding was genuine. We also only tested the divergence limits in our experiment. It has been found both by Stephens & Jones (1990) inducing both eyes toward divergence, and Neveu et al. (2010) inducing both eyes toward convergence, that the divergence and convergence limits both shift by comparable amounts in whatever direction vergence is induced. Although we did not also measure convergence limits, it is likely, based on those studies mentioned above, that convergence limits also shifted away from convergence. Whether this transfer applied equally to both the right and left eyes is also an interesting open question.

4. Transfer of adaptation across eyes in patients. If the unequal transfer of adaptation from one eye to the other is a real effect, testing interocular transfer of vergence adaptation on patients who have difficulty fusing would be of interest. Measuring eye-specific vs general components in, for example, people with convergence insufficiency, or perhaps patients with incomitant or intermittent strabismus, might advance understanding of the neural origins of the disorder.

5. How long does it take to *deadapt*, after vergence adaptation? It would be of interest to adapt the vergence system for different amounts of time (or adapt to different strengths of vergence demand) and then measure how long it takes to deadapt. If, as mentioned above, Sethi and Henson (1987) and Sethi and North (1984) are correct, then phoria reduction down to zero is not a reliable measure of the completeness of adaptation. In that case, one might also expect that adapting for longer periods of time after reaching zero phoria could nevertheless produce stronger and more complete adaptation. This hypothesis predicts that it would take longer to deadapt for longer adaptation durations, even when all durations tested reduced phorias to zero.
6. Could an equal change in accommodation result in further adaptation, when vergence demand is shifted? Which in this case is asking, where does the mechanism limiting fusional limit adaptation exist?

   It is possible that the mismatch in accommodative and vergence cues was hindering the maximum results we were able to attain. Another way to ask this is whether it was a limitation of the EOMs and the nerves that innervate them? It may be something else in the system, for example the accommodative crosslink, which limited the fusional limits in our particular experiment from continuing to adapt, because of the incongruences between the fusional and accommodative cues? This would mean that if we had an accommodation change along with the fusional cues, could

participants have adapted further? This is interesting in either way, because either a) yes they can achieve greater fusional limits while accommodation cues are manipulated along with the fusional cues, or b) if changing accommodative cues does not allow participants to achieve greater fusional limits, then the limiting mechanism is somewhere else in the EOMs, the peripheral nervous system, or the central nervous system. With the flat screen, the viewing distance to the moving image was increasing, and therefore accommodative cues could have changed. The accommodative cues could only have changed up to 1/16Δ, if the image shifted all the way to the edge of the display, but no one was able to diverge that far and maintain fusion, so the change in accommodative demands was even less. It is possible this change in accommodative demand was too small to be significant. However, with one eye diverging and the other eye converging, perhaps the convergence accommodation (the amount of accommodative driven by a change in vergence) could have been disruptive to the vergence angles obtained.

7. Could one develop new therapies using vergence adaptation? Diplopia can be resolved through surgery, the use of prisms, and sometimes through the use of convergence exercises. With the many possible etiologies that can cause diplopia, certain diseases respond better to surgery and/or prisms. For example, skew deviations have a high rate of success with prisms, blowout fractures are more often treated with

surgery, and convergence insufficiency has a low success rate with prisms and is more often treated with convergence exercises (Gunton & Brown, 2012). In general, visual training has a poor history of success in aiding disorders of vergence, though convergence insufficiency is sometimes successfully treated with “pencil pushups”, which help the patient more comfortably converge (Helveston, 2005). However, existing visual training regimens and the studies that support them have used relatively poor experimental design and measurement. Other types of visual training therapies could be explored using more rigorous experimental standards. The pencil pushup exercises used with convergence insufficiency work the fast fusional system, and perhaps vergence adaptation could also be a useful form of therapy, activating the slower, tonic component. For example, perhaps it is possible that post-surgical vergence adaptation therapies could be used to achieve a greater correction.

8. What are the sources of individual differences vergence adaptation? It is clear when looking at the eye-tracker data that there is great variability in the individual differences of eye movements between the different participants. Eye movement patterns are highly specific to an individual and have been proposed as a unique biometric for unlocking smartphones, for example (e.g., Liu, et al., 2015, Holland & Komogortsev, 2013). Are different measures of binocular eye movements (e.g. fusional limits, stereoscopic thresholds, accommodative limits, latent phorias or

tropias) correlated with the degree to which adaptation can shift fusional limits? Answering this question would be informative for both understanding basic mechanisms of vergence adaptation as well as translating them to therapies.

9. Would these results also occur in more ecologically natural eye positions? The positions we directed the eyes to, to have one eye converging and one eye diverging, were arguably an ecologically abnormal configuration. It could be argued that our results would not apply to a more normal configuration. However, we saw a similar pattern of results when the eyes were converging rather than diverging. And also, it could be possible that there would be an even stronger effect with ore normal viewing situations. It may therefore be important to more rigorously look at differences between divergence and convergence, with one and both eyes, as well as possibly test in the vertical meridian as well, to determine if our results apply to vergence adaptation more generally.
10. Are our results simply due to the eyes fatiguing over time? The extraocular muscles are quite resistant to fatigue, but one interpretation of our results is that perhaps near the end of the experiment, the muscles were fatigued, and could not adapt as much as the beginning. One way to confirm this was not happening would be to adapt participants to their pre-test fusional limit for 40 minutes, and also half that amount for 40 minutes at a separate occasion. Again, the rate and amplitude of adaptation could be measured.

And since the duration would be the same, it could not be the amount of time that was fatiguing, and affecting either measure of adaptation.

4.4 Conclusions

Collectively, our studies reveal that there is a limit to vergence adaptation and the increase in fusional limits that it can produce. Adaptation became less efficient as vergence demands increased, resulting in an increasing “debt” of unadapted demand (Experiments 1-3) or increasing time required for adaptation (Experiment 4). Both place a limit on the amount of adaptation attainable. Our findings lay the groundwork for future studies to determine the largest possible increase in fusional limits achievable through adaptation, the optimal protocols to reach these limits, and whether they could be of clinical value.

References

Burian, H. M. (1939). Fusional Movements: Role of Peripheral Retinal Stimuli. *Archives of Ophthalmology*, *21*(3), 486–491.

Carter, D. B. (1965). Fixation disparity and heterophoria following prolonged wearing of prisms. *American Journal of Optometry and Archives of American Academy of Optometry*, *42*(3), 141–152.

Carter, D. B. (1963). Effects of prolonged wearing of prism. *American Journal of Optometry and Archives of American Academy of Optometry*, *40*, 265–273.

Christiansen, S. P., Antunes-Foschini, R. S., & McLoon, L. K. (2010). Effects of recession versus tenotomy surgery without recession in adult rabbit extraocular muscle. *Investigative Ophthalmology and Visual Science*, *51*(11), 5646–5656. https://doi.org/10.1167/iovs.10-5523

Christiansen, S. P., & McLoon, L. K. (2006). The effect of resection on satellite cell activity in rabbit extraocular muscle. *Investigative Ophthalmology and Visual Science*, *47*(2), 605–613. https://doi.org/10.1167/iovs.05-1069

Fender, D., & Julesz, B. (1967). Extension of Panum's fusional area in binocularly stabilized vision. *Journal of the Optical Society of America*, *57*(6), 819–830. https://doi.org/10.1364/JOSA.57.000819

Fincham, B. Y. E. F., & Walton, J. (1957). The Reciprocal Actions of Accommodation and Convergence. *Journal of Physiology*, *137*, 488–508.

Fincham, E. F. (1951). The Accommodation Reflex and its Stimulus. *The British Journal of Ophthalmology*, *35*(7), 381–393. https://doi.org/10.1136/bjo.35.7.381

Fisher, S. K., Ciuffreda, K. J., Tannen, B., & Super, P. (1988). Stability of tonic vergence. *Investigative Ophthalmology and Visual Science*, *29*(10), 1577–1581.

Fray, K. J. (2013). Fusional Amplitudes : Exploring Where Fusion Falters. *American Orthoptic Journal*, *63*, 41–54.

Gegenfurtner, K. R. (2016). The Interaction Between Vision and Eye Movements. *Perception*, (August 2014), 1–25. https://doi.org/10.1177/0301006616657097

Gunton, K. B., & Brown, A. (2012). Prism use in adult diplopia. *Current Opinion in Ophthalmology*. https://doi.org/10.1097/ICU.0b013e3283567276

Harrold, A. L., & Grove, P. M. (2015). Binocular correspondence and the range of fusible horizontal disparities in the central visual field. *Journal of Vision*, *15*, 1–17. https://doi.org/10.1167/15.8.12.doi

Helveston, E. M. (2005). Visual training: Current status in ophthalmology. *American Journal of Ophthalmology*, *140*(5), 903–910. https://doi.org/10.1016/j.ajo.2005.06.003

Henson, D. B., & North, R. (1980). Adaptation to Prism-Induced Heterophoria. *American Journal of Optometry & Physiological Optics*, *57*(3), 129–137.

Hillis, J. M., & Banks, M. S. (2001). Are corresponding points fixed? *Vision Research*, *41*(19), 2457–2473. https://doi.org/10.1016/S0042-6989(01)00137-7

Hoffmann, F. B., & Bielchowsky, A. (1900). Ueber die der Willkur entzogenen Fusionsbewegungen der Augen. *Pflügers Archiv European Journal of Physiology*, *80*(1), 1–40.

Holland, C. D., Komogortsev, O. V, & State, T. (2013). Complex Eye Movement Pattern Biometrics : Analyzing Fixations and Saccades, 1–8.

Howarth, P. A. (2011). The geometric horopter. *Vision Research*, *51*, 397–399. https://doi.org/10.1016/j.visres.2010.12.018

Hung, G. K., Semmlow, J. L., & Ciuffreda, K. J. (1986). A dual-mode dynamic model of the vergence eye movement system. *IEEE Transactions on Bio-Medical Engineering*, *33*(11), 1021–1028. https://doi.org/10.1109/TBME.1986.325868

Hung, G. K., Ciuffreda, K. J., & Rosenfield, M. (1996). Proximal contribution to a linear static model of accommodation and vergence. *Opthalmology and Physiological Optics*, *16*(1), 31–41.

Jaschinski, W., & Walper, N. (2007). Resting positions of vergence and their relation to asthenopic complaints. *Strabismus*, *15*(1), 29–32. https://doi.org/10.1080/09273970601180131

Jiang, B. C. (1996). Accommodative vergence is driven by the phasic component of the accommodative controller. *Vision Research*, *36*(1), 97–102. https://doi.org/10.1016/0042-6989(95)00051-Z

Kalloniatis, M., & Luu, C. (2005). The Perception of Space. In H. Kolb, E. Fernandez, & R. Nelson (Eds.), *Webvision: TheThe Organization of the Retina and Visual System* (pp. 1–12). Salt Lake City (UT): University of Utah Health Sciences Center.

Kersten, D., & Legge, G. E. (1983). Convergence accommodation. *Journal of the Optical Society of America*, *73*(3), 332–338. https://doi.org/10.1364/JOSA.73.000332

Kertesz, A. E. (1981). Effect of stimulus size on fusion and vergence. *Journal of the Optical Society of America*, *71*(3), 289–293. https://doi.org/10.1364/JOSA.71.000289

Krishnan, V. V, & Stark, L. (1977). A heuristic model for the human vergence eye movement system. *IEEE Transactions on Bio-Medical Engineering*, *24*(1), 44–49. https://doi.org/10.1109/TBME.1977.326207

Liu, D., Dong, B., Gao, X., & Wang, H. (2015). Exploiting Eye Tracking for Smartphone Authentication. In T. Malkin, V. Kolesnikov, A. B. Lewko, & M. Polychronakis (Eds.), *Applied Cryptography and Network Security* (pp. 457–477). Cham: Springer International Publishing.

Ludvigh, E., Mckinnon, P., & Zaitzeff, L. (1964). Temporal Course of the Relaxation of Binocular Duction (Fusion) Movements. *Archives of Ophthalmology*, *71*(3), 389–399. https://doi.org/10.1001/archopht.1964.00970010405018

Maddox, E. E. (1893). *The Clinical Use Of Prisms; And the Decentering of Lenses* (2nd ed.). Bristol: J. Wright.

Maunsell, J. H. R., & Van Essen, D. C. (1983). Functional Properties of Neurons in Middle Temporal Visual Area of the Macaque Monkey. II. Binocular Interactions and Sensitivity to Binocular Disparity. *Journal of Neurophysiology*, *49*(5), 1148–1167.

McLoon, L. K. (2011). The extraocular muscles. In *The extraocular muscles* (pp. 182–207). https://doi.org/10.1016/S0002-9394(42)92405-X

Mitchell, D. E. (1966). Retinal disparity and diplopia. *Vision Research*, *6*(441–451).

Morgan, M. W. (1980). The Maddox Classification of Vergence Eye Movements. *American Journal of Optometry & Physiological Optics*, *57*(8), 537–539.

Neveu, P., Priot, A. E., Plantier, J., & Roumes, C. (2010). Short exposure to telestereoscope affects the oculomotor system. *Ophthalmic and Physiological Optics*, *30*(6), 806–815. https://doi.org/10.1111/j.1475-1313.2010.00763.x

North, R. V., Henson, D. B., & Smith, T. J. (1993). Influence of Proximal, Accommodative and Disparity Stimuli upon the vergence system. *Opthalmology and Physiological Optics*, *13*, 239–243.

Ogle, K. N. (1952). On the limits of stereoscopic vision. *Journal of Experimental Psychology*, *44*(4), 253–259. https://doi.org/10.1037/h0057643

Ogle, K. N. (1962). A consideration of the horopter: The Proctor Award Lecture. *Investigative Ophthalmology*, *1*(4), 446–461.

Ogle, K. N., & Prangen, A. deH. (1953). Observations on Vertical Divergences and Hyperphorias. *AMA Archives of Ophthalmology*, *49*(3), 313–334.

Owens, D. A., & Wolf-Kelly, K. (1987). Near Work , Visual Fatigue , and Variations of Oculomotor Tonus. *Investigative Ophthalmology and Visual Science*, *28*(4), 743–749.

Paulus, M. M., Straube, A., & Eggert, T. (2017). Vergence-accommodation conflict in virtual reality displays induces phoria adaptation. *Journal of Neurology*, *264*(s1), S16–S17. https://doi.org/10.1007/s00415-017-8425-z

Poggio, G. F., Gonzalez, F., & Krause, F. (1988). Stereoscopic Mechanisms in Monkey Visual Cortex : Binocular Correlation and Disparity Selectivity. *The Journal Of Neuroscience*, *8*(12), 4531–4550.

Rashbass, C., & Westheimer, G. (1961). Independence of conjugate and disjunctive eye movements. *The Journal of Physiology*, *159*, 361–364. https://doi.org/10.1113/jphysiol.1961.sp006813

Rosenfield, M., Ciuffreda, K. J., & Hung, G. K. (1991). The linearity of proximally induced accommodation and vergence. *Investigative Ophthalmology and Visual Science*, *32*(11), 2985–2991.

Rosenfield, M. (1997). Tonic Vergence and Vergence Adaptation. *Optometry and Vision Science*, *74*(5), 303–328.

Rosenfield, M., Ciuffreda, K. J., Ong, E., & Azimi, A. (1990). Proximally induced accommodation and accommodative adaptation. *Investigative Ophthalmology and Visual Science*, *31*(6), 1162–1167.

Rosenfield, M., & Gilmartin, B. (1990). Effect of Target Proximity on the Open-Loop Accommodative Response. *Optometry and Vision Science*, *67*(2), 74–79.

Schor, C. M. (2011). Adler's Physiology of the eye. In L. A. Levin, S. F. E. Nilsson, J. Ver Hoeve, & S. M. Wu (Eds.) (11th ed., pp. 220–242). Edinburgh: Saunder's Elsevier.

Schor, C. M. (1979). The relationship between fusional vergence eye movements and fixation disparity. *Vision Research*, *19*(12), 1359–1367. https://doi.org/10.1016/0042-6989(79)90208-6

Schor, C. M. (1980). Fixation Disparity: A Steady State Error of Disparity-Induced Vergence. *American Journal of Optometry & Physiological Optics*, *57*(9), 618–631.

Schor, C. M. (1985). Models of Mutual Interactions Between Accommodation and Convergence. *American Journal of Optometry & Physiological Optics*, *62*(6), 369–374.

Schor, C. M. (1979). The influence of rapid prism adaptation upon fixation disparity. *Vision Research*, *19*(7), 757–765. https://doi.org/10.1016/0042-6989(79)90151-2

Schor, C. M., & Tyler, C. W. (1981). Spatio-temporal properties of Panum's fusional area. *Vision Research*, *21*(5), 683–692. https://doi.org/10.1016/0042-6989(81)90076-6

Sethi, B., & Henson, D. B. (1984). Adaptive Chages with Prolonged Effect of Comitant and Incomitant Vergence Disparities. *American Journal of Optometry & Physiological Optics*, *61*(8), 506–512.

Sethi, B., & Henson, D. B. (1985). Vergence-Adaptive Change with a Prism-Induced Noncomitant Disparity. *American Journal of Optometry and Physiological Optics*, *62*(3), 203–206.

Sethi, B., & North, R. V. (1987). Vergence Adaptive Changes with Verying Magnitudes of Prism-Induced Disparities and Fusional Amplitudes. *American Journal of Optometry & Physiological Optics*, *64*(4), 263–268.

Shipley, T., & Rawlings, S. C. (1970). The Nonius Horopter - II. An Experimental Report. *Vision Research*, *10*, 1263–1299.

Shipley, T., & Rawlings, S. C. (1970). The Nonius Horopter - I. History and Theory. *Vision Research*, *10*, 1225–1262.

Siderov, J., Harwerth, R. S., & Bedell, H. E. (1999). Stereopsis, cyclovergence and the backwards tilt of the vertical horopter. *Vision Res*, *39*(7), 1347–1357. https://doi.org/10.1016/S0042-6989(98)00252-1

Stephens, G. L., & Jones, R. (1990). Horizontal fusional amplitudes after adaptation to prism. *Ophthalmic and Physiological Optics*, *10*(1), 25–28. https://doi.org/10.1016/0275-5408(90)90125-I

von Noorden, G. K., & Campos, E. C. (2002). *and Ocular Binocular Vision and Ocular Motility*. (R. Lampert, Ed.) (6th ed.). St. Louis: Mosby.

Willoughby, C. L., Christiansen, S. P., Mustari, M. J., & McLoon, L. K. (2012). Effects of the sustained release of IGF-1 on extraocular muscle of the infant non-human primate: Adaptations at the effector organ level. *Investigative Ophthalmology and Visual Science*, *53*(1), 68–75. https://doi.org/10.1167/iovs.11-8356

Appendices

Appendix A: Extraocular Muscles

This section is summarized from Chapters 3 and 4 of von Noorden & Campos (2002), as well as McLoon (2011).

There are three pairs of extraocular muscles; a pair of horizontal rectus muscles (medial and lateral), a pair of vertical rectus muscles (superior and inferior), and a pair of oblique muscles (superior and inferior).

The rectus muscles (medial, lateral, superior and inferior) begin at the annulus of Zinn, which surrounds the optic nerve, and attach to the sclera on the medial, lateral, superior, and inferior sides of the eye, forming a “cone” of muscle around the eye. The superior oblique muscle has its origin on the bone in the apex of the orbit, runs anteriorly along the medial orbital wall, and passes through the trochlea, a cartilage loop, at the anterior area where the medial and superior walls of the orbit meet; after passing through the trochlea, the superior oblique muscle bends posteriorly at approximately 54°, continues dorsolaterally , passes deep to the superior rectus muscle, and attaches to the sclera on the superior side of the eye posterior to the equator. The inferior oblique muscle begins anteriorly where the medial and inferior walls of the optic cavity meet, and

continues posterolaterally inferior to the eye, and attaches to the sclera on the inferior side of the eye, posterior to the equator.

The primary roles of the extraocular muscles are as follows: the lateral rectus abducts (moves the eye horizontally away from the nose) and the medial rectus adducts (moves the eye horizontally toward the nose). The superior rectus elevates, the inferior rectus depresses, but each has a rotational component; the inferior oblique exocyclorotates (where the upward pole of the eye rotates nasally), and the superior oblique incyclorotates (where the upward pole of the eye rotates nasally).

The horizontal rectus muscles (lateral and medial) have only this primary action. However, the vertical rectus muscles (superior and inferior) and the oblique muscles have a secondary action based on the position of the eye. The superior rectus acts as a pure elevator when the eye is abducted, but in primary position and when adducted it also acts an adductor as well as an elevator, resulting in incycloduction. The inferior rectus acts solely as a depressor when abducted, but in primary position and when adducted it adducts and depresses, resulting in excycloduction. When adducted, the superior oblique muscle acts purely as a depressor, when abducted it acts purely as an incycloductor, and in primary position causes incycloduction, depression and abduction. The inferior oblique

muscle acts as an excyclorotator when abducted, an elevator when adducted, and in primary position it acts as an excyclorotator, an elevator and an abductor. All of the muscles are supplied by 3rd cranial nerve (oculomotor nerve), except for the superior oblique, which is supplied by the 4th nerve (trochlear nerve), and the lateral rectus which is supplied by the 6th nerve (abducens nerve0.

These muscles, and the eye itself, are enveloped in a complex system of fascia and ligaments, collectively referred to as Tenon's capsule, which surrounds, protects, and suspends the eye within the orbit.

There are also check ligaments which limit the contraction of the muscles, and reduce the amount of relaxation of opposing muscle systems; together, these help with the smooth movements of the eye. Smooth and highly controlled eye movements are also possible because of the relatively small muscle fibers, rich supply of nerves, and small motor units, that is each motor neuron innervates only a small number of muscle fibers.

Appendix B: Visual Angle, Prism Diopter, Meter Angle, and Vergence Angle.

Many of the quantitative measures in the paper are reported in degrees or diopters. All these measures rely on the same basic principles of trigonometry.

Visual angle is a way of reporting the size of an image on the retina. The size of an object, and the distance from the eye, are used
to calculate the angle subtended by the image as it enters the eye, which is called visual angle. This calculation is shown in equation 1, where α is visual angle, S is the size of the image, D is the viewing distance, and S and D are in the same units.

$$(1)\ \alpha = 2 * \arctan(S/2D)$$

Vergence angle is the angle between the two optical axes of the eye. This angle becomes larger as the eyes converge, and smaller as the eyes diverge. Vergence angle is calculated in a similar way as visual angle (equation 2), this time using inter-pupillary distance (IPD) instead of image size. Again, IPD and D must be in the same units.

$$(2)\ \alpha = 2 * \arctan(IPD/2D)$$

Fixation offset is the angle of misalignment of the two eyes' fixation points, at the viewing distance, measured in degrees. Equation 1 (the equation for visual angle) can be used to calculate this, where S is the distance between the two eyes' fixations, in the plane of fixation, and D is the distance to the plane of fixation, and S and D are the same units.

Image offset, the misalignment of images in the virtual image plane of a stereoscope, is calculated in the same way as fixation offset, also using Equation 1, the equation for visual angle. The angle, α ,is the angle subtended by the distance between the two images in the virtual image plane, S, at the viewing distance to the virtual image plane, D, and S and D are in the same units.

Prism strength can be reported in diopters, describing how strongly a prism refracts light. For example, at a distance of D meters, a prism that displaces an image H centimeters has a strength of H/D (if H and D are in the same units, the equation is 100*H/D).

Diopters are also used to describe lenses. Lens strength is calculated as the reciprocal focal distance, in meters. For instance, a lens that focuses light at 3 meters is a 1/3Δ lens.

Vergence angle is also sometimes reported as **Meter Angles** (MA), which is reciprocal viewing distance. If a person is fixating at a distance of ½ m, the vergence angle is 2 MA. To convert from MA to diopters, you can multiply MA by IPD in centimeters (equation 3).

$$(3)\ d = IPD*MA$$

Meter angles can be converted to degrees first by converting to diopters (equation 3), and then to degrees (equation 4).

Equations 4 and 5 can be used to convert between diopters and degrees, where d is the prism strength in diopters, and α is any of the above mentioned measurements in degrees. When dealing with small angles, one diopter is roughly 0.57 degrees, and one degree is roughly 1.75 diopters.

$$(4)\ \alpha = \arctan(d/100)$$

$$(5)\ d = 100*\tan(\alpha)$$